

Graduate School for Cellular and Biomedical Sciences

University of Bern

Exploring the pathogen-commensal continuum: Cell wall auxotrophic bacteria in gnotobiotic mice

PhD Thesis submitted by

Miguelangel Cuenca Vera

from **Spain**

for the degree of

PhD in Immunology

Supervisor

Prof. Dr. Siegfried Hapfelmeier

Institute for Infectious Diseases

Faculty of Medicine of the University of Bern

Co-advisor

Dr. Emma Slack-Wetter

Institute for Microbiology

ETH Zürich

Original document saved on the web server of the University Library of Bern



This work is licensed under a

Creative Commons Attribution-Non-Commercial-No derivative works 2.5 Switzerland licence. To see the licence go to <http://creativecommons.org/licenses/by-nc-nd/2.5/ch/> or write to Creative Commons, 171 Second Street, Suite 300, San Francisco, California 94105, USA.

Copyright Notice

This document is licensed under the Creative Commons Attribution-Non-Commercial-No derivative works 2.5 Switzerland. <http://creativecommons.org/licenses/by-nc-nd/2.5/ch/>

You are free:



to copy, distribute, display, and perform the work

Under the following conditions:



Attribution. You must give the original author credit.



Non-Commercial. You may not use this work for commercial purposes.



No derivative works. You may not alter, transform, or build upon this work..

For any reuse or distribution, you must take clear to others the license terms of this work.

Any of these conditions can be waived if you get permission from the copyright holder.

Nothing in this license impairs or restricts the author's moral rights according to Swiss law.

The detailed license agreement can be found at:

<http://creativecommons.org/licenses/by-nc-nd/2.5/ch/legalcode.de>

Accepted by the Faculty of Medicine, the Faculty of Science and the Vetsuisse
Faculty of the University of Bern at the request of the Graduate School for
Cellular and Biomedical Sciences

Bern,

Dean of the Faculty of Medicine

Bern,

Dean of the Faculty of Science

Bern,

Dean of the Vetsuisse Faculty Bern

Acknowledgment

The present work is the compilation of four years of collaborative work, in which many people participated.

I would like to thank my external referee Nassos Typas, for agreeing to review this manuscript in such a short notice.

I thank my thesis committee Emma Slack and Philippe Krebs, for continuous support and constant supply of ideas during the entire period.

I thank my supervisor Siegfried Hapfelmeier, for providing me the tools I needed for professional work and the scientific freedom to use them.

I thank my lab-mates: Miguel, for continuous good mood and willingness to take over all the lab-work that I failed to achieve; Nico, for supporting my bad-lab days and implementing metal Fridays; Simi, for taking the time to teach me all the lab techniques even when I am not the best learner; Steff, for always being willing to help despite my horrifying disorganization; Stefi, for being my late night lab company during the long days; Tephi, for using her knowledge to cover my immunological holes; Firuza, for being so cheerful and never complain over taking more work and Nanda, for providing me infinite advices and guidance.

I thank all my friends, who continuously supported me during this period, went with me on all those Aareböötle trips, heard all my complaints, cheered me up on the bad days and partied with me on the good days.

And last I thank my family for the continuous support from afar, despite the Venezuelan disaster always lingering there.

General index

Abstract	5
Introduction	6
Chapter 1	
Author contributions	18
Abstract	19
Introduction	20
Results	21
Discussion	27
Materials and Methods	29
References	34
Supplementary Material	36
Chapter 2	
Abstract	41
Introduction	42
Results and discussion	43
Materials and Methods	49
References	51
Supplementary Material	53
Chapter 3	
Author contributions	56
Abstract	57
Introduction	58
Results	60
Discussion	69
Supplementary Material	72
Materials and Methods	76
References	79
General Discussion	84
Curriculum vitae	87
Declaration of originality	89

Abstract

The intestinal tract of all known vertebrate animals is colonized with a high density of bacteria, forming host-specific communities. These communities are usually composed of a broad range of different species that have co-evolved with the host, to form very close and beneficial. In this thesis we developed a new tool for the study of host-microbiota interactions, based on the use of a proliferation controlled commensal *E. coli* strain and germ-free mice. This strain, contained a severe cell wall synthesis defect leading to the inability of proliferate without external supplementation. To guarantee the tightness of our system and its similarity to the wild type strain, we tested extensively the strain properties even under extreme cell wall starvation. This tool was further adapted to *Salmonella enterica* Typhimurium allowing us to simulate artificially the first six hours of a natural *Salmonella* infection, without the actual induction of disease. Our ability of simulating the early phase of an infection led to recognition of crucial *in vivo* bacterial adaptations, induced by the adaptive immunity, which led to the shift from pathogenic to commensal behavior in several *Salmonella* strains. The mechanism of this behavioral shift was explored, leading to the recognition of a *Salmonella* O-antigen shift, specific IgA induction and, exclusion of a pathogenic strain combined in to protection against disease when exposed to wild type *Salmonella enterica*. The additive effect of the discovered mechanisms was able to only partly explain the observed behavior, suggesting that other mechanisms remain to be uncovered to fully explain the behavioral shift.

Introduction

Microbiota constitution

The mammalian microbiota begins to form at birth and continues its development until death of the host (Zhang et al., 2014). During this period, four major groups colonize the intestinal tract, and dominate the community: Firmicutes, Bacteroidetes, Actinobacteria and Proteobacteria (Bäckhed et al., 2015). The Firmicutes are a group of Gram-positive anaerobic bacteria, which include well known members as the genus *Clostridium*. The Bacteroidetes are a group of Gram-negative bacteria abundant in soil, sea water and the intestines of homoeothermic animals. The Actinobacteria comprise a phylum of Gram-positive bacteria, containing the well-studied genus *Streptomyces*, and associated with the production of several antibiotics. The last major group of gut-associated bacteria is the Gram-negative Proteobacteria phylum, which includes the well-studied commensal *E. coli*, as well as several important human pathogens including *Salmonella enterica*, *Yersinia pestis*, *Campylobacter jejunii*, *Helicobacter pylori* and *Vibrio cholerae* (Khanna and Tosh, 2014; Macpherson and McCoy, 2014).

The process of colonization of the newborn germ-free mammal in a rapid succession of maternally and environmentally derived early colonizers and the maturation of the postnatally acquired consortium into an adult microbiota requires a delicate interplay of all species involved (Bäckhed et al., 2015). This ecological succession is highly influenced by dietary factors, exposition to new immigrants and the host immune system (Koenig et al., 2010). The mode of birth is the first major factor that influences the bacterial compositions, as it has been shown that vaginally delivered babies have a different microbiota composition compared to those delivered by C-section (Dominguez-Bello and Costello, 2010). After the primary microbiota has been established, a major compositional shift happens upon weaning, when the diet changes from milk to solid food, leading in to an adult-type microbiota (Koenig et al., 2010).

Even established adult microbiotas show a high degree of inter- and intra-individual (temporal) phylogenetic variability, which makes their direct comparison complex. The colonization of germ-free mice intestinal tract with a myriad of species from a variety of environmental sources, all lead to extremely different communities (Seedorf et al., 2014). These different species interact between themselves in either beneficial (complementary metabolism and degradation of toxic products) or detrimental (production of antibiotics, competition for nutrients and direct attack) relationships that shape the final structure of the community. The bacteria-bacteria interactions vary with the changes in host nutrition or

incorporation of new species, dynamically changing the community structure in a daily basis (Bäckhed et al., 2015; Dishaw et al., 2014)

Despite the high variability of the microbiome between age-matched individuals, they at the functional level encode a rather similar set of metabolic pathways, regardless of phylogenetic composition (Bashan et al., 2016). The resulting microbial metabolic repertoire provides many nutritional advantages to the host, such as synthesis of micronutrients, degradation of toxic compounds, increase in the efficiency of nutrient absorption and protection from obesity (Blanton et al., 2016; Bäckhed et al., 2015; Cummings and Macfarlane, 1997; Dishaw et al., 2014; Maltby et al., 2013; McFall-Ngai and Casadevall, 2012; Ridaura et al., 2013; Tremaroli and Bäckhed, 2012)

Advantages of the microbiota

The stability of an adult microbiota comes from a tight and intricate nutritional connection between species, induced by an overlay of all the different metabolic pathways. This state is achieved by a specific subset of bacteria, able to fully co-exist and resist change, referred to as residents (Bäckhed et al., 2015). This concept separates the resident microbiota from tourist species (organisms that only transit in the gut before being shed). The selection of resident species and continuous exclusion of tourist (and pathogenic) species are the main signs of a mature microbiota (Bäckhed et al., 2015; Cummings and Macfarlane, 1997; Tremaroli and Bäckhed, 2012)

A fully developed intact microbiota provides protection against pathogens due to a phenomenon long known as “colonization resistance”, where the resident bacteria deplete nutrients needed for the newcomer’s proliferation while inducing an specific immune response (Leatham et al., 2009; Maltby et al., 2013; Stecher et al., 2007a). Colonization resistance also favors resident bacteria, as seen in *E. coli*, that after a period of adaptation in the gut becomes more efficient in carbon source utilization, preventing the bloom of other *E. coli* strains (Leatham et al., 2005). Since this protection is able to deter the invasion of newcomers, many pathogens developed mechanisms to break this colonization resistance.

A well-studied mechanism for bypassing the colonization resistance is known to be crucial in enteric infection with *Salmonella enterica* serovar Typhimurium (Stm) (Stecher et al., 2007b). In this disease, Stm uses the type three secretion system (TTSS) encoded on salmonella pathogenicity island-1 (SPI-1) to invade the intestinal mucosa (Hapfelmeier et al., 2005). Driven by bacterial invasion and inflammasome activation, the host induces an acute inflammatory response leading to the decrease of butyrate-producing *Clostridium spp.*, and hence a decrease in the *Clostridium* induced local anoxia (Rivera-Chávez et al., 2016). Inflammation-related increases in the levels of reactive oxygen and nitrogen species allows

Stm to boost its proliferation rate and overcome colonization resistance. The increase in Stm numbers leads to diarrhea, loss of weight, prolonged discomfort and depending on the host's immune competence death. This strategy has the side effect of giving rise to spontaneous avirulent mutant, able to overgrow the virulent Stm, which can be interpreted as a population-level regulatory mechanism leading to the clearance of the pathogen by the resident microbiota, ensuring the survival of the host (Diard et al., 2013; Endt et al., 2010; Sturm et al., 2011).

Methods for microbiota study

The microbiota disruption observed in Stm colitis can be artificially achieved by treating mice with antibiotics, to lower the colonization resistance, allowing the establishment of Stm. This antibiotic treatment is the most widely used mouse model for the study of Stm-induced colitis (Barthel et al., 2003; Rivera-Chávez et al., 2016). This method has been very successfully used for studying the pathogen-host interactions. However, since it leads to an artificially disrupted microbiota it has limited use for studying the healthy host-microbiota interactions and microbiota-pathogen-host relationship.

Depleting mice of their native microbiota by using highly concentrated antibiotic cocktails was proposed as a method to assess the delicate microbiota-pathogen continuum and its relationship with the host (Reikvam et al., 2011). This treatment has low reproducibility and the microbiota recovers as soon as the antibiotic cocktail is removed (Macpherson and McCoy, 2014). The method of choice to avoid this problem is the utilization of germ-free animals. Germ-free mice are derived from sterile neonates that had been delivered by aseptically performed Cesarean section, hand-reared, and then bred under sterile conditions. Already established germ-free mouse vivaria can be efficiently extended with additional mouse strains by axenic embryo transfer (Macpherson and McCoy, 2014).

Germ-free (sterile) and gnotobiotic (ex-germ-free mice colonized with a defined subset of isolated species) mice provide powerful tools to study reduced-complexity and fully defined microbial communities, as well as detailed host-microbiota interactions. In such animals it is possible to assess which species-specific microbiota subsets are able to provide an efficient colonization resistance, what are the long term effects of small microbiota changes and if the microbiota is transferable between hosts (Chung et al., 2012; Lichtman et al., 2016; Ridaura et al., 2013). But even with the use of germ-free mice researchers have been bound to permanently expose mice to bacteria, obscuring reversible from irreversible bacterially induced changes. To be able to transiently colonize mice, "cell wall auxotrophic" (CWA) bacteria were developed (Hapfelmeier et al., 2010).

CWA bacterial strains provide a tool for limiting the host-bacterial interactions to a short duration, effectively separating short- from long-lived responses (Hapfelmeier et al., 2010). This tool is based on the auxotrophy for two bacteria-specific amino acids, D-alanine (D-ala) and *meso*-diaminopimelic acid (m-Dap). These amino acids are main constituents of the peptidoglycan, the essential and ubiquitous support structure in the gram-negative cell wall, and can be substituted by other (also bacteria-specific) metabolites only under extreme conditions (Cava et al., 2011; Lupoli et al., 2011; Xin et al., 2012). The other important factor is that neither of these compounds are produced by mammals, leading to D-Ala/m-Dap deprivation of the CWA strains upon inoculation into germ-free animals. The D-amino acids starvation that CWA strains undergo should induce a phenotype similar to that induced by beta-lactam antibiotic treatment. Beta-lactam antibiotics bind to penicillin binding proteins (PBPs) inducing an accumulation of peptidoglycan precursors in the cytosol, eventually leading to cellular arrest or lytic death (Park and Uehara, 2008; Uehara and Park, 2008; Yao et al., 2012).

Using a CWA *E. coli* K-12 strain it was possible to determine that a short lived intestinal mucosal exposition to live bacteria was sufficient to induce long-lasting specific immunoglobulin A (IgA), a clear sign that adaptive immune responses could be formed independently from continuous colonization (Hapfelmeier et al., 2010). The same strain was used for studying the role of continuous microbiota presence in the induction of granulopoiesis, where germ-free mice had an increase on their neutrophils after being exposed to bacteria, suggesting that live bacteria induce different responses than mere bacterial component exposition such as LPS or dead bacterial particles (Balmer et al., 2014)

Microbiota and immunity

The immune system holds an important role in shaping and especially containing the microbiota in the gut by several layers of redundant or complementary mechanisms. The immune response is comprised of two main components: innate and adaptive immunity. The function of these two components is based on the ability to recognize conserved non-mammalian/microbial molecular patterns by germ-line encoded (hence, "innate") and undefined non-self-antigens that are not limited to microbes by a combinatorically encoded and evolving set of ("adaptive") immune receptors (the B and T cell receptors), respectively. The combined effects of these two mechanisms account for most of the direct effect from the host to manipulate the microbiota (Dishaw et al., 2014)

The intestinal innate immunity consists of a series of relatively unspecific mechanisms of microbial containment, mostly by forming barriers and eliminating any type of microbe that invades the tissues. The primary physical intestinal barrier is the epithelium that covers the

entire intestinal surface while being permeable to nutrients (Dishaw et al., 2014). This barrier is covered by intestinal mucus, a biological gel primarily composed of mucin 2 (MUC2). The mucus covers the entire intestinal tract and constitutes a physical barrier that separates the microbiota from the epithelial brush border. There are two distinct mucus layers: an inner mucus, mostly composed of tightly packed MUC2 and nearly sterile; and an outer layer, composed of loosely packed MUC2 (Jakobsson et al., 2015). The outer mucus is permanently colonized, and provides carbon source to a distinct microbiota that differs from the luminal, digestive-associated microbiota (Jakobsson et al., 2015; Li et al., 2015). For the normal formation of the mucus barrier a continuous microbial colonization for > 8 weeks is necessary, leading to the full activation of goblet cells (the producers of the intestinal mucus) (Jakobsson et al., 2015).

Moreover, innate immunity is the first line of pathogen-commensal differentiation in the gut. Pro-inflammatory signaling induces a rapid release of highly fucosylated proteins, that have been shown to promote the proliferation of commensals while downregulating the virulence in *pathogenic E. coli* strains (Pickard et al., 2014). It has also been shown that the lipopolysaccharide (LPS) of *Bacteroides*, a genus of known commensals, dampens the pro-inflammatory response (Vatanen et al., 2016). Another method of limiting the epithelial exposition to bacteria is by production of antimicrobial peptides, a group of molecules that has been shown to be important in the maintenance of the inner mucus sterility (Meyer-Hoffert et al., 2008). The production of antimicrobial peptides by Paneth cells is tightly regulated by NOD2, an intracellular innate receptor for bacterial peptidoglycan fragments/subunits, and its malfunctioning has been linked to diseases as Crohn's ileitis (Boneca et al., 2007; Kobayashi et al., 2005). Moreover, deficiency in innate immunity, for example in impaired toll-like receptor (TLR) signaling leads to a hyper-induction of compensatory adaptive immune responses, to maintain the intestinal homeostasis (Slack et al., 2009).

The adaptive immune responses are characterized by the recognition of specific non-self-antigen and the expansion of highly antigen-specific effector T and B cells, which also give rise to the formation of long-lived memory cells providing long live immunological memory. The initial recognition of relevant antigens is primarily done by dendritic cells (DCs), the main antigen-presenting cells of the innate immune system, which process and present antigen to T-cells. After antigen presentation has occurred, the T-cells mediate a large array of immune mechanisms to eradicate the foreign organism, including B-cells (main mediators of immunoglobulin responses), regulating the innate immunity and activating phagocytic cells (Hapfelmeier and Macpherson, 2010).

In the gut, B-cells and T-cells are mostly organized in special structures that maximize the interaction with DCs. These structures are classified by size or position in to: mesenteric lymph nodes (MLNs), Peyer's patches, or minor lymph nodes. In these structures, primed DCs carrying relevant antigens interact with T-cells. The DC-T-cell interaction, denominated antigen presentation, leads to the specific activation of naïve T-cells and their differentiation. From the two main T-cell types, CD8+ (cytotoxic, mostly antiviral function) and CD4+ (helper, Th, mostly activation of other cellular types), the helper T-cells are the ones mostly involved in host-bacterial interactions (Perez-Lopez et al., 2016).

The helper T-cells are mainly classified in four types: Th1 (classical anti-intracellular pathogens), Th2 (classical anti-extracellular pathogens), Th17 (common in mucosal sites and associated to bacterial responses) and Treg (associated with anti-inflammatory responses) (Dong, 2010).

The role of immunity in the microbiota structure

Traditionally the adaptive immune response has been attributed the role to counter and eradicate pathogens. This role has been further supported by the observations that mice could be vaccinated against intestinal bacterial pathogens like *Salmonella enterica* or *Vibrio cholerae*, or that known colitogenic bacteria are stronger inducers of IgA (the main intestinal immunoglobulin). Even though IgA was shown to be relevant for acquired immunity against several intestinal pathogens, there are several examples for immunoglobulin-independent responses crucial to mucosal protective immunity. Immunized mice deficient in IgA are able to fend off enteric Stm infection, but B-cell deficient or MyD88 deficient mice are not (Ko et al., 2009; Nanton et al., 2012). Also the presence of commensal-specific mucosal regulatory T-cells (Treg) is crucial for the maintenance of the intestinal homeostasis, even during a pathogen associate inflammatory response (Ivanov and Honda, 2012). Whenever the balance between the host and the microbiota is lost, commensal-specific pro-inflammatory T-cells are induced, the unbalanced production of which may cause pathology (Hand et al., 2012).

The traditional pathogenesis-centered view of adaptive immune responses has recently shifted with the description of Th17-cells, a subgroup of commensal induced T-cells that provide extra protection against pathogens (Ivanov et al., 2009). Certain commensal species such as segmented filamentous bacteria (SFB), *Bacteroides* spp. or *Clostridium* spp. are known to induce Treg or Th17 responses (Geuking et al., 2011; Peterson et al., 2007; Smith et al., 2013; van Beelen et al., 2007). These commensal-bacteria induced responses dampen or prevent the mucosal inflammation, while also supporting the colonization of beneficial strains. These observations led several authors to suggest that the adaptive

immune system primarily functions to support and maintain a rich, physiological microbiota (Dishaw et al., 2014). There is concrete evidence supporting the idea that functional adaptive immune system increases the predictability and stability of the microbiota. When the microbiota of B-cell and T-cell deficient mice was studied over time, it was found that the rate of bacterial evolution was altered, as well as the species composition (Barroso-Batista et al., 2015; Brown et al., 2013; Zhang et al., 2014).

Aims

The study of host-induced effects on the microbiota structure and composition is the central aspect to be covered in this thesis. For this purpose we defined three main aims which will be further explored in each of three result chapters:

1. Design, construction and testing of a new bacterial tool that allows us to dissect short from long lived bacteria-host interactions in mice.
2. Characterization of the early innate immune responses against a known pathogen, in a transient infection model.
3. Study the influence of adaptive immunity in intestinal bacterial-bacterial interactions.

Original contribution

Even though the effect of the adaptive immune system on microbiota structure and composition are well-supported, the precise mechanisms of action are poorly understood. In this work we explored this and other questions, generating three fundamental pieces of new evidence:

1. A new tool to study transient host-microbiota interactions, using a cell wall auxotrophic strain of a biologically representative commensal bacterium, showed that neither the bacterial behavior nor bacteria-host interaction are affected by the mutations. This finding confirms that the CWA strains can be used to simulate short term host-microbiota interactions.
2. The infection of mice with the CWA Stm strain was able to induce an increase in the variability of inflammatory markers, without leading to inflammation. This represents an effective separation of the primary pathogen-induced responses from the pathology it normally causes. As a consequence, the model simulates the first 6 h of Stm induced colitis, without inducing pathology.
3. The combination of adaptive immune response and *in vivo* bacterial adaptation are crucial in the microbiota development from immigrant to resident status, by disfavoring the colonization of bacterial newcomers. Chapter three describes novel information on the underlying mechanism.

References

- Balmer, M.L., Schürch, C.M., Saito, Y., Geuking, M.B., Li, H., Cuenca, M., Kovtonyuk, L.V., McCoy, K.D., Hapfelmeier, S., Ochsenbein, A.F., et al. (2014). Microbiota-derived compounds drive steady-state granulopoiesis via MyD88/TICAM signaling. *J. Immunol.* **193**, 5273-83.
- Barroso-Batista, J., Demengeot, J., and Gordo, I. (2015). Adaptive immunity increases the pace and predictability of evolutionary change in commensal gut bacteria. *Nature Communications* **6**, 8945.
- Barthel, M., Hapfelmeier, S., Quintanilla-Martínez, L., Kremer, M., Rohde, M., Hogardt, M., Pfeffer, K., Rüssmann, H., and Hardt, W. (2003). Pretreatment of mice with streptomycin provides a *Salmonella enterica* serovar Typhimurium colitis model that allows analysis of both pathogen and host. *71*, 2839-2858.
- Bashan, A., Gibson, T.E., Friedman, J., Carey, V.J., Weiss, S.T., Hohmann, E.L., and Liu, Y. (2016). Universality of human microbial dynamics. *Nature* **534**, 259-62.
- Blanton, L.V., Charbonneau, M.R., Salih, T., Barratt, M.J., Venkatesh, S., Ilkaveya, O., Subramanian, S., Manary, M.J., Trehan, I., Jorgensen, J.M., et al. (2016). Gut bacteria that prevent growth impairments transmitted by microbiota from malnourished children. *Science* **351**, aad3311.
- Boneca, I.G., Dussurget, O., Cabanes, D., Nahori, M., Sousa, S., Lecuit, M., Psyllinakis, E., Bouriotis, V., Hugot, J., Giovannini, M., et al. (2007). A critical role for peptidoglycan N-deacetylation in *Listeria* evasion from the host innate immune system. *Proc. Natl. Acad. Sci. U.S.A.* **104**, 997-1002.
- Brown, E.M., Sadarangani, M., and Finlay, B.B. (2013). The role of the immune system in governing host-microbe interactions in the intestine. *Nature Immunology* **14**, 660.
- Bäckhed, F., Roswall, J., Peng, Y., Feng, Q., Jia, H., Kovatcheva-Datchary, P., Li, Y., Xia, Y., Xie, H., Zhong, H., et al. (2015). Dynamics and Stabilization of the Human Gut Microbiome during the First Year of Life. *Cell Host & Microbe* **17**, 690.
- Cava, F., Pedro, M.A., Lam, H., Davis, B.M., Waldor, M.K., and de Pedro, M.A. (2011). Distinct pathways for modification of the bacterial cell wall by non-canonical D-amino acids. *The EMBO Journal* **30**, 3442-3453.
- Chung, H., Pamp, S., Hill, J., Surana, N., Edelman, S., Troy, E., Reading, N., Villablanca, E., Wang, S., Mora, J., et al. (2012). Gut Immune Maturation Depends on Colonization with a Host-Specific Microbiota. *Cell* **149**, 1578-1593.
- Cummings, J.H., and Macfarlane, G.T. (1997). Role of intestinal bacteria in nutrient metabolism. *JPEN J Parenter Enteral Nutr* **21**, 357-65.
- Diard, M., Garcia, V., Maier, L., Remus-Emsermann, M.N., Rol, Regoes, R., Ackermann, M., Hardt, W., and Regoes, R.R. (2013). Stabilization of cooperative virulence by the expression of an avirulent phenotype. *Nature* **494**, 353-356.
- Dishaw, L.J., Cannon, J.P., Litman, G.W., and Parker, W. (2014). Immune-directed support of rich microbial communities in the gut has ancient roots. *Developmental & Comparative Immunology* **47**, 36.

Dominguez-Bello, M., and Costello, E. (2010). Delivery mode shapes the acquisition and structure of the initial microbiota across multiple body habitats in newborns. In *Proceedings Of The*.

Dong, C. (2010). Helper T-cell heterogeneity: a complex developmental issue in the immune system. *Cellular And Molecular Immunology* 7, 163.

Endt, K., Stecher, B., Chaffron, S., Slack, E., Tchitchek, N., Benecke, A., Van Maele, L., Sirard, J., Mueller, A.J., Heikenwalder, M., et al. (2010). The microbiota mediates pathogen clearance from the gut lumen after non-typhoidal *Salmonella* diarrhea. *PLOS Pathogens* 6, e1001097.

Geuking, M., Cahenzli, J., Lawson, M.E., Ng, D.K., Slack, E., Hapfelmeier, S., McCoy, K., and Macpherson, A. (2011). Intestinal Bacterial Colonization Induces Mutualistic Regulatory T Cell Responses. *Immunity* 34, 794-806.

Hand, T.W., Santos, L.M., Bouladoux, N., Molloy, M.J., Pagan, A.J., Pepper, M., Maynard, C.L., Elson, C.O., and Belkaid, Y. (2012). Acute Gastrointestinal Infection Induces Long-Lived Microbiota-Specific T Cell Responses. *Science* 337, 1553-1556.

Hapfelmeier, S., Lawson, M.A., Slack, E., Kirundi, J.K., Stoel, M., Heikenwalder, M., Cahenzli, J., Velykoredko, Y., Balmer, M.L., Endt, K., et al. (2010). Reversible Microbial Colonization of Germ-Free Mice Reveals the Dynamics of IgA Immune Responses. *Science* 328, 1705-1709.

Hapfelmeier, S., and Macpherson, A.J. (2010). In remembrance of commensal intestinal microbes. *Communicative & Integrative Biology* 3, 569.

Hapfelmeier, S., Stecher, B., Barthel, M., Kremer, M., Müller, A.J., Heikenwalder, M., Stallmach, T., Hensel, M., Pfeffer, K., Akira, S., et al. (2005). The *Salmonella* pathogenicity island (SPI)-2 and SPI-1 type III secretion systems allow *Salmonella* serovar typhimurium to trigger colitis via MyD88-dependent and MyD88-independent mechanisms. *J. Immunol.* 174, 1675-85.

Ivanov, I.I., Atarashi, K., Manel, N., Brodie, E.L., Shima, T., Karaoz, U., Wei, D., Goldfarb, K.C., Santee, C.A., Lynch, S.V., et al. (2009). Induction of Intestinal Th17 Cells by Segmented Filamentous Bacteria. *Cell* 139, 485-498.

Ivanov, I., and Honda, K. (2012). Intestinal Commensal Microbes as Immune Modulators. *Cell Host & Microbe* 12, 496-508.

Jakobsson, H.E., Holmén-Larsson, J., Schütte, A., Ermund, A., Rodríguez-Piñeiro, A.M., Arike, L., Wising, C., Svensson, F., Bäckhed, F., and Hansson, G.C. (2015). Normalization of Host Intestinal Mucus Layers Requires Long-Term Microbial Colonization. *Cell Host & Microbe* 18, 582-92.

Khanna, S., and Tosh, P.K. (2014). A clinician's primer on the role of the microbiome in human health and disease. *Mayo Clin. Proc.* 89, 107-14.

Ko, H.J., Yang, J.Y., Shim, D.H., Yang, H., Park, S.M., Curtiss, R., and Kweon, M.N. (2009). Innate Immunity Mediated by MyD88 Signal Is Not Essential for Induction of Lipopolysaccharide-Specific B Cell Responses but Is Indispensable for Protection against *Salmonella enterica* serovar Typhimurium infection. *The Journal Of Immunology* 182, 2305.

- Kobayashi, K.S., Chamaillard, M., Ogura, Y., Henegariu, O., Inohara, N., Nuñez, G., and Flavell, R.A. (2005). Nod2-dependent regulation of innate and adaptive immunity in the intestinal tract. *Science* 307, 731-4.
- Koenig, J.E., Spor, A., Scalfone, N., Fricker, A.D., Stombaugh, J., Knight, R., Angenent, L.T., and Ley, R.E. (2010). Succession of microbial consortia in the developing infant gut microbiome. *Proceedings Of The National Academy Of Sciences* 108, 4578.
- Leatham, M.P., Banerjee, S., Autieri, S.M., Mercado-Lubo, R., Conway, T., and Cohen, P.S. (2009). Precolonized Human Commensal *Escherichia coli* Strains Serve as a Barrier to *E. coli* O157:H7 Growth in the Streptomycin-Treated Mouse Intestine. *Infection And Immunity* 77, 2876-2886.
- Leatham, M.P., Stevenson, S.J., Gauger, E.J., Krogfelt, K.A., Lins, J.J., Haddock, T.L., Autieri, S.M., Conway, T., and Cohen, P.S. (2005). Mouse Intestine Selects Nonmotile *flhDC* Mutants of *Escherichia coli* MG1655 with Increased Colonizing Ability and Better Utilization of Carbon Sources. *Infection And Immunity* 73, 8039-8049.
- Li, H., Limenitakis, J.P., Fuhrer, T., Geuking, M.B., Lawson, M.A., Wyss, M., Brugiroux, S., Keller, I., Macpherson, J.A., Rupp, S., et al. (2015). The outer mucus layer hosts a distinct intestinal microbial niche. *Nature Communications* 6, 8292.
- Lichtman, J.S., Ferreyra, J.A., Ng, K.M., Smits, S.A., Sonnenburg, J.L., and Elias, J.E. (2016). Host-Microbiota Interactions in the Pathogenesis of Antibiotic-Associated Diseases. *Cell Reports* 14, 1049.
- Lupoli, T.J., Tsukamoto, H., Doud, E.H., Wang, T.A., Walker, S., and Kahne, D. (2011). Transpeptidase-mediated incorporation of D-amino acids into bacterial peptidoglycan. *J. Am. Chem. Soc.* 133, 10748-51.
- Macpherson, A.J., and McCoy, K.D. (2014). Standardised animal models of host microbial mutualism. *Mucosal Immunology* 8, 476.
- Maltby, R., Leatham-Jensen, M.P., Gibson, T., Cohen, P.S., and Conway, T. (2013). Nutritional basis for colonization resistance by human commensal *Escherichia coli* strains HS and Nissle 1917 against *E. coli* O157:H7 in the mouse intestine. *Plos ONE* 8, e53957.
- McFall-Ngai, M., and Casadevall, A. (2012). A Global Forum for Clinical Microbiologists and Immunologists. *Microbe Magazine* 7, 30.
- Meyer-Hoffert, U., Hornef, M.W., Henriques-Normark, B., Axelsson, L., Midtvedt, T., Putsep, K., and Andersson, M. (2008). Secreted enteric antimicrobial activity localises to the mucus surface layer. *Gut* 57, 764.
- Nanton, M.R., Way, S.S., Shlomchik, M.J., and McSorley, S.J. (2012). Cutting Edge: B Cells Are Essential for Protective Immunity against *Salmonella* Independent of Antibody Secretion. *The Journal Of Immunology* 189, 5503.
- Park, J.T., and Uehara, T. (2008). How Bacteria Consume Their Own Exoskeletons (Turnover and Recycling of Cell Wall Peptidoglycan)[†]. *Microbiology And Molecular Biology Reviews* 72, 211.

- Perez-Lopez, A., Behnsen, J., Nuccio, S., and Raffatellu, M. (2016). Mucosal immunity to pathogenic intestinal bacteria. *Nature Reviews Immunology* 16, 135.
- Peterson, D.A., McNulty, N.P., Guruge, J.L., and Gordon, J.I. (2007). IgA Response to Symbiotic Bacteria as a Mediator of Gut Homeostasis. *Cell Host & Microbe* 2, 328.
- Pickard, J.M., Maurice, C.F., Kinnebrew, M.A., Abt, M.C., Schenten, D., Golovkina, T.V., Bogatyrev, S.R., Ismagilov, R.F., Pamer, E.G., Turnbaugh, P.J., et al. (2014). Rapid fucosylation of intestinal epithelium sustains host-commensal symbiosis in sickness. *Nature* 514, 638.
- Reikvam, D.H., Erofeev, A., Sandvik, A., Grcic, V., Jahnsen, F.L., Gaustad, P., McCoy, K.D., Macpherson, A.J., Meza-Zepeda, L.A., and Johansen, F. (2011). Depletion of Murine Intestinal Microbiota: Effects on Gut Mucosa and Epithelial Gene Expression. *Plos ONE* 6, e17996.
- Ridaura, K.V., Faith, J.J., Rey, F.E., Cheng, J., Duncan, A.E., Kau, A.L., Griffin, N.W., Lombard, V., Henrissat, B., Bain, J.R., et al. (2013). Gut Microbiota from Twins Discordant for Obesity Modulate Metabolism in Mice. *Science* 341, 1241214-1241214.
- Rivera-Chávez, F., Zhang, L.F., Faber, F., Lopez, C.A., Byndloss, M.X., Olsan, E.E., Xu, G., Velazquez, E.M., Lebrilla, C.B., Winter, S.E., et al. (2016). Depletion of Butyrate-Producing Clostridia from the Gut Microbiota Drives an Aerobic Luminal Expansion of Salmonella. *Cell Host & Microbe* 19, 443.
- Seedorf, H., Griffin, N.W., Ridaura, V.K., Reyes, A., Cheng, J., Rey, F.E., Smith, M.I., Simon, G.M., Scheffrahn, R.H., Woebken, D., et al. (2014). Bacteria from Diverse Habitats Colonize and Compete in the Mouse Gut. *Cell* 159, 253.
- Slack, E., Hapfelmeier, S., Stecher, B., Velykoredko, Y., Stoel, M., Lawson, M.A., Geuking, M.B., Beutler, B., Tedder, T.F., Hardt, W., et al. (2009). Innate and adaptive immunity cooperate flexibly to maintain host-microbiota mutualism. *Science (New York, N.Y.)* 325, 617-20.
- Smith, P.M., Howitt, M.R., Panikov, N., Michaud, M., Gallini, C.A., Bohlooly-Y, M., Glickman, J.N., and Garrett, W.S. (2013). The Microbial Metabolites, Short-Chain Fatty Acids, Regulate Colonic Treg Cell Homeostasis. *Science* 341, 569-573.
- Stecher, B., Robbiani, R., Walker, A.W., Westendorf, A.M., Barthel, M., Kremer, M., Chaffron, S., Macpherson, A.J., Buer, J., Parkhill, J., et al. (2007a). Salmonella enterica serovar typhimurium exploits inflammation to compete with the intestinal microbiota. *5*, 2177-2189.
- Stecher, B., Robbiani, R., Walker, A.W., Westendorf, A.M., Barthel, M., Kremer, M., Chaffron, S., Macpherson, A.J., Buer, J., Parkhill, J., et al. (2007b). Salmonella enterica Serovar Typhimurium Exploits Inflammation to Compete with the Intestinal Microbiota. *Plos Biology* 5, e244.
- Sturm, A., Heinemann, M., Arnoldini, M., Benecke, A., Ackermann, M., Benz, M., Dormann, J., Hardt, W., Zürich, Z.S., Groningen, T.N., et al. (2011). The Cost of Virulence: Retarded Growth of Salmonella Typhimurium Cells Expressing Type III Secretion System 1. *PLOS Pathogens* 7, e1002143-10.
- Tremaroli, V., and Bäckhed, F. (2012). Functional interactions between the gut microbiota and host metabolism. *Nature* 489, 242-249.

- Uehara, T., and Park, J.T. (2008). Growth of *Escherichia coli*: Significance of Peptidoglycan Degradation during Elongation and Septation. *Journal Of Bacteriology* *190*, 3914.
- Vatanen, T., Kostic, A.D., d’Hennezel, E., Siljander, H., Franzosa, E.A., Yassour, M., Kolde, R., Vlamakis, H., Arthur, T.D., Hämäläinen, A., et al. (2016). Variation in Microbiome LPS Immunogenicity Contributes to Autoimmunity in Humans. *Cell* *165*, 842.
- Xin, W., Wanda, S.Y., Zhang, X., Santander, J., Scarpellini, G., Ellis, K., Alamuri, P., and Curtiss, R. (2012). The Asd+-DadB+ Dual-Plasmid System Offers a Novel Means To Deliver Multiple Protective Antigens by a Recombinant Attenuated *Salmonella* Vaccine. *Infection And Immunity* *80*, 3621.
- Yao, Z., Kahne, D., and Kishony, R. (2012). Distinct single-cell morphological dynamics under beta-lactam antibiotics. *Molecular Cell* *48*, 705-12.
- Zhang, H., Sparks, J.B., Karyala, S.V., Settlage, R., and Luo, X.M. (2014). Host adaptive immunity alters gut microbiota. *The ISME Journal* *9*, 770.
- van Beelen, A.J., Zelinkova, Z., Taanman-Kueter, E.W., Muller, F.J., Hommes, D.W., Zaat, S.A.J., Kapsenberg, M.L., and de Jong, E.C. (2007). Stimulation of the intracellular bacterial sensor NOD2 programs dendritic cells to promote interleukin-17 production in human memory T cells. *Immunity* *27*, 660-9.

Chapter 1. D-alanine-controlled transient intestinal mono-colonization with non-laboratory adapted commensal E. coli strain HS

Author Contributions

This manuscript describes the design, construction and testing of a transient colonization model for the study of host-microbiota interactions. This work was possible thanks to the contribution of several authors:

- Animal Experimentation: Miguelangel Cuenca, Simona Pfister and Stefanie Buschor
- Strain design, construction and characterization: Miguelangel Cuenca, Simona Pfister, Firuza Bayramova and Siegfried Hapfelmeier
- *Ex vivo* IgA analysis: Simona Pfister
- Cell Wall probes design and construction: Erkin Kuru, Yves Brun and Michael S. Van Nieuwenhze.
- Cell wall biochemical analysis: Sara B. Hernandez and Felipe Cava.
- 2-Photon imaging: Fernanda Coelho and Miguelangel Cuenca
- Statistical analysis: Miguelangel Cuenca
- Concept and writing the manuscript: Miguelangel Cuenca and Siegfried Hapfelmeier

RESEARCH ARTICLE

D-Alanine-Controlled Transient Intestinal Mono-Colonization with Non-Laboratory-Adapted Commensal *E. coli* Strain HS

Miguelangel Cuenca^{1,2}✉, Simona P. Pfister^{1,2}✉, Stefanie Buschor^{1,2}, Firuza Bayramova¹, Sara B. Hernandez³, Felipe Cava³, Erkin Kuru^{4,5}, Michael S. Van Nieuwenhze⁴, Yves V. Brun⁵, Fernanda M. Coelho¹, Siegfried Hapfelmeier¹*

1 Institute for Infectious Diseases, University of Bern, Bern, Switzerland, 2 Graduate School GCB, University of Bern, Bern, Switzerland, 3 Laboratory for Molecular Infection Medicine Sweden, Department of Molecular Biology, Umeå Centre for Microbial Research, Umeå University, Umeå, Sweden, 4 Department of Chemistry, Indiana University, Bloomington, Indiana, United States of America, 5 Department of Biology, Indiana University, Bloomington, Indiana, United States of America

✉ These authors contributed equally to this work.

* siegfried.hapfelmeier@ifik.unibe.ch



OPEN ACCESS

Citation: Cuenca M, Pfister SP, Buschor S, Bayramova F, Hernandez SB, Cava F, et al. (2016) D-Alanine-Controlled Transient Intestinal Mono-Colonization with Non-Laboratory-Adapted Commensal *E. coli* Strain HS. PLoS ONE 11(3): e0151872. doi:10.1371/journal.pone.0151872

Editor: Michael Hensel, University of Osnabrueck, GERMANY

Received: September 12, 2015

Accepted: March 4, 2016

Published: March 22, 2016

Copyright: © 2016 Cuenca et al. This is an open access article distributed under the terms of the [Creative Commons Attribution License](http://creativecommons.org/licenses/by/4.0/), which permits unrestricted use, distribution, and reproduction in any medium, provided the original author and source are credited.

Data Availability Statement: All relevant data are within the paper and its Supporting Information files.

Funding: SH was supported by the Swiss National Science Foundation (<http://www.snf.ch>; Grant 310030_138452) and an ERC Starting Grant from the European Research Council (<http://erc.europa.eu>) under the European Union's Seventh Framework Programme (FP/2007-2013), ERC Grant Agreement 281904. The FC laboratory received funding support by Molecular Infection Medicine Sweden (<http://www.mims.umu.se>), Knut and Alice Wallenberg Foundation (<https://www.wallenberg.com/kaw/en>).

Abstract

Soon after birth the mammalian gut microbiota forms a permanent and collectively highly resilient consortium. There is currently no robust method for re-deriving an already microbially colonized individual again-germ-free. We previously developed the *in vivo* growth-incompetent *E. coli* K-12 strain HA107 that is auxotrophic for the peptidoglycan components D-alanine (D-Ala) and meso-diaminopimelic acid (Dap) and can be used to transiently associate germ-free animals with live bacteria, without permanent loss of germ-free status. Here we describe the translation of this experimental model from the laboratory-adapted *E. coli* K-12 prototype to the better gut-adapted commensal strain *E. coli* HS. In this genetic background it was necessary to complete the D-Ala auxotrophy phenotype by additional knock-out of the hypothetical third alanine racemase *metC*. Cells of the resulting fully auxotrophic strain assembled a peptidoglycan cell wall of normal composition, as long as provided with D-Ala and Dap in the medium, but could not proliferate a single time after D-Ala/Dap removal. Yet, unsupplemented bacteria remained active and were able to complete their cell cycle with fully sustained motility until immediately before autolytic death. Also *in vivo*, the transiently colonizing bacteria retained their ability to stimulate a live-bacteria-specific intestinal Immunoglobulin (Ig)A response. Full D-Ala auxotrophy enabled rapid recovery to again-germ-free status. *E. coli* HS has emerged from human studies and genomic analyses as a paradigm of benign intestinal commensal *E. coli* strains. Its reversibly colonizing derivative may provide a versatile research tool for mucosal bacterial conditioning or compound delivery without permanent colonization.

grant KAW 2012-0184), Kempe foundation (<http://www.kempe.com>; grant JCK-1422) and the Swedish Research Council (<http://www.vr.se>; grant K2014-57X-22450-01-5). SB was supported by a Boehringer Ingelheim Foundation (<https://www.bifonds.de>) PhD scholarship. SBH was supported by an Alfonso Martin Escudero Foundation (<http://www.fundame.org>) postdoctoral scholarship. The funders had no role in study design, data collection and analysis, decision to publish, or preparation of the manuscript.

Competing Interests: The authors have declared that no competing interests exist.

Introduction

The mammalian microbiota influences the biology of its host at many levels. As a consequence, a large number of human conditions are not only shaped by the host's genetic predisposition, external environment and diet, but also the microbiota composition. However, the high microbiota variability between individuals and between different experimental vivaria (often synonymously referred to as "hygiene status") generates a growing demand for new and improved animal models that provide better experimental control over microbiota composition. Numerous studies, spanning many decades, have utilized axenic/ germ-free animals [1] and gnotobiotic animal models with simplified defined microbial compositions [2,3] to greatly advance our current understanding of host-microbial interactions. Comparing host phenotypes in complete or selective absence and presence of microbes can be highly informative. Manipulating simple microbiotas by experimentally increasing the complexity with new immigrants is generally technically easier than permanently eliminating members of an established consortia. Although antibiotic treatments provide a means for the reduction of density and complexity of an already established microbiota, it is incomplete and unsustainable without continued antibiotic administration [4] and can lead to blooms of unsusceptible or resistant microbes. Also the recovery from the antibiotic treatment back to the original state is often incomplete and irreproducible [5], potentially causing persistent dysbiosis.

We recently developed a reversible live microbial colonization model that allowed the fully transient intestinal association of germ-free animals with a live commensal bacterium, the *in vivo* auxotrophic commensal *E. coli* strain K-12 mutant HA107 (relevant genotype: $\Delta alr \Delta dadX \Delta asd$). This mutant strain strictly depends on external supplementation with the bacteria-specific amino acids D-alanine (D-Ala) and *meso*-diaminopimelic acid (Dap) for growth. Both compounds are essential bacterial cell wall (= peptidoglycan) components without which mucopeptide crosslinks between peptidoglycan polymers cannot be formed. Unless supplemented with both compounds, these bacteria cannot synthesize a rigid cell wall and fail to proliferate. Unlike the standard L-amino acids, host metabolism and diet cannot supply intestinal *E. coli* HA107 with these two necessary bacteria-specific amino acids, allowing the quantitative and fully transient controlled association of germ-free animals with (*in vitro*-grown) live microbes followed by the rapid recovery to again-germ-free status [6]. This reversible colonization model has since been successfully used to study the dynamics of intestinal microbiota-induced immunity and disease [6–9].

Although commensal *E. coli* represents a highly relevant early colonizer of the human gut [10] and includes strains with probiotic potential (e.g. *E. coli* Nissle 1920; [11]), the rather lab-adapted K-12 strain is not the most biologically representative *E. coli* strain. Its rough phenotype alone (repeated *in vitro* passaging over decades led to loss-of-function of O-antigen biosynthesis due to a spontaneous mutation), among numerous other mutations, have decreased its intestinal fitness [12].

To allow studies of reversible commensal *E. coli* colonization in a more representative bacterial genetic background we therefore re-constructed the genotype of K-12 strain HA107 in the well-characterized, smooth (complete LPS O-antigen structure), better colonizing, and human-trial-tested benign human commensal strain *E. coli* HS [13,14] by introducing genomic deletions of the genes *alr*, *dadX* and *asd*. Here, we describe the necessary genetic optimizations required in this bacterial genetic background and the improved phenotype of the new bacterial strain *in vitro* and *in vivo*. This improved transient *E. coli* colonization model may be further extended in similar form to other microbial species and utilized for probing a multitude of host responses to bacterial inoculation, or as vector for bacterial metabolite and protein delivery without permanent colonization of the host.

Results

Genetic engineering of fully D-Ala- and Dap-auxotrophic *E. coli* HS

We reconstructed the genotype of the reversible intestinal colonization prototype strain *E. coli* K-12 HA107 [6] in the genetic background of the less laboratory-adapted commensal *E. coli* strain HS [13,14] by deleting the genes *alr* (alanine racemase-1), *dadX* (alanine racemase-2) and *asd* (aspartatesemialdehyde dehydrogenase). We characterized the resulting D-Ala- and Dap-auxotrophic (D-Ala^{aux} Dap^{aux}) strain HS $\Delta alr \Delta dadX \Delta asd$ in an *in vivo* pilot experiment by quantifying fecal bacterial shedding from germ-free mice following gavage with approximately 4×10^{10} bacteria. The intestinal bacterial clearance of HS $\Delta alr \Delta dadX \Delta asd$ was delayed compared to *E. coli* K-12 HA107 (Fig 1A), suggesting a leaky phenotype in this strain background. Others have recently demonstrated that an *alr dadX* double mutation in *E. coli* K-12 confers D-Ala auxotrophy only in methionine-rich complex media, but not in methionine-limited minimal media. Moreover, the abolition of methionine repression of the putative alanine racemase *metC* by mutation of the repressor *metJ* confers D-Ala-independent growth of *alr dadX* mutants in all media [15]. We found that whilst D-Ala auxotrophy revertants with a spontaneous Insertion Element (IS)-1-mediated disruption of *metJ* could readily be selected *in vitro* (Fig 1B), intestinal *ex vivo* re-isolates of *E. coli* HS $\Delta alr \Delta dadX \Delta asd$ remained D-Ala-dependent on rich media (8 clones isolated up to 5 days post gavage were tested).

Thus, the intestinal habitat does not appear to select for D-Ala^{aux} revertants but may be permissive for residual growth of *alr dadX asd* mutants due to methionine limitation, leading to an *in vivo* colonization phenotype solely limited by Dap auxotrophy that we previously found to be leaky [6]. This hypothesis was corroborated by the finding that spontaneous Dap-independent mutants, selected on LB + D-Ala medium, were much more frequent in the HS (mean frequency = 1.5×10^{-5}) than in the K-12 (frequency < 1×10^{-9}) background (Fig 1C, red symbols). To block this escape route, we therefore additionally deleted *metC*, generating the fully D-Ala auxotrophic quadruple mutant HS $\Delta metC \Delta alr \Delta dadX \Delta asd$ (D-Ala^{full-aux} Dap^{aux}). Further selection experiments on LB + Dap media confirmed a marked decrease of D-Ala reversion frequency of HS $\Delta metC \Delta alr \Delta dadX \Delta asd$ compared to HS $\Delta alr \Delta dadX \Delta asd$ and K-12 $\Delta alr \Delta dadX \Delta asd$ (Fig 1C, blue symbols). Thus, in the HS strain background D-Ala auxotrophy confers markedly more effective growth control than Dap auxotrophy. Since the reversion rates on LB media were below the detection limit for many conditions, we additionally employed a more advanced culture method with a better recovery rate for bacterial strains with instable cell wall structure: L-form-like (LFL) media [16], an osmoprotective sucrose- and Mg²⁺-supplemented rich medium. On LFL, D-Ala^{aux} revertants could be selected at roughly 10-fold higher frequencies than on LB media (Fig 1D, blue symbols), with a no longer significant difference between HS $\Delta metC \Delta alr \Delta dadX \Delta asd$ and HS $\Delta alr \Delta dadX \Delta asd$, indicative of a *metC*-independent mechanism. Moreover, on LFL medium we observed an increased frequency of slow-growing Dap revertants of HS $\Delta metC \Delta alr \Delta dadX \Delta asd$ (Fig 1D; compare red symbols in panels C and D). These clones are reminiscent of an older report that showed that *metC* mutation in Dap-auxotrophic *E. coli* can lead to the over-accumulation and incorporation of the Dap homologues meso-lanthionine and L-allo-cystathionine instead of Dap into the cell wall [17]. However, also under the highly permissive stabilizing conditions in LFL medium, D-Ala and Dap auxotrophies combined acted synergistically to reduce double-reversion frequency to very low levels (Fig 1D, black symbols). To allow the detection of such revertants also *ex vivo*, LFL media (un-supplemented and D-Ala/ Dap supplemented) were also used for all following animal experiments.

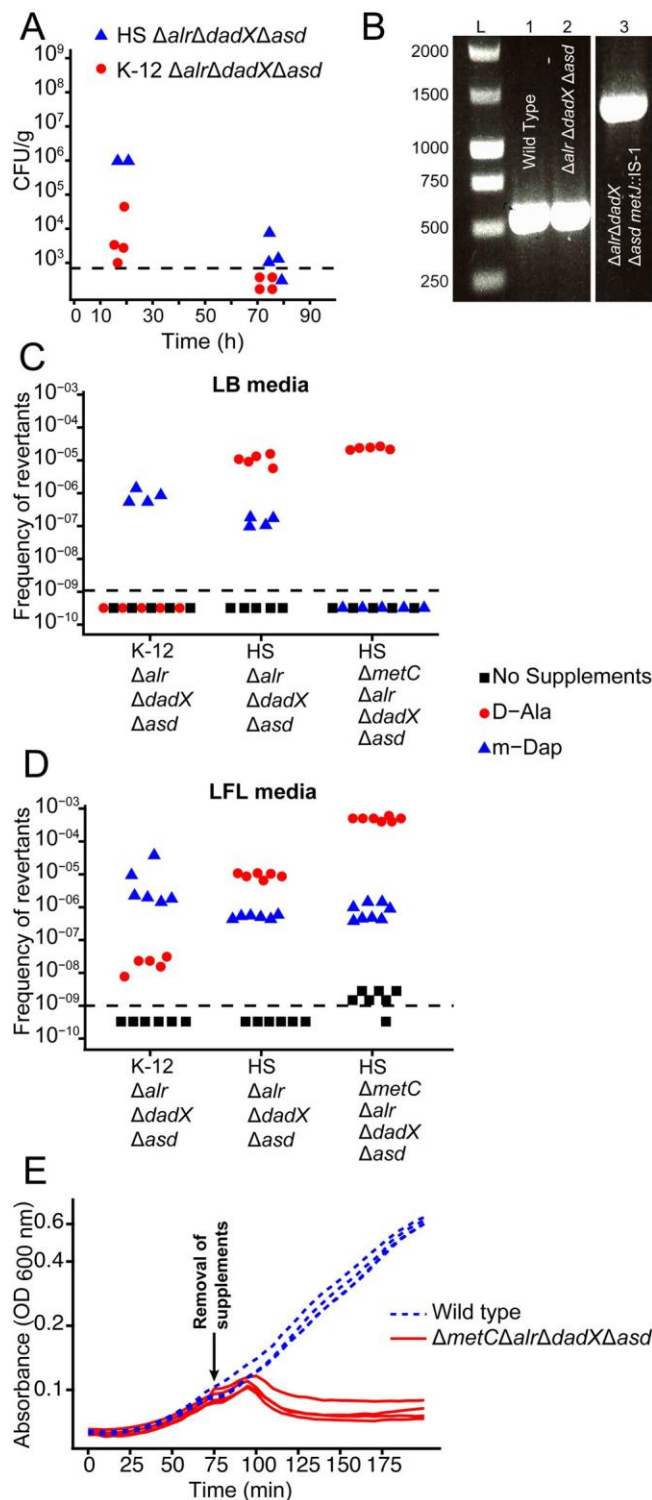


Fig 1. Phenotypic characterization of auxotrophic *E. coli* HS mutants. (A) Fecal bacterial loads from mice that had been gavaged with 10^{10} CFU of *E. coli* HS $\Delta metC \Delta alr \Delta dadX \Delta asd$ (filled blue triangles) or *E. coli* K-12 $\Delta alr \Delta dadX \Delta asd$ (strain HA107; filled red circles), each symbol represents one individual. (B) Insertion sequence (IS-)1 insertion observed in HS $\Delta alr \Delta dadX \Delta asd$ after *in vitro* selection for D-Ala auxotrophy reversion. PCR amplification of the genomic region of *metJ* from *E. coli* HS wild type (lane 1), *E. coli* HS $\Delta alr \Delta dadX \Delta asd$ original stock (lane 2), and *E. coli* HS $\Delta alr \Delta dadX \Delta asd$ D-Ala⁺ revertant selected on LB + Dap (lane 3) reveals a mobile genetic element insertion in the *metJ* ORF that was identified by

sequencing as IS-1. (C, D) Frequency of auxotrophy revertants in K-12 $\Delta alr \Delta dadX \Delta asd$, HS $\Delta alr \Delta dadX \Delta asd$ and HS $\Delta metC \Delta alr \Delta dadX \Delta asd$ selected on LB (C) or LFL (D) containing Dap (blue triangles, D-Ala^{aux} revertants), D-Ala (red circles, Dap^{aux} revertants), or no supplements (black squares; D-Ala^{aux} Dap^{aux} double-revertants). (E) Bacterial growth curves of *E. coli* HS $\Delta metC \Delta alr \Delta dadX \Delta asd$ (solid red line) and wild type (dotted blue line) before and after removal of D-Ala and Dap from the media (arrow indicates time point of removal).

doi:10.1371/journal.pone.0151872.g001

Normal cell wall biochemistry of *in-vitro* grown auxotrophs

Despite its complete dependence on externally supplied D-Ala and Dap, HS $\Delta metC \Delta alr \Delta dadX \Delta asd$ has a normal growth rate (compared to its parental wild-type strain as control) in appropriately supplemented medium (Fig 1E). As confirmation of this conditional phenotype we carried out biochemical cell wall analyses to evaluate if auxotrophic HS $\Delta metC \Delta alr \Delta dadX \Delta asd$ was able to incorporate externally acquired D-Ala and Dap into a peptidoglycan of normal composition. First, we confirmed the complete absence of endogenous D-Ala racemization activity in HS $\Delta metC \Delta alr \Delta dadX \Delta asd$. Alanine racemase activity was quantified by measuring the production of D-Ala from L-Ala in bacterial crude extracts (see [material and methods](#)) by two different techniques: Marfey's (FDAA) derivatization and D-amino acid oxidase (DAAO) assays (Fig 2A and 2B). No residual alanine racemase activity was detectable in HS $\Delta metC \Delta alr \Delta dadX \Delta asd$. Second, we compared the peptidoglycan structure between laboratory-grown (D-Ala and Dap supplemented) HS $\Delta metC \Delta alr \Delta dadX \Delta asd$ and wild type. The mucopeptide profile obtained by UPLC analysis showed that the peptidoglycan structures of both strains were indistinguishable (Fig 2C). Thus, *in-vitro* grown HS $\Delta metC \Delta alr \Delta dadX \Delta asd$, externally supplied with D-Ala and Dap, has a cell wall of normal composition.

Sustained bacterial activity under non-permissive conditions

We have previously shown that the initial gastrointestinal passage of D-Ala/Dap auxotrophs and wild-type *E. coli* is similar [6] showing that the majority of bacteria survive the intestinal passage but cannot sustain colonization without reproduction *in vivo*. D-Ala/Dap deficiency has a highly cell cycle-dependent phenotype. Whereas non-dividing cells are stable, dividing cells at initiation of binary fission undergo a programmed autolytic cell death, an active process that is linked to the cell wall rearrangements preceding binary fission [18]. Whilst autolysis itself is an activity-dependent cellular process, little is known about the impact of D-Ala/Dap-deficiency on bacterial activity prior to autolysis. We therefore used 2-photon microscopy to dynamically track the swimming velocity of D-Ala/Dap-deprived HS $\Delta metC \Delta alr \Delta dadX \Delta asd$ (which is flagellated and motile) over time as a proxy for bacterial energy status and functional integrity of the bacterial cell envelope (into which the flagellar rotor is embedded). Tracking growth of live HS $\Delta metC \Delta alr \Delta dadX \Delta asd$ that had been cultured in medium containing D-Ala/Dap as well as the metabolic peptidoglycan label hydroxycoumarin-carbonyl-amino-D-alanine (HADA; [19]) after transfer to D-Ala/Dap-supplemented and non-supplemented medium, respectively, we could confirm that bacteria in supplemented media were able to proliferate with intact cellular septum formation and division (Fig 3A, bottom panels; Fig 3C top). In sharp contrast non-supplemented bacteria at this stage began to display mid-lateral bulging with cytoplasm membrane protrusion due to a breach in the cell wall rigidity and the consequent loss of turgency (Fig 3A, top panels; Fig 3C bottom panels), later followed by lysis leaving behind empty peptidoglycan sacculi (Fig 3A, middle panels). To study bacterial activity prior to these processes, GFP-expressing bacteria were diluted into D-Ala/Dap-deprived and non-deprived soft agar medium (to slow down swimming for more accurate velocity measurement) and tracked by time-lapse 2-photon microscopy over an observation period between 5 and

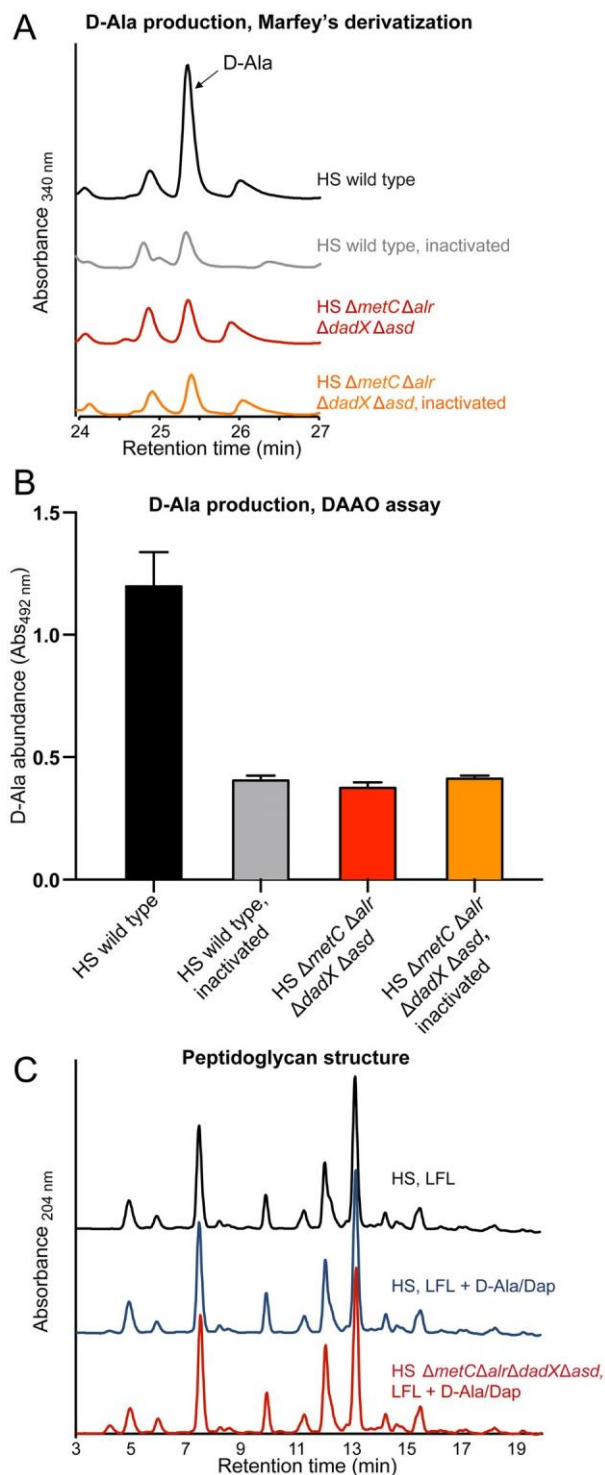


Fig 2. Determination of Ala-racemase activity and peptidoglycan analysis. (A, B). D-Ala production by crude extracts of HS wild-type (black line/ bar) and HS $\Delta metC \Delta alr \Delta dadX \Delta asd$ (red line/ bar) determined by (A) Marfey's derivatization-HPLC analysis and (B) D-amino acid oxidase (DAAO) assay. Heat-inactivated crude extracts of HS wild type (grey line/ bar) and HS $\Delta metC \Delta alr \Delta dadX \Delta asd$ (orange line/ bar) served as negative controls. (C) UPLC peptidoglycan analysis of HS wild type grown in LFL medium with (blue line) and without (black line) supplementation with D-Ala and Dap and HS $\Delta metC \Delta alr \Delta dadX \Delta asd$ (red line) grown in supplemented LFL. LFL: L-form-like medium. Analysis was repeated 3 times; chromatograms from one representative experiment are shown.

doi:10.1371/journal.pone.0151872.g002

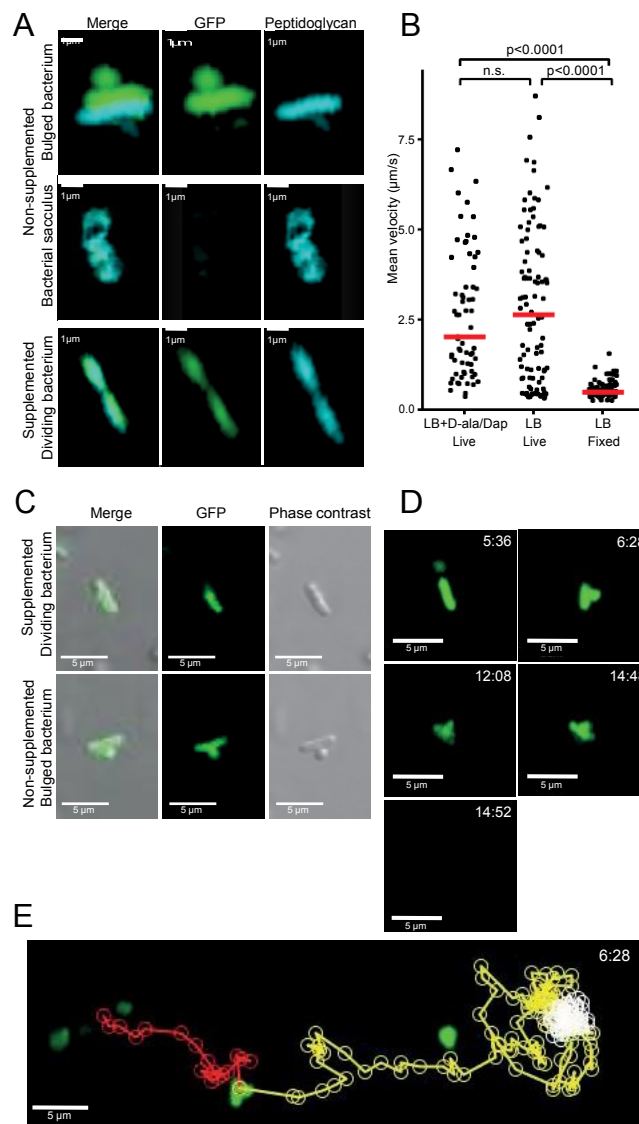


Fig 3. Bacterial activity and survival under non-permissive conditions. (A) Frame shots of a bacterium displaying cellular bulging (top), an empty bacterial sacculus after autolysis (middle), and a dividing bacterium undergoing septum formation with intact cell wall formation (bottom). Green, cytoplasmic eGFP; blue, HADA-labelled cell wall. (B-D) eGFP-expressing (green) bacteria grown in LB medium containing D-Ala and Dap were diluted in soft agar medium containing no supplements (LB, Live), D-Ala and Dap (LB + D-Ala/Dap, Live), or fixed with 4% *para*-formaldehyde (LB, Fixed) on a microscopy slide. Time-lapse videos were recorded using a 2-photon microscope and quantified with Velocity software. (B) Mean velocities of individual HS $\Delta\text{metC} \Delta\text{alr} \Delta\text{dadX} \Delta\text{asd}$ under the three indicated conditions. Statistical analysis: Kruskal-Wallis test with KruskalMC as post hoc. (C) Frame shots of confocal eGFP overlaid with phase contrast images of a D-Ala/Dap-depleted bacterium displaying cellular bulging (bottom), and a D-Ala/Dap-supplemented control of normal morphology (top). (D) Frame shots of bacterium displaying cellular bulging. Top right time stamps indicate time after D-Ala/Dap depletion. (E) Track of the bacterium shown in panel C, before bulge formation (red path), after bulge formation (yellow path), after stopping and until lysis (white path).

doi:10.1371/journal.pone.0151872.g003

60 min after D-Ala/Dap depletion. We observed that HS $\Delta\text{metC} \Delta\text{alr} \Delta\text{dadX} \Delta\text{asd}$ maintained identical mean velocities in non-supplemented medium as in supplemented control medium (Fig 3B). Although in a small proportion (6%) of tracked cells the early stages of autolysis with mid-lateral outer-membrane bulge formation (as previously described for beta-lactam

antibiotic-induced autolysis in [18]; Fig 3D) could be observed, even bulge formation had no immediate impact on motility of the affected cells; bulged cells stopped swimming only approximately 3 min before cell death (sudden release of cytoplasmic GFP within <4 seconds; see example shown in S1 Video and Fig 3D and 3E), having little impact on mean velocity. These data collectively show that the activity and agility of D-Ala/ Dap-deprived HS $\Delta metC \Delta alr \Delta dadX \Delta asd$ remains largely unaffected until immediately before autolytic cell death, closely resembling beta-lactam antibiotic-induced cell death [18].

Transient intestinal mono-colonization

Next, we evaluated the intestinal colonization kinetics of the optimized, fully D-Ala auxotrophic strain by gavaging germ-free mice with identical doses ($4.3 \pm 1.0 \times 10^{10}$ CFU; mean \pm SD in 200 μ L PBS) of the congenic mutants HS Δasd (D-Ala⁺ Dap^{aux}), HS $\Delta metC \Delta alr \Delta dadX$ (D-Ala^{full-aux} Dap⁺), HS $\Delta alr \Delta dadX \Delta asd$ (D-Ala^{aux} Dap^{aux}) and HS $\Delta metC \Delta alr \Delta dadX \Delta asd$ (D-Ala^{full-aux} Dap^{aux}), respectively (Fig 4). The oral-fecal passage and intestinal persistence of the 4 strains was compared over the course of 11 days by quantification of LFL-culturable bacteria from fresh feces. Dap^{aux} single-auxotroph HS Δasd showed prolonged bacterial shedding until at least day 11, indicative of residual *in vivo* proliferation (Fig 4A). In one cage of 4 mice inoculated with HS Δasd , spontaneous occurrence and transmission of a m-Dap auxotrophy revertant led to high-level colonization of all 4 affected individuals (Fig 4A and S1 Fig). Mice that were inoculated with either HS $\Delta metC \Delta alr \Delta dadX$ or HS $\Delta alr \Delta dadX \Delta asd$ returned to germ-free status within 3–6 days, but with highly variable and irregular kinetics (Fig 4B and 4C). In contrast, all animals inoculated with HS $\Delta metC \Delta alr \Delta dadX \Delta asd$ consistently returned to again-germ-free status within 3–4 days (Fig 4D). No double-revertants were recovered *ex vivo* on D-Ala/ Dap-free LFL medium. These data collectively show that the additional deletion of *metC* effectively prevented the occurrence of prolonged intestinal persistence and increased robustness of reversible colonization of germ-free animals.

The early gastrointestinal transit between 5 and 9 hours post inoculation was sampled in 1-hour intervals (S2 Fig), revealing that the peak fecal bacterial densities of HS $\Delta metC \Delta alr \Delta dadX \Delta asd$ remained within an order of magnitude as the density of the gastric inoculum (around 2×10^{10} – 2×10^{11} CFU/g; S2 Fig), indicating that a large fraction of the inoculated bacteria survived the intestinal passage.

Intact IgA-stimulatory activity *in vivo*

Transiently colonizing D-Ala/ Dap-auxotrophic *E. coli* strains were originally developed to study the dynamics and dose-response relationship of commensal bacterial induction of intestinal immunoglobulin A (IgA) [6]. In these studies we showed that the bacterial induction of IgA strongly depended on a mucosal exposure to live *E. coli*, and killed bacteria were highly attenuated in their IgA stimulatory potential [6]. We therefore used the induction of live-*E. coli* HS-specific IgA as a sensitive readout for testing if additional mutation of *metC* negatively affected the IgA stimulatory activity. We compared the intestinal IgA immunogenicity of HS $\Delta metC \Delta alr \Delta dadX \Delta asd$ and its parental strain HS $\Delta alr \Delta dadX \Delta asd$ *in vivo*. The intestinal secretory IgA for this analysis was isolated from the germ-free mice presented in Fig 4B and 4D, 28 days after they had received equivalent doses of HS $\Delta metC \Delta alr \Delta dadX \Delta asd$ and HS $\Delta alr \Delta dadX \Delta asd$, respectively. Quantification of the anti-*E. coli* HS IgA titers in a live bacterial flow cytometry assay (see Methods section and S3 Fig for details) revealed no decrease of IgA induction by *metC* mutation (Fig 5). Thus, the described genetic optimization in *E. coli* HS $\Delta metC \Delta alr \Delta dadX \Delta asd$ improved reversibility of intestinal colonization without compromising its intestinal IgA stimulatory activity.

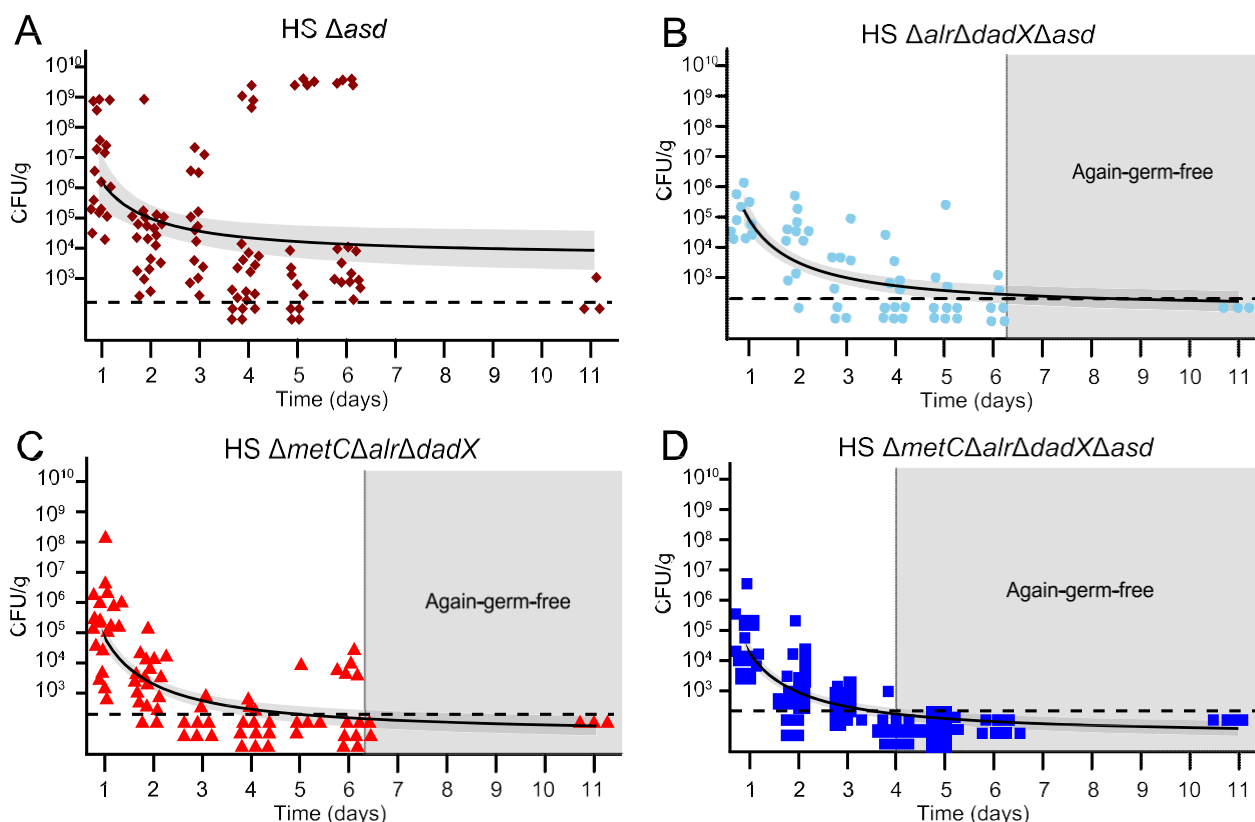


Fig 4. Transient intestinal colonization kinetics of auxotrophic *E. coli* HS. Germ-free mice were inoculated by gavage with $4.3 \pm 1.0 \times 10^{10}$ CFU of either (A) HS Δasd (brown symbols), (B) HS $\Delta alr \Delta dadX \Delta asd$ (light blue symbols), (C) HS $\Delta metC \Delta alr \Delta dadX$ (red symbols), or (D) HS $\Delta metC \Delta alr \Delta dadX \Delta asd$ (blue symbols). Bacterial numbers in fresh feces were quantified at the indicated time points by plating on D-Ala- and Dap-supplemented LFL medium. Each symbol represents one individual. Data of three independent experiments were combined. Light-grey shaded area indicates the time point upon which all mice have regained germ-free status. Black line represents the exponential-decay-fitted curve ($CFU = a1/time$); the dark-grey shaded area around the curve indicated the confidence interval of the fitted curve (95% confidence); horizontal dotted line indicates the lower detection limit.

doi:10.1371/journal.pone.0151872.g004

Discussion

Early attempts to generate *E. coli* strains that can no longer survive in their natural environment (primarily the lower intestinal lumen) date back to the 70s with the purpose to more effectively confine recombinant genetic material to controlled laboratory environments. One of the most prominent “safety” strains from this early era of biotechnology, *E. coli* K-12 Chi1776 (genotype: $F^- \Delta[gal-uvrB]40 \Delta[bioH-asd]29 supE42 thyA142 glnV42 hsdR2 cycB2 cycA1 gyrA25 tonA53 dapD8 minA1 minB2 rfb-2 oms-1 oms-2 \lambda$) [20] combines Dap and thymidine auxotrophies with several other debilitating mutations that make it sensitive to bile salts, UV light, and osmotic stress, resulting in an environmentally very unstable organism that does not survive the gastrointestinal transit in germ-free rats [21]. The less enfeebled Dap and thymidine auxotroph *E. coli* DP50 (genotype: $fhuA53 dapD8 lacY glnX44 \Delta(gal-uvrB)47 \lambda tyrT58 gyrA29 \Delta thyA57 hsdS3$) was designed to be more stable under permissive laboratory conditions. It also better survives the gastrointestinal transit, but persistently colonized germ-free animals in the form of Dap⁺ revertants, if inocula of greater than 10^7 CFU were administered [22], similar to our HS Δasd mono-colonization data in this study (see Fig 4A).

Following a similar strategy we more recently developed an *in vivo* growth-defective strain of K-12 by combining Dap auxotrophy (which alone was insufficient to reliably control germ-

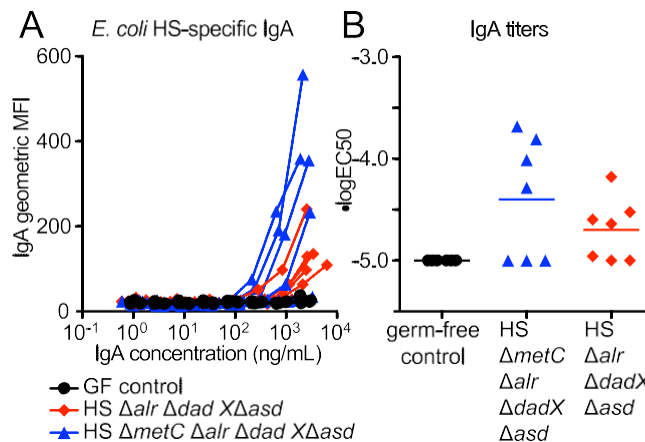


Fig 5. IgA stimulatory activity of transiently colonizing *E. coli* HS $\Delta metC \Delta alr \Delta dadX \Delta asd$. IgA-containing Intestinal lavages were prepared from the animals 28 days post inoculation with *E. coli* HS $\Delta alr \Delta dadX \Delta asd$ (red symbols) and HS $\Delta alr \Delta dadX \Delta asd \Delta metC$ (blue symbols), and germ-free control animals (black symbols). (A) IgA decoration of *E. coli* HS incubated with varying concentrations of intestinal secretory IgA. Geometric means of IgA-fluorescence intensities (IgA geoMFI) were plotted against IgA concentration in the assay, resulting in titration curves. (B) Anti-live-*E. coli* HS IgA antibody titers, expressed as $-\log EC_{50}$, calculated by 4-parameter-curve-fitting of the data shown in (A). Dotted line, lower detection limit.

doi:10.1371/journal.pone.0151872.g005

free intestinal colonization) with the synergistically acting auxotrophy for D-Ala to generate a fully reversibly colonizing K-12 derivative strain HA107 that could be inoculated repeatedly in doses above 10¹⁰ CFU without permanent intestinal colonization [6]. Although HA107 does not escape from its *in vivo* cell wall biosynthesis deficiency, it survives the gastrointestinal transit similarly well as its congenic non-auxotrophic parental strain, making it an effective tool for live bacterial conditioning of germ-free animals [6]. In the present report we further refined this approach by adapting it to the more resilient and less laboratory-adapted commensal strain *E. coli* HS, which required optimization of D-Ala auxotrophy.

Our data demonstrate that in *E. coli* HS and likely also other *Enterobacteriaceae* D-Ala is a more essential metabolite than Dap for peptidoglycan biosynthesis and growth. We continue to combine D-Ala auxotrophy with Dap auxotrophy as a “second hit” strategy, since it was still possible to select *in vitro* (but never *in vivo*) D-Ala^{aux} revertants with $\Delta metC \Delta alr \Delta dadX$ genotype that can grow (albeit poorly) without D-Ala supplementation by an unknown mechanism. Additional work will be required to identify (and prevent) this yet unknown escape pathway. An advantage of purely D-Ala auxotrophic strains would be the entirely cell-wall-specific phenotype and the universal applicability of D-Ala auxotrophy since D-Ala, in contrast to Dap, is an essential metabolite of all known Eubacteria.

A main scientific application of this model is the bacterial conditioning and concomitant “normalization” of microbially shaped body functions (such as the immune system) in germ-free animals without permanent microbial colonization. Many bacterially modulated processes depend on live microbes. We therefore deliberately did not target enterobacterial colonization factors like bile acid resistance (LPS-O-antigen), adhesion (fimbriae etc.) factors or motility that may be important for productive microbe-host interaction in the intestinal mucosa. As a consequence transiently colonizing *E. coli* HS retains a high IgA immunogenicity and survives the intestinal transit. Also for applications using inactivated bacterial preparations or products in biological systems *in vivo* or *in vitro* the use of this model for production of such materials effectively avoids the contamination with surviving bacteria.

In conclusion, we extended a robust transient mono-colonization model from a laboratory strain to a biologically more representative and more resilient intestinal commensal *E. coli* strain. This model can serve as a technology platform for numerous scientific applications. It may be used as a “sterile” biological vector for proteins, metabolites or signaling molecules that need to be delivered directly *in situ* or cannot be stably purified. More generally, it represents a live bacterial conditioning system for axenic animals or other sterile biological systems for the detailed study of host-microbial interactions. Many other future applications are thinkable, and the genetic approach may be extended to other microbial species.

Materials and Methods

Animal colonization experiments

Germ-free animals were re-derived from C57BL/6 mice and maintained germ-free in flexible film isolators in the Genaxen Foundation Clean Mouse Facility (CMF) of the University of Bern as described [23]. Experimental germ-free mice were aseptically transferred to autoclaved sealsafe-plus IVCs under positive pressure (Tecniplast, Italy) in a barrier unit of the Genaxen Clean Mouse Facility. Cage changes were carried out under strictly aseptic conditions. In all experiments animals were provided with sterile mouse chow (Kliba 3437; autoclaved) and autoclaved water *ad libitum*. All experiments were performed according to protocols approved by the Bernese Cantonal Ethical committee for animal experiments and carried out in accordance with Swiss Federal law for animal experimentation (license number BE91/14).

To generate contamination-free bacterial inoculums, D-Ala (200 µg/µl)- and Dap (50 µg/mL)-supplemented autoclaved LB medium in sterile-filter-sealed flasks, was aseptically inoculated from single colonies of the test bacterium and incubated shaking at 150 rpm at 37°C for 16 hours. Bacteria were harvested by centrifugation (10 min, 4816 x g, 4°C) in a sterile aerosol-proof assembly, washed in autoclaved sterile PBS and concentrated to a density of 2×10^{11} CFU/mL in sterile PBS, performed aseptically under a sterile laminar airflow. The bacterial suspensions were aseptically aliquoted in autoclaved plastic tubes and sealed in a sterilized secondary containment. The sterile tubes containing the inocula and germ-free mice were aseptically imported into a sterilized laminar flow hood laid out with sterile surgical drapes, and each animal inoculated with 200 µL of bacterial suspension (containing 4×10^{10} CFU in sterile PBS, at a density of 2×10^{11} CFU/mL) by gavage, carried out wearing sterile surgical gowns and sterile surgical gloves. Fresh fecal pellets were collected aseptically, suspended in sterile PBS, and plated in serial dilutions on D-Ala/ Dap-supplemented or non-supplemented LFL agar and incubated aerobically at 37°C for 2: 24 hours.

Bacterial culture

LB medium (Sigma-Aldrich) was used as the standard growth media. Where required, the following supplements were added to the media: ampicillin (Sigma, 100 µg/mL), tetracycline (Sigma, 12.5 µg/mL), kanamycin (Sigma, 50 µg/mL), meso-diaminopimelic acid (Sigma, 50 µg/mL), D-alanine (Sigma, 200 µg/mL). L-form-like media (LFL) was prepared in two parts: 75.2 g/L brain-heart infusion broth, 20 g/L agar; and separately 10 mM MgSO₄, 200 g/L, sucrose, and mixed in equal parts after autoclaving. The frequencies of auxotrophy revertants were measured by plating stationary phase bacterial culture on LB or LFL agar plates containing D-Ala+Dap, D-Ala only, Dap only, or no supplements and incubated at 37°C. Revertant frequencies are equivalent to the ratio revertant CFU/ total CFU.

Bacterial genetic engineering

All bacterial strains used or generated in this study are specified in [S1 Table](#). The *E. coli* HS wild type strain was kindly provided by Jim Nataro from the University of Virginia School of Medicine, Charlottesville VA, USA and is a replicate of the same bacterial stock that was fully sequenced by Rasko *et al.* [14] (GenBank accession no. CP000802). All deletions were carried out by Lambda Red recombineering. Mutagenesis primer sequences are specified in [S2 Table](#). (i) Strain HA126 ($\Delta asd::tetRA$) was generated by deletion of *asd* using recombineering plasmid pKD46 as described [24] with minor modifications: a *tetRA* recombineering amplicon was amplified from genomic *tetRA* template DNA (isolated from a Tn10-containing bacterial strain) with primers HS-*asd*-mutF and HS-*asd*-mutR, and 2 mM L-arabinose added to express recombinase for 1 hour before the culture was stopped. (ii), Following the same protocol, *alr* in HA126 was deleted using recombinase plasmid pKD46 and a *flp-kan-flp* recombineering cassette amplified with primers HS-*alr*-mutF and HS-*alr*-mutR from template plasmid pKD4, followed by elimination of the *kan* resistance gene using FLP recombinase plasmid pCP20 as previously described [25], resulting in strain HA130 ($\Delta alr::flp \Delta asd::tetRA$); this procedure leaves behind one *flp* site. (iii), following the same procedure, *dadX* was deleted in HA130, using primers HS-*dadX*-mut-F and HS-*dadX*-mutR, to generate strain HA132 ($\Delta alr::flp \Delta dadX::flp-kan-flp \Delta asd::tetRA$). (iv), the *kan* resistance was removed from HA132 using pCP20, and *metC* was deleted using the heat-shock regulated recombinase expression plasmid pSIM6, primers HS-*metC*-mutF and HS-*metC*-mutR, and the *flp-kan-flp* template plasmid pKD4, following a recently published protocol [26], resulting in strain HA416 ($\Delta metC::flp-kan-flp \Delta alr::flp \Delta dadX::flp \Delta asd::tetRA$). (v), To generate strain HA417 ($\Delta metC::flp-kan-flp \Delta alr::flp \Delta dadX::flp$), the $\Delta asd::tetRA$ allele in HA416 was replaced with the wild-type *asd* allele, using pSIM6 in combination with a recombineering amplicon produced with primers *asd_F* and *asd_B* and wild type genomic template DNA. HA417 was isolated by positive selection of recombinants on LB containing D-Ala. All deletions were verified phenotypically and by control PCR (control primers specified in [S2 Table](#)). Plasmids (see [S1 Table](#) for a complete list) were introduced by electroporation following standard protocols.

Insertion element identification

The genomic *metJ* region of *E. coli* HS was amplified by PCR using primers *metJ_F* and *metJ_B* ([S2 Table](#)), and Sanger sequenced (Microsynth, TWON, Switzerland) using the same primers. The obtained sequences were compared using BLAST with the nr database and the best match was considered to be the correct.

Two-photon and confocal microscopy

A subculture of HS $\Delta metC \Delta alr \Delta dadX \Delta asd$ harboring eGFP expression plasmid pM979 was grown in LB containing D-Ala, Dap, ampicillin, 50 nM HADA, [27] for approximately 3 hours to reach $OD_{600} = 0.6$ and cooled down on ice. Small aliquots of this culture were sedimented by centrifugation and re-suspended 1:100 in fresh medium containing ampicillin, and either (i) no further chemicals, (ii) D-Ala and Dap, or (III) 4% *para*-formaldehyde (end concentration), and poured on a microscopy slide with matching media covered with low-melting-point 0.1% agarose. Time lapse videos were recorded immediately using an Olympus BX50WI fluorescence 15 microscope (three z-stacks with 3 μm spacing, 150 μm square sections, fast mode) attached to a 2-PM scanner (TrimScope system, LaVision Biotec, Bielefeld, Germany) equipped with a 20X objective (numerical aperture = 0.95) and heated stage. Image sequences were transformed into volume-rendered four-dimensional movies using Volocity software (Improvision), which was also used for semi-automated tracking of bacteria motility. From the

acquired videos 85 (supplemented) or 100 (non-supplemented and PFA) bacterial tracks were selected based on duration (2:10 consecutive time points, 3.3 frames/s), size (2:3 μm diameter) and the intensity of the objects (more than 1900 voxels). These tracks were imported into R and processed into plots using ggplot2 and dplyr.

For confocal microscopy, identically prepared bacterial preparations were imaged with a Zeiss LSM 710 confocal laser-scanning microscope, time-lapse movies of GFP and Phase contrast (three z-stacks with 3 μm spacing, 150 μm square sections, fast mode channels) were recorded simultaneously using a beam splitter with a 40X oil objective (numerical aperture = 1.3) and heated stage. Image sequences were transformed using Imaris software.

Enzyme-linked immune sorbent assay (ELISA) for IgA

Total concentrations of IgA in mouse intestinal lavage were determined by sandwich ELISA. Coating antibodies were goat anti-mouse IgA (Southern Biotech, 1040–01); detection antibodies were horseradish peroxidase (HRP)–conjugated goat-anti-mouse IgA (A3673, Sigma). Purified monoclonal isotype control IgA (Becton Dickinson, clone M18-254, 553476) served as standard.

Live bacterial flow cytometry and IgA response quantification

Live bacterial flow cytometry quantification of *E. coli* HS-specific Immunoglobulin (Ig)A titers (expressed as EC_{50} values) were carried out previously described [6]. Briefly, *E. coli* HS was grown in 0.2 μm membrane-filtered LB broth overnight at 37°C without shaking. 1 mL of culture was gently pelleted for 3 min at 4816 \times g in a Heraus Fresco 21 centrifuge and washed 3 times with sterile-filtered 2% BSA/0.005% NaN_3 /PBS before re-suspending at a density of approximately 10^7 bacteria/mL. Intestinal IgA lavages were collected by rinsing the small intestine with 5 mL of 1% soybean-trypsin-inhibitor/0.05 M EDTA/PBS. The intestinal washes were then centrifuged at 4816 \times g, 20 min; the supernatant sterile-filtered to remove bacteria-sized particles, and serially diluted in sterile-filtered 2% BSA/0.005% NaN_3 /PBS. Serially diluted IgA-solution and bacterial suspension were mixed 1:1 and incubated at 4°C for 1 h. Bacteria were washed twice in sterile-filtered 2% BSA/0.005% NaN_3 /PBS before re-suspending in monoclonal FITC-anti-mouse IgA (clone 10.3; Becton Dickinson). After 1 h incubation at 4°C the bacteria were washed twice with sterile-filtered 2% BSA/0.005% NaN_3 /PBS and re-suspended in 2% *para*-formaldehyde/PBS for acquisition on a FACSArray SORP flow cytometer (Becton Dickinson) using FSc and SSc parameters in logarithmic mode. GeoMean fluorescence intensities were plotted against IgA concentrations analyzed using FlowJo software (Treestar, USA) and Graphpad prism software 4-parameter curve fitting to calculate EC_{50} titers as previously described [6] and summarized in [S3 Fig](#).

Isolation of peptidoglycan and UPLC analysis

To isolate murein sacculi, cultures were pelleted, resuspended in 2 mL of medium and slowly added to 2 mL of boiling 10% SDS while stirring. After boiling for 2 h, they were stirred overnight at room temperature. Cell wall material was then pelleted by ultracentrifugation (60'000 rpm, 10 min) and washed with purified water to remove SDS. Samples were digested with pronase E (100 $\mu\text{g/mL}$) in 10 mM Tris-HCl, pH 7.5, 1 h at 60°C to remove Braun's lipoprotein. After addition of SDS to a final concentration of 1% (w/v), reactions were heat-inactivated and detergent was removed by washing in MQ water. Purified peptidoglycan was re-suspended in 100 μL of 50 mM NaPO_4 buffer pH 4.9 and treated with 100 $\mu\text{g/mL}$ muramidase (Cellosyl) for 16 h at 37°C. Muramidase digestion was stopped by boiling and coagulated proteins were removed by 10 min centrifugation at 14'000 rpm. Supernatants were reduced by adding sodium borate pH 9.5 and sodium borohydride to a final concentration of 10 mg/mL and

incubating at RT for 30 min. Finally, samples were adjusted to pH 3.5 with phosphoric acid. Muropeptides were separated in a 20-min linear gradient of 50 mM NaPO₄, pH 4.35, to 50 mM NaPO₄, pH 4.95, and 15% (v/v) methanol on an AQUITY ultra-performance liquid chromatography (UPLC) BEHC18 column (130 Å, 1.7 µm, 2.1 mm × 150 mm; Waters, USA), and detected by absorption at wavelength 204 nm.

Alanine racemase activity assay

Cleared cell lysates were prepared from cultures and assayed for alanine racemase activity. Lysates were prepared from cultures grown in LB supplemented with D-Ala and Dap (OD600 was measured for normalizing the number of cells in each sample). Cells were collected by centrifugation and then washed twice with ice-cold HEPES 50 mM pH 7.5. By three passages through a French press re-suspended cells were disrupted and then lysates were cleared of cell debris and membranes by centrifugation at 20'000 rpm for 30 min at 4°C. Alanine racemization assays (adapted from [28,29]) were performed in 1.5 mL Eppendorf tubes in a total volume of 200 µL by adding 160 µL of the soluble fraction of crude extract, L-Ala and pyridoxal phosphate (PLP) at 50 mM and 20 µM respectively (final concentrations). After incubation at 37°C for 45 min the reaction was quenched by adding 40 µl of 2 M HCl.

L-FDAA (1-fluoro-2-4-dinitrophenyl-5-L-alanine amide, Marfey's reagent, Thermo Scientific) was used for the derivatization of amino acids [28,30]. First quenched enzyme reactions were neutralized with 40 µL of 2 M NaOH and then a 50 µL aliquot of the sample was mixed with 100 µL Marfey's reagent (0.5% solution in acetone) and 20 µL 1 M NaHCO₃. The derivatization mixture was incubated at 80°C for 10 min and the reaction was stopped with 2 M HCl. After cooling down to room temperature samples were diluted with 200 µL of a mixture 9:1 of buffers A (triethylamine-phosphate 50 mM pH 3) and B (triethylamine-phosphate 50 mM pH3, 40% acetonitrile). Samples were filtered and 100 µL were injected in the HPLC (high-pressure liquid chromatography). Amino acids were separated in a 45 min linear gradient of triethylamine phosphate/acetonitrile with an Aeris peptide column (250 x 4.6 mm; 3.6 µm particle size, Phenomenex, USA) and detected at Abs. 340 nm. D-Ala and L-Ala were used as standards of to establish retention times.

DAAO reaction coupled to peroxidase and 2,3-diaminophenazine was performed for detection of the D-Ala produced by the *in vitro* as previously described [31]. The formation of the colorimetric product was measured at 492 nm.

Data analysis and statistical analysis

All data analysis was done using the R 3.1.1 statistical program [32] and the ggplot2 [33], dplyr [34] and pgirmess [35] packages. All scripts can be downloaded from <https://github.com/cuencam/HA416>, and data are available on request. Statistical tests are specified in the figure legends.

Supporting Information

S1 Fig. Selection of spontaneous *asd* auxotrophy revertants in *E. coli* HS Δasd -inoculated animals. 4 Germ-free mice (also depicted in Fig 4A) were inoculated by gavage with approximately 4×10^{10} CFU of HS Δasd . (A) CFU counts from each mouse over time, each individual highlighted in a different color. (B) PCR amplification of the genomic *asd* region of HS wild-type (lane 1), HS Δasd (exact genotype: $\Delta asd::tetRA$; longer PCR fragment verifies allelic exchange of *asd* by *tetRA* cassette) original stock (lane 2), and HS Δasd re-isolate from mouse 3 (verifying the correct genotype of this revertant), verifying colonization with a revertant clone of the correct inoculated. Lane L contains molecular ladder. (C, D) Colony morphology of 4 revertant clones re-isolated

from mouse 3 on day 2 (clone 1) and day 3 (clone 2), mouse 1 on day 3 (clone 3), and mouse 2 on day 3 (clone 4) on supplemented (C) and unsupplemented (D) LFL agar plates.
(PDF)

S2 Fig. Early intestinal colonization kinetics of auxotrophic *E. coli* HS. Early time points of the experiment presented in main Fig 4 are shown. Germ-free mice were inoculated by gavage with around 4×10^{10} CFU of either (A) HS Δasd (brown symbols), (B) HS $\Delta alr \Delta dadX \Delta asd$ (light blue symbols), (C) HS $\Delta metC \Delta alr \Delta dadX$ (red symbols), or (D) HS $\Delta metC \Delta alr \Delta dadX \Delta asd$ (blue symbols). Each symbol represents one individual; data are combined from three independent experiments. Black line represents the exponential-decay-fitted curve ($CFU = a1/time$) with the 95% confidence interval shown as dark-grey shaded area. The vertical gray line marks the time point at which all individuals have reached fecal bacterial densities 100-fold below the mean inoculum density (from top of light gray area).
(PDF)

S3 Fig. Live bacterial FACS analysis and titer calculations. IgA-stained bacteria were analyzed using a BD FACSArray SORP and acquired data were exported to Treestar FlowJo. (A) Gating procedure: Single bacteria were defined as forward-scatter-width-(FSC-W)-low events. Forward scatter area (FSC-A) and Side scatter area (SSC-A) were used to eliminate electrical noise, bubbles and debris from the analysis. Gating Red (APC channel)-low events allowed to reduce unspecific fluorescence. Three serial 3-fold dilutions of a representative positive sample are shown. (B) Three representative histograms of FITC-anti-IgA resulting from 3 serial dilutions and their overlay are shown. (C) Titration curves shown in main Fig 5A. Geometric mean fluorescent intensities (geoMFI; accounting for the Log Normal distribution of fluorescence data) of IgA bacterial FACS staining (y-axis) was plotted against IgA concentration in the assay (x-axis) (determined by isotype-specific sandwich ELISA). (D) 4-parameter curve fitting of the data shown panel C and main Fig 5A. Graphpad Prism 6 software was used to fit 4-parameter logistic curves to the data. Equation: $Y = Bottom + (Top - Bottom) / (1 + 10^{((LogEC50 - X) * HillSlope)})$. (E)—LogEC50 IgA titers. The LogEC50 values were extracted from the curve parameters, which when anti-logged corresponds to the concentration of IgA required to give half-maximum IgA binding. The —LogEC50 titer thus corresponds to the $\text{Log}(1/[IgA]_{\text{giving 50\% binding}})$ the dotted line to the lower detection limit.
(PDF)

S1 Table. Bacterial strains and plasmids.
(DOCX)

S2 Table. Primers used in this study.
(DOCX)

S1 Video. Representative example of a swimming bacterium undergoing bulging and autolysis. The red circle highlights the bacterium of interest; white arrow indicates the moment at which the cells starts bulging. After approximately 7 min the bacterium stops active movement, followed 3 min later by autolysis, causing an instant drop of cytoplasmatic GFP signal as it is released into the extracellular medium. The video is part of the data shown in Fig 4.
(MOV)

Acknowledgments

We thank all laboratory members, Emma Slack and Maria Balmer for reading and commenting on the manuscript. We thank the Clean Mouse Facility of the Department of Clinical Research,

Kathy McCoy, and all members of the CMF Curatorium of the University of Bern for support of the gnotobiotic animal work. We thank Jens Stein and Britta Engelhardt from the Theodor Kocher Institute for the support with the two-photon microscope and Fabian Blank, the MIC and the LCI Core Facility for the support with the LSM 710 Confocal microscope at University of Bern.

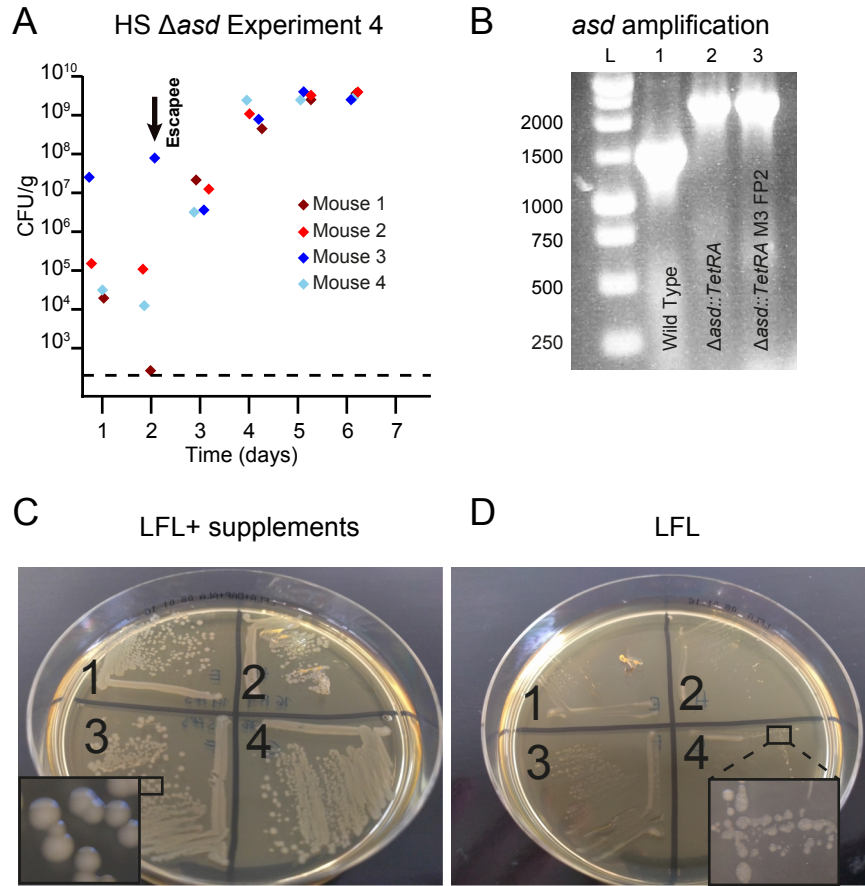
Author Contributions

Conceived and designed the experiments: SH MC SPP EK MSV YVB FC FMC. Performed the experiments: MC SPP SB FB SBH FMC. Analyzed the data: SH MC SPP SB SBH FC FMC. Contributed reagents/materials/analysis tools: MSV YVB. Wrote the paper: MC SH.

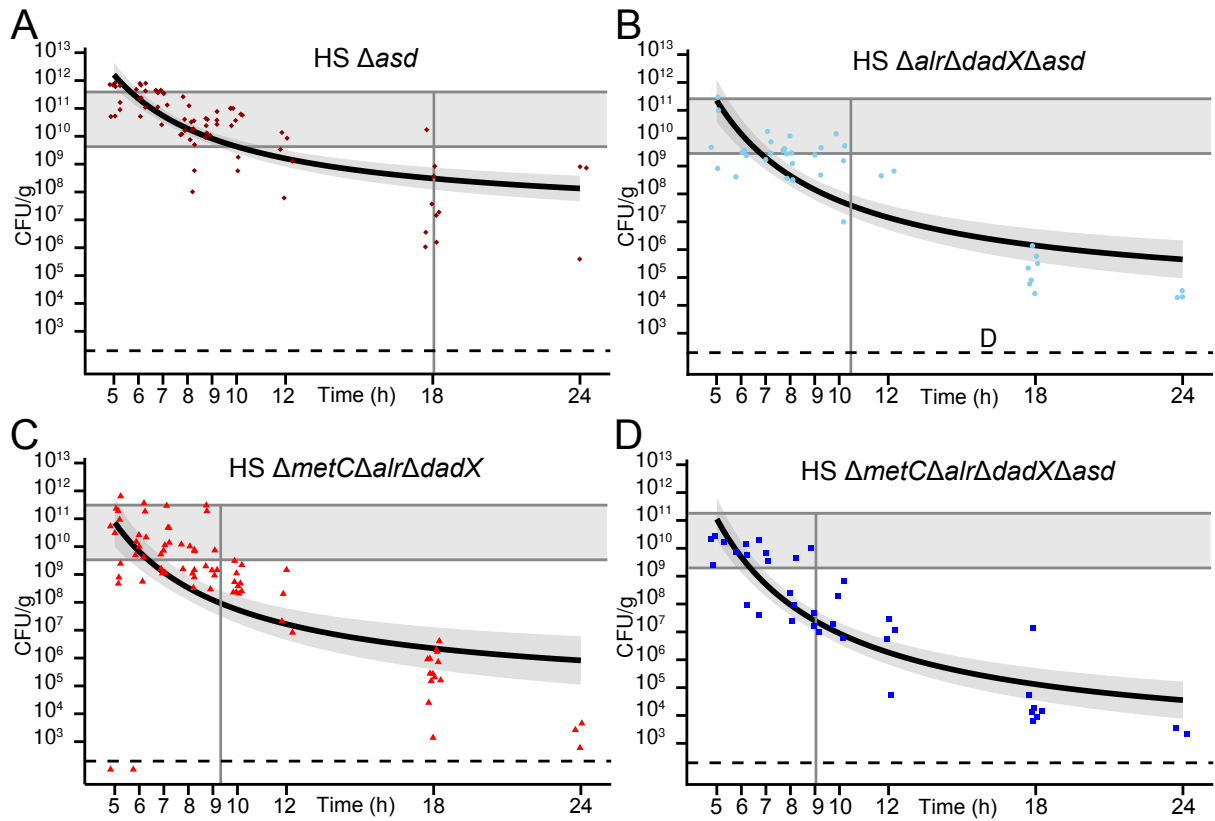
References

1. Smith K, McCoy KD, Macpherson AJ. Use of axenic animals in studying the adaptation of mammals to their commensal intestinal microbiota. *Semin Immunol*. 2007; 19: 59–69. doi: [10.1016/j.smim.2006.10.002](https://doi.org/10.1016/j.smim.2006.10.002) PMID: [17118672](https://pubmed.ncbi.nlm.nih.gov/17118672/)
2. Macpherson AJ, McCoy KD. Standardised animal models of host microbial mutualism. *Mucosal Immunol*. 2014; 8: 476–486. doi: [10.1038/mi.2014.113](https://doi.org/10.1038/mi.2014.113) PMID: [25492472](https://pubmed.ncbi.nlm.nih.gov/25492472/)
3. Faith JJ, Ahern PP, Ridaura VK, Cheng J, Gordon JL. Identifying gut microbe-host phenotype relationships using combinatorial communities in gnotobiotic mice. *Sci Transl Med*. 2014; 6: 220ra11. doi: [10.1126/scitranslmed.3008051](https://doi.org/10.1126/scitranslmed.3008051) PMID: [24452263](https://pubmed.ncbi.nlm.nih.gov/24452263/)
4. Reikvam DH, Erofeev A, Sandvik A, Grcic V, Jahnsen FL, Gaustad P, et al. Depletion of murine intestinal microbiota: effects on gut mucosa and epithelial gene expression. *PLoS ONE*. 2011; 6: e17996. doi: [10.1371/journal.pone.0017996](https://doi.org/10.1371/journal.pone.0017996) PMID: [21445311](https://pubmed.ncbi.nlm.nih.gov/21445311/)
5. Dethlefsen L, Relman DA. Incomplete recovery and individualized responses of the human distal gut microbiota to repeated antibiotic perturbation. *Proc Natl Acad Sci USA*. 2011; 108 Suppl 1: 4554–4561. doi: [10.1073/pnas.1000087107](https://doi.org/10.1073/pnas.1000087107) PMID: [20847294](https://pubmed.ncbi.nlm.nih.gov/20847294/)
6. Hapfelmeier S, Lawson MAE, Slack E, Kirundi JK, Stoeckl M, Heikenwalder M, et al. Reversible microbial colonization of germ-free mice reveals the dynamics of IgA immune responses. *Science*. 2010; 328: 1705–1709. doi: [10.1126/science.1188454](https://doi.org/10.1126/science.1188454) PMID: [20576892](https://pubmed.ncbi.nlm.nih.gov/20576892/)
7. Fritz JH, Rojas OL, Simard N, McCarthy DD, Hapfelmeier S, Rubino S, et al. Acquisition of a multifunctional IgA+ plasma cell phenotype in the gut. *Nature*. 2012; 481: 199–203. doi: [10.1038/nature10698](https://doi.org/10.1038/nature10698)
8. Balmer ML, Slack E, de Gottardi A, Lawson MAE, Hapfelmeier S, Miele L, et al. The liver may act as a firewall mediating mutualism between the host and its gut commensal microbiota. *Sci Transl Med*. 2014; 6: 237ra66–237ra66. doi: [10.1126/scitranslmed.3008618](https://doi.org/10.1126/scitranslmed.3008618) PMID: [24848256](https://pubmed.ncbi.nlm.nih.gov/24848256/)
9. Balmer ML, Schürch CM, Saito Y, Geuking MB, Li H, Cuenca M, et al. Microbiota-derived compounds drive steady-state granulopoiesis via MyD88/TICAM signaling. *J Immunol*. 2014; 193: 5273–5283. doi: [10.4049/jimmunol.1400762](https://doi.org/10.4049/jimmunol.1400762) PMID: [25305320](https://pubmed.ncbi.nlm.nih.gov/25305320/)
10. Rautava S, Luoto R, Salminen S, Isolauri E. Microbial contact during pregnancy, intestinal colonization and human disease. *Nat Rev Gastroenterol Hepatol*. 2012; 9: 565–576. doi: [10.1038/nrgastro.2012.144](https://doi.org/10.1038/nrgastro.2012.144) PMID: [22890113](https://pubmed.ncbi.nlm.nih.gov/22890113/)
11. Schultz M. Clinical use of *E. coli* Nissle 1917 in inflammatory bowel disease. *Inflamm Bowel Dis*. 2008; 14: 1012–1018. PMID: [18240278](https://pubmed.ncbi.nlm.nih.gov/18240278/)
12. Browning DF, Wells TJ, França FLS, Morris FC, Sevastyanovich YR, Bryant JA, et al. Laboratory adapted *Escherichia coli* K-12 becomes a pathogen of *Caenorhabditis elegans* upon restoration of O antigen biosynthesis. *Mol Microbiol*. 2013; 87: 939–950. doi: [10.1111/mmi.12144](https://doi.org/10.1111/mmi.12144) PMID: [23350972](https://pubmed.ncbi.nlm.nih.gov/23350972/)
13. Levine MM, Bergquist EJ, Nalin DR, Waterman DH, Hornick RB, Young CR, et al. *Escherichia coli* strains that cause diarrhoea but do not produce heat-labile or heat-stable enterotoxins and are non-invasive. *Lancet*. 1978; 1: 1119–1122. PMID: [77415](https://pubmed.ncbi.nlm.nih.gov/77415/)
14. Rasko DA, Rosovitz MJ, Myers GSA, Mongodin EF, Fricke WF, Gajer P, et al. The pangenome structure of *Escherichia coli*: comparative genomic analysis of *E. coli* commensal and pathogenic isolates. *J Bacteriol*. 2008; 190: 6881–6893. doi: [10.1128/JB.00619-08](https://doi.org/10.1128/JB.00619-08) PMID: [18676672](https://pubmed.ncbi.nlm.nih.gov/18676672/)
15. Kang L, Shaw AC, Xu D, Xia W, Zhang J, Deng J, et al. Upregulation of MetC is essential for D-alanine-independent growth of an *alr*/*dadX*-deficient *Escherichia coli* strain. *J Bacteriol*. 2011; 193: 1098–1106. doi: [10.1128/JB.01027-10](https://doi.org/10.1128/JB.01027-10) PMID: [21193606](https://pubmed.ncbi.nlm.nih.gov/21193606/)
16. Glover WA, Yang Y, Zhang Y. Insights into the molecular basis of L-form formation and survival in *Escherichia coli*. *PLoS ONE*. 2009; 4: e7316. doi: [10.1371/journal.pone.0007316](https://doi.org/10.1371/journal.pone.0007316) PMID: [19806199](https://pubmed.ncbi.nlm.nih.gov/19806199/)

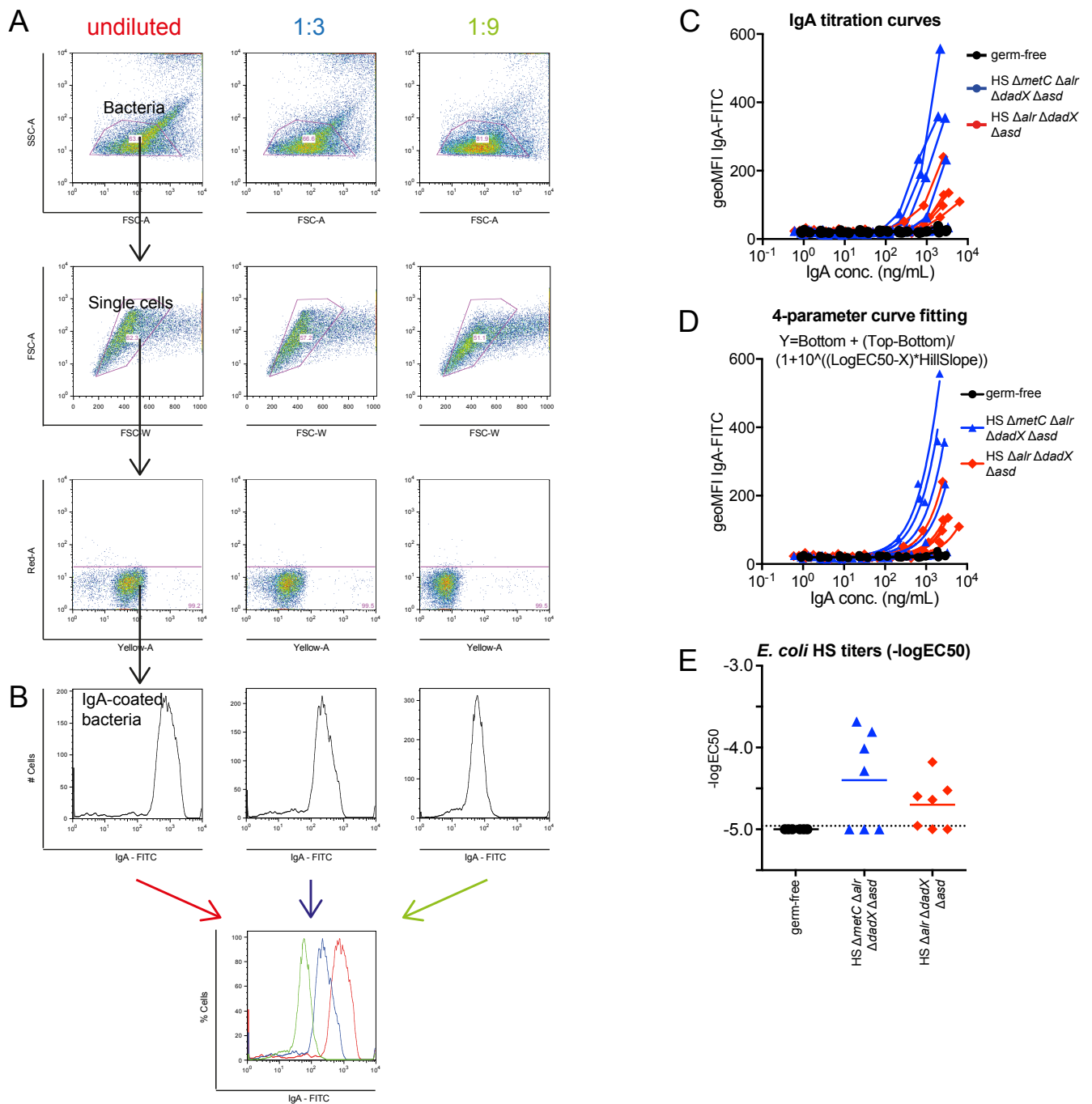
17. Richaud C, Mengin-Lecreux D, Pochet S, Johnson EJ, Cohen GN, Marlière P. Directed evolution of biosynthetic pathways. Recruitment of cysteine thioethers for constructing the cell wall of *Escherichia coli*. *J Biol Chem*. 1993; 268: 26827–26835. PMID: [8262915](#)
18. Yao Z, Kahne D, Kishony R. Distinct single-cell morphological dynamics under beta-lactam antibiotics. *Mol Cell*. 2012; 48: 705–712. doi: [10.1016/j.molcel.2012.09.016](#) PMID: [23103254](#)
19. Kuru E, Tekkam S, Hall E, Brun YV, Van Nieuwenhze MS. Synthesis of fluorescent D-amino acids and their use for probing peptidoglycan synthesis and bacterial growth in situ. *Nat Protoc*. 2015; 10: 33–52. doi: [10.1038/nprot.2014.197](#) PMID: [25474031](#)
20. Curtiss R 3rd. Modified microorganisms and method of preparing and using same. US Patent 1980; US4190495 A.
21. Wells CL, Johnson WJ, Kan CM, Balish E. Inability of debilitated *Escherichia coli* chi 1776 to colonise germ-free rodents. *Nature*. 1978; 274: 397–398. PMID: [353563](#)
22. Ducluzeau R, Ladiré M, Raibaud P. [Implantation of a mutant of *Escherichia coli* requiring diaminopimelic acid in the digestive tract of gnotobiotic mice]. *Ann Inst Pasteur Microbiol*. 1986; 137A: 79–87. PMID: [3314677](#)
23. Macpherson AJ, Geuking MB, Kirundi J, Collins S, McCoy KD. Gnotobiotic and Axenic Animals. *Encyclopedia of Microbiology*. Elsevier; 2009. pp. 237–246. doi: [10.1016/B978-012373944-5.00215-7](#)
24. Datsenko KA, Wanner BL. One-step inactivation of chromosomal genes in *Escherichia coli* K-12 using PCR products. *Proc Natl Acad Sci USA*. 2000; 97: 6640–6645. doi: [10.1073/pnas.120163297](#) PMID: [10829079](#)
25. Cherepanov PP, Wackernagel W. Gene disruption in *Escherichia coli*: TcR and KmR cassettes with the option of Flp-catalyzed excision of the antibiotic-resistance determinant. *Gene*. 1995; 158: 9–14. PMID: [7789817](#)
26. Thomason L, Court DL, Bubunenko M, Costantino N, Wilson H, Datta S, et al. Recombineering: genetic engineering in bacteria using homologous recombination. *Current protocols in molecular biology* / edited by Ausubel FM [et al]. 2007; Chapter 1: Unit 1.16. doi: [10.1002/0471142727.mb0116s78](#)
27. Kuru E, Hughes HV, Brown PJ, Hall E, Tekkam S, Cava F, et al. In Situ probing of newly synthesized peptidoglycan in live bacteria with fluorescent D-amino acids. *Angew Chem Int Ed Engl*. 2012; 51: 12519–12523. doi: [10.1002/anie.201206749](#) PMID: [23055266](#)
28. Radkov AD, Moe LA. Amino acid racemization in *Pseudomonas putida* KT2440. *J Bacteriol. American Society for Microbiology*; 2013; 195: 5016–5024. doi: [10.1128/JB.00761-13](#)
29. Arias CA, Weisner J, Blackburn JM, Reynolds PE. Serine and alanine racemase activities of VanT: a protein necessary for vancomycin resistance in *Enterococcus gallinarum* BM4174. *Microbiology (Reading, Engl)*. 2000; 146 (Pt 7): 1727–1734.
30. Marfey P. Determination of D-amino acids. II. Use of a bifunctional reagent, 1,5-difluoro-2,4-dinitrobenzene. *Carlsberg Research Communications*. Springer-Verlag; 1984; 49: 591–596. doi: [10.1007/BF02908688](#)
31. Espaillet A, Carrasco-López C, Bernardo-García N, Pietrosevoli N, Otero LH, Álvarez L, et al. Structural basis for the broad specificity of a new family of amino-acid racemases. *Acta Crystallogr D Biol Crystallogr*. 2014; 70: 79–90. doi: [10.1107/S1399004713024838](#) PMID: [24419381](#)
32. R Development Core Team. R: A Language and Environment for Statistical Computing. R Foundation for Statistical Computing 2014. <http://www.R-project.org/>. Accessed 01 Aug 2015.
33. Wickham H. ggplot2: Elegant Graphics for Data Analysis. Springer New York; 2009. Available: <http://had.co.nz/ggplot2/book>.
34. Wickham H, Francois R. dplyr: A Grammar of Data Manipulation. In: R package version 0.4.1. 2015. Available: <http://CRAN.R-project.org/package=dplyr>. Accessed 17 Jul 2015.
35. Giraudoux P. pgirmess: Data Analysis in Ecology. In: R package version 1.6.2. 2015. Available: <http://CRAN.R-project.org/package=pgirmess>. Accessed 17 Jul 2015.



S1 Fig. Selection of spontaneous *asd* auxotrophy revertants in *E. coli* HS Δasd -inoculated animals. 4 Germ-free mice (also depicted in [Fig 4A](#)) were inoculated by gavage with approximately 4×10^{10} CFU of HS Δasd . (A) CFU counts from each mouse over time, each individual highlighted in a different color. (B) PCR amplification of the genomic *asd* region of HS wild-type (lane 1), HS Δasd (exact genotype: $\Delta asd::tetRA$; longer PCR fragment verifies allelic exchange of *asd* by *tetRA* cassette) original stock (lane 2), and HS Δasd re-isolate from mouse 3 (verifying the correct genotype of this revertant), verifying colonization with a revertant clone of the correct inoculated. Lane L contains molecular ladder. (C, D) Colony morphology of 4 revertant clones re-isolated



S2 Fig. Early intestinal colonization kinetics of auxotrophic *E. coli* HS. Early time points of the experiment presented in main Fig 4 are shown. Germ-free mice were inoculated by gavage with around 4×10^{10} CFU of either (A) HS Δasd (brown symbols), (B) HS $\Delta alr \Delta dadX \Delta asd$ (light blue symbols), (C) HS $\Delta metC \Delta alr \Delta dadX$ (red symbols), or (D) HS $\Delta metC \Delta alr \Delta dadX \Delta asd$ (blue symbols). Each symbol represents one individual; data are combined from three independent experiments. Black line represents the exponential-decay-fitted curve ($CFU = a1/time$) with the 95% confidence interval shown as dark-grey shaded area. The vertical gray line marks the time point at which all individuals have reached fecal bacterial densities 100-fold below the mean inoculum density (from top of light gray area).
(PDF)



S3 Fig. Live bacterial FACS analysis and titer calculations. IgA-stained bacteria were analyzed using a BD FACSArray SORP and acquired data were exported to Treestar FlowJo. (A) Gating procedure: Single bacteria were defined as forward-scatter-width-(FSC-W)-low events. Forward scatter area (FSC-A) and Side scatter area (SSC-A) were used to eliminate electrical noise, bubbles and debris from the analysis. Gating Red (APC channel)-low events allowed to reduce unspecific fluorescence. Three serial 3-fold dilutions of a representative positive sample are shown. (B) Three representative histograms of FITC-anti-IgA resulting from 3 serial dilutions and their overlay are shown. (C) Titration curves shown in main Fig 5A. Geometric mean fluorescent intensities (geomFI; accounting for the Log Normal distribution of fluorescence data) of IgA bacterial FACS staining (y-axis) was plotted against IgA concentration in the assay (x-axis) (determined by isotype-specific sandwich ELISA). (D) 4-parameter curve fitting of the data shown panel C and main Fig 5A. Graphpad Prism 6 software was used to fit 4-parameter logistic curves to the data. Equation: $Y = Bottom + (Top - Bottom) / (1 + 10^{((LogEC50 - X) * HillSlope)})$. (E) -LogEC50 IgA titers. The LogEC50 values were extracted from the curve parameters, which when anti-logged corresponds to the concentration of IgA required to give half-maximum IgA binding. The -LogEC50 titer thus corresponds to the $\text{Log}(1/[IgA]_{\text{giving 50\% binding}})$ the dotted line to the lower detection limit. (PDF)

Strain/ Plasmid	Relevant genotype/phenotypes/description	Source, Reference
<i>E. coli</i> HS	Wild type	Jim Nataro ^a , [13,14]
HA126	$\Delta asd::tetRA$; Tet ^R	This study
HA130	$\Delta alr::flp \Delta asd::tetRA$; Tet ^R	This study
HA132	$\Delta alr::flp \Delta dadX::flp-kan-flp \Delta asd::tetRA$; Kan ^R Tet ^R	This study
HA416	$\Delta metC::flp-kan-flp \Delta alr::flp \Delta dadX::flp \Delta asd::tetRA$; Kan ^R Tet ^R	This study
HA417	$\Delta alr::flp \Delta dadX::flp \Delta metC::flp-kan-flp$; Kan ^R	This study
pSIM6	Lambda red expression plasmid, Amp ^R	[36]
pKD46	Lambda red expression plasmid, Amp ^R	[24]
pCP20	Recombinase plasmid FLP ⁺ , $\lambda cl857^+$, λp_R Rep ^{ts} , Amp ^R	[25]
pM979	Constitutive GFP-expression plasmid, Amp ^R	W.-D. Hardt ^b , [37]

^aDepartment of Pediatrics, University of Virginia School of Medicine ; Charlottesville VA, USA

^bETH Zurich, Institute for microbiology, Zurich, Switzerland

Additional References:

36. Datta S, Costantino N, Court DL. A set of recombineering plasmids for gram-negative bacteria. *Gene*. 2006;379: 109–115. doi:10.1016/j.gene.2006.04.018
37. Stecher B, Hapfelmeier S, Müller C, Kremer M, Stallmach T, Hardt W-D. Flagella and chemotaxis are required for efficient induction of *Salmonella enterica* serovar Typhimurium colitis in streptomycin-pretreated mice. *Infect Immun*. 2004;72: 4138–4150. doi:10.1128/IAI.72.7.4138-4150.2004

Name	Description	Sequence
HS-<i>asd</i>-mutF	<i>asd tetRA</i> cassette construction forward	ACA TTT ATA CAG CAC ACA TCT TTG CAG GAA AAA AAC GCT TTT AAG ACC CAC TTT CAC ATT
HS-<i>asd</i>-mutR	<i>asd tetRA</i> cassette construction reverse	AGG GGC GGC ATC GCG CCC CAG ATT TAA TGA ATA AAG ATT ACT AAG CAC TTG TCT CCT G
HS-<i>alr</i>-mutF	<i>alr kan</i> cassette construction forward	GAA TTA GGT AAT TAA AGC AAA CAC TTA TCA AGG AAC ACA AGT GTA GGC TGG AGC TGC TTC
HS-<i>alr</i>-mutR	<i>alr kan</i> cassette construction reverse	ACG CCG CAT CCG GCA CAG ACA ATC AAA TAT TAC AGA ACG AGA TAT GAA TAT CCT CCT TA
HS-<i>dadX</i>-mutF	<i>dadX kan</i> cassette construction forward	TCC GGG CCA TTT ACA TGG CGC ACA CAG CTA AG AAA GA GGT GTA GGC TGG AGC TGC TTC
HS-<i>dadX</i>-mutR	<i>dadX kan</i> cassette construction reverse	GCA CCC AGA AGA CGT TGC CTC CGA TCC GGC TTA CAA CAA GCA TAT GAA TAT CCT CCT TA
HS-<i>metC</i>-mutF	<i>metC kan</i> cassette construction forward	TAG TTT AGA CAT CCA GAC GTA TAA AAA CAG GAA TCC CGA CGT GTA GGC TGG AGC TGC TTC
HS-<i>metC</i>-mutR	<i>metC kan</i> cassette construction reverse	AAT AAA ATG TCT GCA AAA TTG TCC AAA AGT GGC AAT GTT ACA TAT GAA TAT CCT CCT TA
<i>asd_F</i>	Forward <i>asd</i> control primer	GCG TGC TAA CAA AGC AGG AT
<i>asd_R</i>	Reverse <i>asd</i> control primer	TCC CGG TAA ATC ATG AAA CA
<i>alr2_F</i>	Forward <i>alr</i> control primer	GAC GGT ACG CCT GAC CTT TA
<i>alr2_R</i>	Reverse <i>alr</i> control primer	GCG ATG GTT CTC CAG GTT TA
<i>dadX2_F</i>	Forward <i>dadX</i> control primer	GTT TCG ATA ACC GCA TTC GT
<i>dadX2_R</i>	Reverse <i>dadX</i> control primer	GCG ATG GTT CTC CAG GTT TA
<i>metC_F</i>	Forward <i>metC</i> control primer	AGGCGACGCTTCTGATTGAA
<i>metC_B</i>	Reverse <i>metC</i> control primer	GCCATGGACTTTCCTGTGGA
<i>metJ_F</i>	Forward <i>metJ</i> control primer	ATCCGGCCTACAAGTTCGTG
<i>metJ_B</i>	Reverse <i>metJ</i> control primer	TGTCGGTGAAATGTCAGGCA

Chapter 2. Simulation of early intestinal infection of *Salmonella enterica* Typhimurium in a disease-independent model

Abstract

Discrimination between intestinal pathogenic and commensal bacteria is a critical function of the mammalian immune system. The ability to recognize pathogenic bacteria and mount an appropriate immune response is crucial for the maintenance of the homeostasis. Here, we formulated the question if there was a different expression pattern from known mucosal biomarkers in response to growth-proficient and *in vivo* growth-deficient (cell wall auxotrophic; CWA) virulent strains of *Salmonella enterica* serovar Typhimurium (Stm), which would allow us to predict possible outcome of the disease. A panel of 86 genes related to intestinal inflammation in inflammatory bowel disease (IBD) was measured in mouse cecum at 6 hours post inoculation with either wild type (WT) Stm, avirulent Stm, CWA Stm, commensal *E. coli* HS or PBS. We built a classifier model to predict the occurrence of inflammation, based on the assumptions that growth proficient *Salmonella* was the only positive condition and all others as antigen or manipulation controls. When tested in an independently generated dataset, the model failed to classify with enough confidence to be used as a predictive tool. This led us to the recognition that at time point 6 h there is a high variability in an interesting biomarker subset that is similar between WT Stm and CWA Stm, but not present in the untreated control, avirulent Stm or *E.coli* HS. Based on this observation the experiment was repeated at 9 h post inoculation and we observed that in response to WT Stm these biomarkers had increased or maintained at the same level, whereas in CWA Stm there was no change. This observation led to the interpretation that during the first measured time point (6h) this increase of variability is related to the start of an immune response, sustained until 9h in the presence of WT Stm, but is resolved after CWA Stm exposition. We conclude that the inability of the predictive model to distinguish between the different groups at 6 h is due to the absence of a clear difference between the groups, which is more apparent at 9h post-gavage. These early similarities suggest that the mucosal inoculation with CWA Stm is able to simulate the early steps of a WT Stm infection, which underscores the usefulness of this experimental system for the study of immune responses, for which reason the model for identifying differences between both responses fails to identify a differential pattern in the biomarker set available.

Introduction

A critical aspect of the maintenance of intestinal homeostasis is the effective discrimination between pathogenic and commensal bacteria. The ability to discern pathogenic bacteria efficiently and timely is crucial, and is mediated by the interaction between innate and adaptive immunity (Jakobsson et al., 2015). The difference between these two parts of the immune system is based on the ability to recognize general foreign patterns of the former and the recognition of specific non-self-antigens of the latter.

The innate immune system is composed of overlapping layers of all-purpose mechanisms to exclude or eliminate any type of non-self-object or organisms. The first layer of protection in the lumen is achieved by the intestinal mucus, a gel-like structure that separates the particulate luminal contents from the epithelium while allowing the absorption of soluble nutrients (Jakobsson et al., 2015). The mucus is also enriched with antimicrobial peptides and other small molecules known to regulate bacterial behavior, helping in the active maintenance of intestinal homeostasis (Jakobsson et al., 2015; Li et al., 2015; Meyer-Hoffert et al., 2008). When these mechanisms are not sufficient for the containment of luminal microorganisms, an inflammatory response is activated to clear the foreign particle or organism.

The factors regulating the activation of inflammatory responses are not fully understood. It is known that certain pathogenic microorganisms and types of antigen elicit a strong inflammatory response, however the defining characteristics of these activators are ill-described, since there is always an overlap between innate and adaptive responses (Hapfelmeier et al., 2005; Sellin et al., 2014). Previously in our lab, we have shown that transient colonization of germ-free mice with cell wall auxotrophic (CWA) *Salmonella enterica* Typhimurium (Stm) induces high titers of species-specific IgA, without inducing inflammation (Pfister *et al*, unpublished), effectively separating the innate inflammation from the induction of a protective adaptive immune response. This uncoupling of adaptive immunity from inflammation provides us with a model of pathogen exposition ideal to dissect the early bacteria-innate immunity interaction, and further expand our understanding of inflammatory responses.

In this section we explore the early host - CWA Stm interaction and compare it with the host-WT Stm infection. For this approach we decided to generate a multivariate statistical model that would be able to identify pathogen-induced innate immunity genes different between these two strains, and separate them from general responses elicited by commensal bacteria. Our statistical model was unable to separate the CWA Stm-induced from the WT

Stm-induced responses, leading to the recognition that both strains are able to elicit similar early innate immunity expression. Based on this we concluded that CWA Stm can simulate the first hours of a WT Stm without leading to the well characterized Stm induced colitis.

Results and Discussion

The first step to study the early responses of mice against cell wall auxotrophic (CWA) *Salmonella enterica* Typhimurium (Stm) was to characterize the *in-vivo* behavior of the strain. To address this objective we exposed germ-free mice to a mixed gavage of 10^{10} CFU of CWA Stm and 10^{10} CFU of CWA *E. coli* K-12, and followed the bacterial shedding in the feces over time to estimate the time of bacterial intestinal passage. This experiment showed that initially both strains show the same shedding pattern, where the first CFU are already detectable 6 h post gavage, the peak of excretion is between 8-9 h post gavage and most of the total CFU have been shed after 24 h (**Figure 2.1 A-B**)

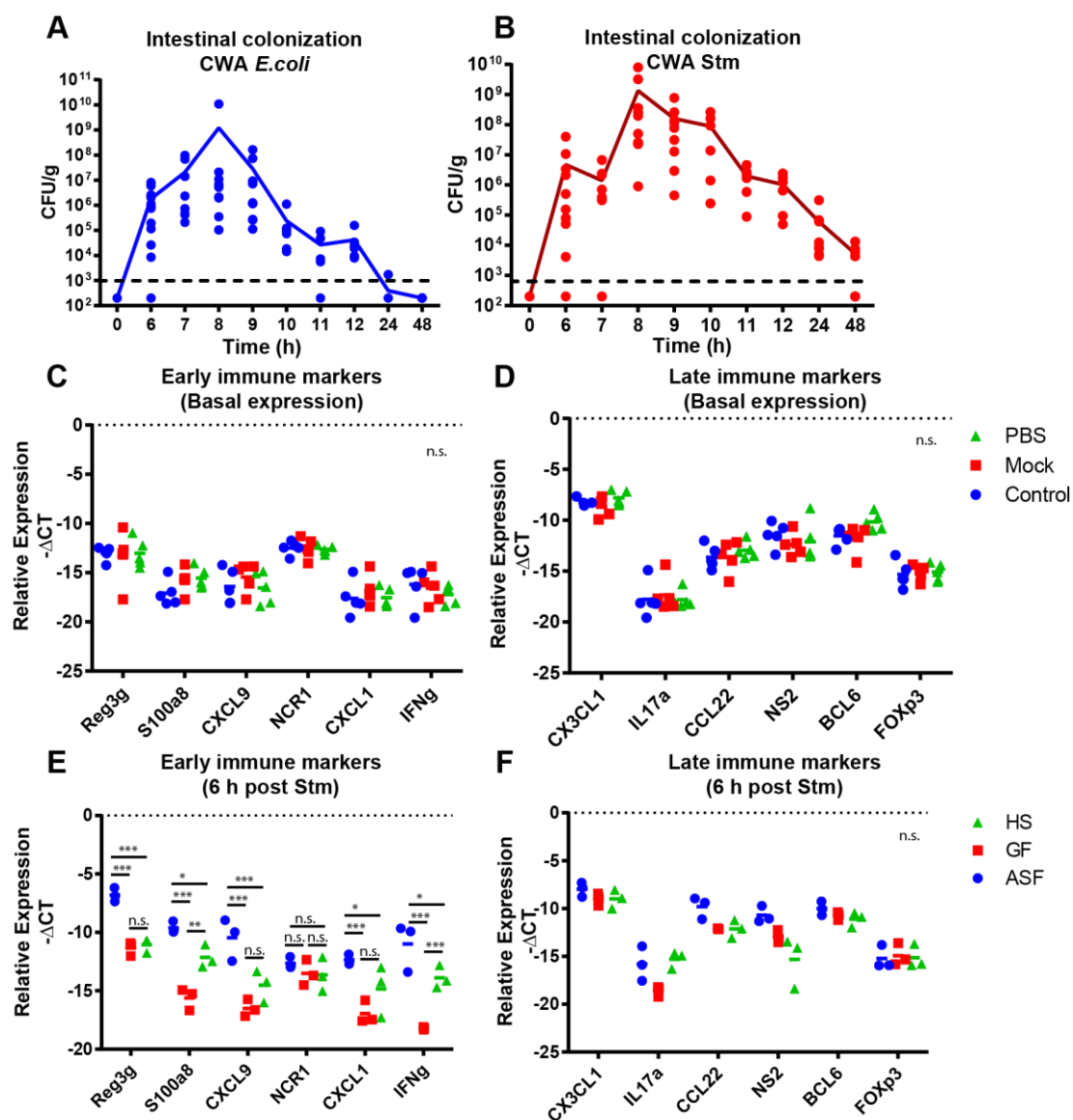


Figure 2.1. Early response of mice to cell wall auxotrophic bacteria. Germ-free mice were gavaged with a 1:1 mixture of 10^{10} CFU of cell wall auxotrophic (CWA) *E.coli* (A) and 10^{10} CFU of CWA Stm (B), and the luminal colonization was followed for 48 h. (C-D) Background expression of mRNA in cecum from Naïve (green triangles), mock gavaged (red squares) or PBS gavaged (blue circles). (E-F) Intestinal immune response to a 10^{10} CFU CWA Stm infection of HS colonized (green triangles), germ-free (red squares) or ASF colonized (blue circles) mice. All animals were sacrificed 6 h after treatment and cecal mRNA was quantified with qPCR. The expression is normalized to actin beta. Each dot represents one mouse. Anova with Tukey as posttest, ***< 0.001, ** <0.01, *<0.05, n.s = not significant.

Besides the evident similarities between the strains, CWA Stm maintained higher shedding numbers for a longer period of time than CWA *E. coli*, clearly evident from residual CFU still being shed at 48 h post gavage (**figure 2.1 A-B**). The bacterial shedding of CWA *E. coli* corresponded well with the published colonization kinetics of this strain (Hapfelmeier et al., 2010), suggesting that the observed longer persistence of CWA Stm might be due to better *in vivo* survival than in comparable *E. coli* strains (Cuenca et al., 2016).

Once the average transit time was estimated, we proceeded to measure 12 immune markers selected rationally to cover the spectrum of known intestinal responses, as a means to establish the basal immune status in the experimental mice (Table S1). Since our main objective was to determine the early responses that would eventually lead to inflammation, we decided to use 6 h post gavage as the measuring time point. At this time point we estimated that in average the bulk of bacteria was present in the cecum, inflammation would not yet be induced. This assumption goes in line with the observations in the streptomycin-pretreated mouse model of invasive non-typhoid salmonellosis, where the first intra-epithelial Stm have been observed at 6 h post infection and reaching the maximum at 9 h post infection (Sellin et al., 2014).

Since our experimental procedures induce stress and anxiety in the experimental animal by handling and gavage, we decided to measure the expression of the 12 mRNA markers compared to control mice that were left untreated, mock gavaged (introducing the feeding needle into the stomach without liquid administration) or gavaged with sterile PBS (our standard vehicle) 6 h post gavage. This basal analysis showed that the basic experimental procedures do not cause major alterations to the gene expression of any marker measured (**figure 2.1 C-D**). We could also measure that the variability of the assay is low, encouraging its usage for measuring small but critical differences.

The results from this experiment led us to speculate, if marker expression in response to CWA Stm infection was influenced by hygiene status/microbiota composition. To test this hypothesis, 3 germ-free mice, 3 ASF (Altered Schaedler Flora-colonized) mice and 3 two-week commensal *E. coli* HS-monocolonized mice were gavaged with CWA Stm (**figure 2.1 E-F**). The ASF mice showed an elevated expression pattern in nearly all the early immune markers, but not in the late immune markers. Germ-free mice showed lower

expression than ASF-colonized mice. *E. coli* HS-monocolonized mice had an intermediate expression pattern. The clear and microbiota-complexity-dependent separation between different colonization statuses suggested that the baseline expression of these markers depends on the colonization status and that the monocolonization with *E. coli* HS is sufficient to partially revert the germ-free phenotype. Another possible interpretation is that there is a differential responsiveness to pathogens between the experimental groups; however this interpretation cannot be fully assessed due to the lack of uninfected controls.

Instead of generating further data to explain the differential response between health statuses, we decided to use the information obtained in this experiment to start a more comprehensive analysis of the immune response at 6 h post-gavage. The main objective of this project was to build a predictive model for the induction of intestinal inflammation, based on the early response to an incoming pathogen. To achieve this goal, a panel of 86 genes related to human IBD was measured in mouse cecum at 6 h post-gavage with either WT *Stm*, avirulent *Stm* (SPI-1⁻, SPI-2⁻), CWA *Stm*, *E. coli* HS or PBS.

To analyze this complex dataset we used multinomial logistic regression, with lasso as a variable selector, based on the following assumptions:

- WT *Salmonella* is the only inducer of pathological inflammation.
- Avirulent *Salmonella* shares antigen composition but does not induce inflammation.
- CWA *Salmonella* shares all antigens (including virulence factors), invades in to the epithelial cells but is unable to induce inflammation.
- *E. coli* HS is a physiological, non-pathogenic bacterial stimulus.
- PBS is a control, defining the expression baseline of all markers.
- The model should contain the minimal number of variables needed to obtain a classification of at least 80% accuracy.

The animal experiments necessary to generate this dataset were performed twice, amounting to a total up to 5 mice per group (original dataset). The resulting model is composed of three equations that do a step wise classification of a sample in either “WT *Salmonella*”, “avirulent *Salmonella*”, “*E. coli*” or “CWA *Salmonella*”, based on the values of 19 variables (table 2.1). The graphical representation of this model can be observed as a linear discriminant analysis in figure 2.2.

Table 2.1. Coefficients of the logistic regression classifier to predict the occurrence of inflammation .

Mice were gavaged with either WT *Salmonella*, avirulent *Salmonella*, CWA *Salmonella*, *E. coli* HS or PBS and sacrificed after 6 h. The cecal mRNA was extracted and quantified with an 86 immune marker array. The values were used to build a multinomial logistic model composed of the least possible variables that still retain 80% classification power.

WT <i>Salmonella</i>		Avirulent <i>Salmonella</i>		<i>E. coli</i>	
Intercept	-3.03809	Intercept	2.524692	Intercept	0.513398
Cr2	0.093589	Cxcl11	-0.03441	Cxcl2	-0.08405
Cxcl1	-0.02515	Cxcl9	0.014873	Il17a	-0.12395
Cxcl2	0.012145	Ifng	-0.04822	S100a8	0.096239
Cxcr1	0.029334	Il1b	-0.01461	Sele	-0.13581
Il13	0.072258	Il23a	-0.019		
Il17a	0.048485	Tdo2	0.058935		
Il23a	0.003085	Timp1	-0.12876		
Il5	-0.02804				
Mmp10	0.094274				
Sele	0.127861				

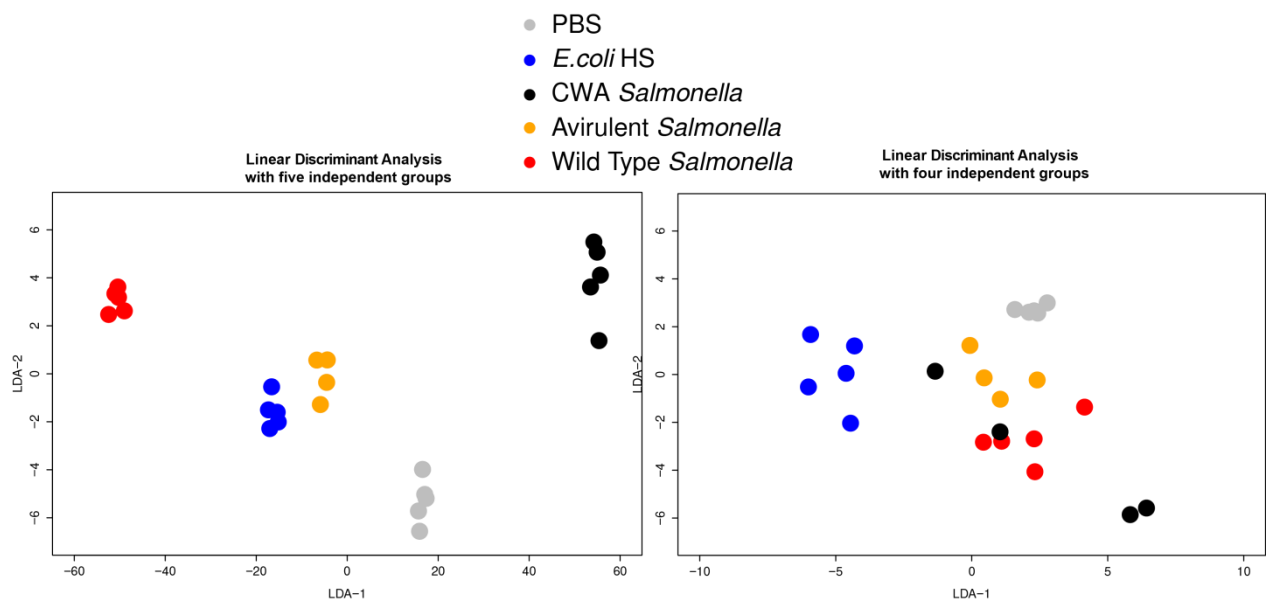


Figure 2.2. Linear Discriminant Analysis of mRNA expression in cecum 6h post-gavage. Left, linear discriminant analysis using the variables selected with the multinomial logistic regression to classify the samples in to five different groups (WT Stm, avirulent Stm, reversible Stm, *E. coli* HS and PBS). Right, model made with four groups (WT Stm, avirulent Stm, *E. coli* HS and PBS) and used to re-classify CWA Stm.

Figure 2.2 left shows a clear separation between the different experimental groups, leading to the conclusion that our model is able to recognize immune responses from our experimental groups, based on this particular marker subset. This clear separation is no longer observed when we attempt to classify CWA Stm with the statistical model, in to WT Stm, avirulent Stm, *E. coli* or PBS. This phenomenon suggests that the response induced by CWA Stm is distinct to the other groups. Another possible interpretation of the results is that our model is recognizing intrinsic patterns in the dataset that have no biological meaning, and hence the classification would have no predictive value. It is known that linear discriminant analysis have strong biases to repetitive differences between groups, regardless their scientific relevance.

To address the possibility of a technical bias on our data we decided to test our model with a newly generated dataset. This dataset would come from an identical experiment, hence eliminating the possibility of technical bias. If the new dataset classifies in the same groups, we would be able to assess the biological relevance of our predictor.

This newly generated dataset was run through the model and the predicted classification was compared to the actual treatment of each sample. Our model was accurate only in 30% of the cases, suggesting that the ability to separate the original dataset into the correct class was only due to irrelevant technical variability and not due to important biological differences (figure 2.3).

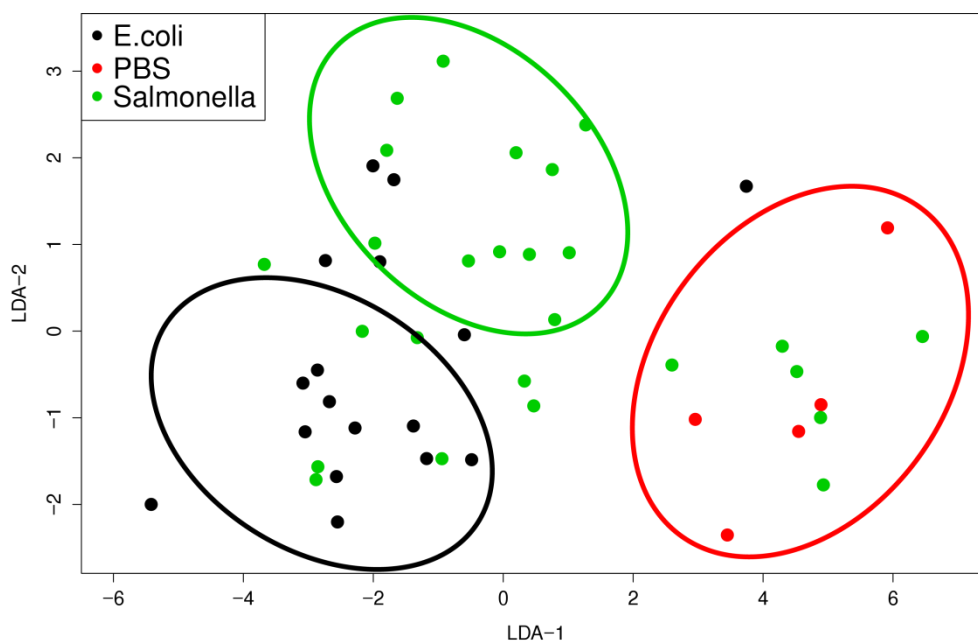


Figure 2.3. Classification of an independent dataset. The previously generated model from figure 2.2 was used to classify a newly generated dataset in to four groups (*E. coli*, *Salmonella* and, PBS). Each dot represents a samples and the circles represent the expected area where each class should be.

As an attempt to understand the source of this variability, we manually analysed the expression pattern of known *Salmonella*-related markers at 6 h and compared them with a 9 h -infection (**figure 2.4**). We observed a very high variability in the WT *Salmonella* and CWA *Salmonella* groups at 6 h, that is absent in the avirulent *Salmonella* or PBS group. Despite this variability we observe an increase in markers associated to cell migration (S100a8 and Cxcl2) in response to WT and CWA Stm harbouring functional virulence factors.

This high variability seemed to decrease by 9 h post-gavage in the WT *Salmonella* group, and in most cases showed a marked increase in inflammation markers. The increase in the expression of inflammation markers was not observed in CWA at 9 h post gavage.

The spread in the observations at 6h post-gavage is probably related to the high variability in the intestinal transit flow during the first hours, that we also observed in a previous study using this colonization model, showing that the passage of the bolus occurs with a one-hour precision (Cuenca et al., 2016). Since the activation of these immune markers is highly dependent on active bacterial invasion of the epithelium, the added variability caused by the bacterial transit variability makes such an early time point difficult to analyse. This goes in line with the increase in consistency of the marker expression at 9 h in the WT Stm, when the influence of the temporal variation in the bacterial transit becomes less significant, and generates a more consistent inflammation-related signal.

In previous work from our lab, we have described that after 9 h post-gavage mucosal histological differences between WT *Salmonella* and CWA *Salmonella* appear (Pfister *et al*, unpublished). Since the main objective of this project was the differentiation between the effects of both strains before development of histopathology, the idea of using a complex multivariate mRNA based model was not further explored. Nonetheless the absence of a clear difference between CWA Stm and WT Stm at early time points, combined with the known ability of CWA Stm to generate species-specific IgA led us to conclude that the CWA *Salmonella* infection model simulates a 6-hour-limited wild-type *Salmonella enterica* Typhimurium infection and then rapidly and fully resolves.

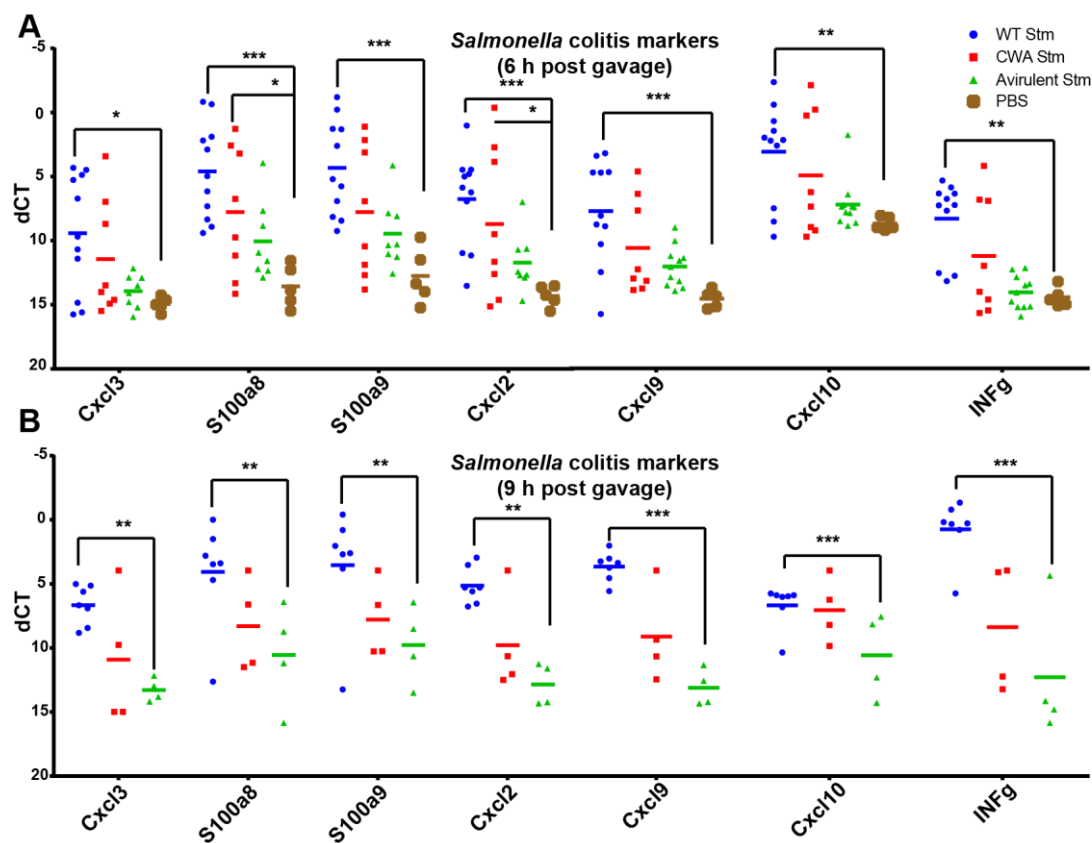


Figure 2.4 *Salmonella*-related markers expressed at 6 or 9 h post-gavage. Mice were gavaged with either 10^{10} CFU WT Stm, 10^{10} CFU CWA Stm, 10^{10} CFU avirulent Stm or PBS. **(A)** Gene expression in mouse cecum 6 hours post gavage (ANOVA with tukey post-test using PBS as comparison). **(B)** Gene expression in mouse cecum 6 hours post gavage (ANOVA with tukey post-test using avirulent as comparison).

Table S2.1 Bacterial strains and plasmids

Strain/ Plasmid	Strain name	Relevant genotype/phenotypes/description	Source, Reference
WT Stm	χ4138	Wild type, UK-1 background	Roy Curtiss (Dieye et al., 2009)
Avirulent Stm	χ9650	gyrA1816 Δ(<i>avrA-invH</i>)-2::cat Δ(<i>ssaG-ssaU</i>)-1::kan, NalR, CmR, KmR. χ4138 derivate	Roy Curtiss (Dieye et al., 2009)
CWA Stm	χ9052	Δ <i>alr</i> -3 Δ <i>dadB</i> 4 Δ <i>asd</i> A33 χ4138 derivate	Roy Curtiss (Xin et al., 2012)
<i>E. coli</i> HS		Wild type	Jim Nataro (Levine et al., 1978)
CWA <i>E.coli</i>	HA107	Δ <i>alr</i> Δ <i>dadx</i> Δ <i>asd</i>	Siegfried Hapfelmeier (Hapfelmeier et al., 2010)

Material and Methods

Animal colonization experiments

Germ-free animals were re-derived from C57BL/6 mice and maintained germ-free in flexible film isolators in the Genaxen Foundation Clean Mouse Facility (CMF) of the University of Bern as described (Macpherson and McCoy, 2014). For experiments mice were aseptically transferred to autoclaved sealfsafe-plus IVCs under positive pressure (Tecniplast, Italy) in a barrier unit of the Genaxen Clean Mouse Facility. Cage changes were carried out under strictly aseptic conditions. In all experiments animals were provided with sterile mouse chow (Kliba 3437; autoclaved) and autoclaved water ad libitum. All experiments were performed according to protocols approved by the Bernese Cantonal Ethical committee for animal experiments and carried out in accordance with Swiss Federal law for animal experimentation (license numbers BE94/11 and BE91/14).

To generate contamination-free *Salmonella enterica* Typhimurium inoculums, NaCl (0.3M), D-Ala (200 µg/mL) and Dap (50 µg/ mL) supplemented autoclaved LB medium in sterile-filter-sealed flasks, was aseptically inoculated from single colonies of the test bacterium and incubated shaking at 150 rpm at 37°C for 16 hours. This subculture was then diluted 1:10⁶ in 500mL of the same media and incubated shaking at 150 rpm at 37°C for 16 hours. Bacteria were harvested by centrifugation (10 min, 4816 x g, 4°C) in a sterile aerosol-proof assembly, washed in autoclaved sterile PBS and concentrated to a density of 1x10¹¹ CFU/mL in sterile PBS, performed aseptically under a sterile laminar airflow. To generate contamination free *E.*

coli inoculums, the same procedure was followed with the exception of the media: LB supplemented with D-Ala (200 µg/mL) and Dap (50 µg/ mL). The bacterial suspensions were aseptically aliquoted in autoclaved plastic tubes and sealed in a sterilized secondary containment. The sterile tubes containing the inocula and the mice were aseptically imported into a sterilized laminar flow hood, and each animal inoculated with 200 µL of bacterial suspension (containing 1×10^{10} CFU in sterile PBS, at a density of 1×10^{11} CFU/mL) by gavage, carried out wearing sterile surgical gowns and sterile surgical gloves. Fresh fecal pellets were collected aseptically, suspended in sterile PBS, and plated in serial dilutions on D-Ala/ Dap-supplemented or non-supplemented LB agar and incubated aerobically at 37°C for 24 hours.

RT-qPCR

Cecum samples were collected 6 h or 9 h post infection with 10^{10} CFU of bacteria, washed in sterile PBS and immediately preserved in RNeasy lysis buffer (QIAGEN) for RNA stabilization overnight. The samples were then transferred to -80°C for long term storage. Total RNA was extracted from approximately 15 mg of tissue using the RNeasy mini kit (Qiagen) and the quality was assessed using the Agilent RNA 6000 Nano Kit to be higher than RIN 9. The samples of interest were reverse transcribed with the RT² easy first strand kit (Qiagen) and then the cDNA libraries were analyzed using either the 12 gene custom plate CAPM11698 (SABiosciences) or the mouse crohn's disease RT² profiler PCR array (SABiosciences, PAMM-169ZE-4) with SYBR green reagents (Qiagen) in a Viia 7 Real-Time PCR System (Thermo Scientific). For the plate PAMM-169ZE-4 five housekeeping genes (Actb, B2m, Gapdh, Gusb and Hsp90ab1) were averaged and used for calculating the ΔCT ($CT_{sample} - CT_{average \text{ housekeeping genes}}$). In the plate CAPM11698 only Actb was used.

Data analysis

All multivariate data analysis was done using the R 3.1.1 statistical program and the ggplot2 (Wickham and Chang, 2015), dplyr (Wickham and Francois, 2015), glmnet (2010; 2010) and MASS packages. The scripts used for this analysis are provided as supplementary data. Figures 2.1 and 2.3 were done using the program Prism 6

Acknowledgments

We thank the Clean Mouse Facility for all the animal work and the Genomics Core Facility, from the Department of Clinical Research University of Bern for the access to the qPCR machines. This work was funded by the grants ERC 281904 and SNF 310030_138452.

References

(2010). Regularization Paths for Generalized Linear Models via Coordinate Descent. *Journal Of Statistical Software* 33, 1--22.

Cuenca, M., Pfister, S.P., Buschor, S., Bayramova, F., Hernandez, S.B., Cava, F., Kuru, E., Van Nieuwenhze, M.S., Brun, Y.V., Coelho, F.M., et al. (2016). D-Alanine-Controlled Transient Intestinal Mono-Colonization with Non-Laboratory-Adapted Commensal *E. coli* Strain HS. *Plos ONE* 11, e0151872.

Dieye, Y., Ameiss, K., Mellata, M., and Curtiss, R. (2009). The *Salmonella* Pathogenicity Island (SPI) 1 contributes more than SPI2 to the colonization of the chicken by *Salmonella enterica* serovar Typhimurium. *BMC Microbiology* 9, 3.

Hapfelmeier, S., Lawson, M.A., Slack, E., Kirundi, J.K., Stoel, M., Heikenwalder, M., Cahenzli, J., Velykoredko, Y., Balmer, M.L., Endt, K., et al. (2010). Reversible Microbial Colonization of Germ-Free Mice Reveals the Dynamics of IgA Immune Responses. *Science* 328, 1705-1709.

Hapfelmeier, S., Stecher, B., Barthel, M., Kremer, M., Müller, A.J., Heikenwalder, M., Stallmach, T., Hensel, M., Pfeffer, K., Akira, S., et al. (2005). The *Salmonella* pathogenicity island (SPI)-2 and SPI-1 type III secretion systems allow *Salmonella* serovar typhimurium to trigger colitis via MyD88-dependent and MyD88-independent mechanisms. *J. Immunol.* 174, 1675-85.

Jakobsson, H.E., Holmén-Larsson, J., Schütte, A., Ermund, A., Rodríguez-Piñeiro, A.M., Arike, L., Wising, C., Svensson, F., Bäckhed, F., and Hansson, G.C. (2015). Normalization of Host Intestinal Mucus Layers Requires Long-Term Microbial Colonization. *Cell Host & Microbe* 18, 582-92.

Levine, M.M., Bergquist, E.J., Nalin, D.R., Waterman, D.H., Hornick, R.B., Young, C.R., and Sotman, S. (1978). *Escherichia coli* strains that cause diarrhoea but do not produce heat-labile or heat-stable enterotoxins and are non-invasive. *1*, 1119-1122.

Li, H., Limenitakis, J.P., Fuhrer, T., Geuking, M.B., Lawson, M.A., Wyss, M., Brugiroux, S., Keller, I., Macpherson, J.A., Rupp, S., et al. (2015). The outer mucus layer hosts a distinct intestinal microbial niche. *Nature Communications* *6*, 8292.

Macpherson, A.J., and McCoy, K.D. (2014). Standardised animal models of host microbial mutualism. *Mucosal Immunology* *8*, 476.

Meyer-Hoffert, U., Hornef, M.W., Henriques-Normark, B., Axelsson, L., Midtvedt, T., Putsep, K., and Andersson, M. (2008). Secreted enteric antimicrobial activity localises to the mucus surface layer. *Gut* *57*, 764.

Sellin, M.E., Müller, A.A., Felmy, B., Dolowschiak, T., Diard, M., Tardivel, A., Maslowski, K.M., and Hardt, W. (2014). Epithelium-Intrinsic NAIP/NLRC4 Inflammasome Drives Infected Enterocyte Expulsion to Restrict Salmonella Replication in the Intestinal Mucosa. *Cell Host & Microbe* *16*, 237.

Wickham, H., and Chang, W. (2015). *Ggplot2: An implementation of the grammar of graphics*, Version 1.0. 1.

Wickham, H., and Francois, R. (2015). *dplyr: A grammar of data manipulation*. R Package Version 0.4.

Xin, W., Wanda, S.Y., Zhang, X., Santander, J., Scarpellini, G., Ellis, K., Alamuri, P., and Curtiss, R. (2012). The Asd⁺-DadB⁺ Dual-Plasmid System Offers a Novel Means To Deliver Multiple Protective Antigens by a Recombinant Attenuated Salmonella Vaccine. *Infection And Immunity* *80*, 3621.

Supplementary figure 2.1. Script to build a log- logistic model

Lasso.R

```
setwd("//ifik.unibe.ch/users/Homes/cuenca/Desktop")
library(glmnet)
library(reshape2)
#####Aquiring and shaping the training data
rnadb=read.table("Data_mc14_001.csv",
header=T, sep=";") class(rnadb) # The data are
stored as a list names(rnadb) # The names of
the list elements are x and y x <- rnadb[3:85]
X<-
data.matrix(x
) y<-rnadb[2]
Y<-data.matrix(y)
#####Fitting the model
fit = glmnet(X, Y, family = "multinomial", type.multinomial = "grouped", intercept=FALSE,
dfmax=20,)# fit the model
fit
#Plot the paths for the fit
plot(fit, xvar = "lambda", label = TRUE, type.coef = "2norm")

title(main="20-variable coefficient paths",cex=0.8)
#####Cross validation of the fitted model
cv.fit = cv.glmnet(X, Y, family = "multinomial", type.measure="class")
plot(cv.fit)# Plot the mean sq error for the cross validated fit as a function
# of lambda the shrinkage parameter
# First vertical line indicates minimal mse
# Second vertical line is one sd from mse: indicates a smaller model
# is "almost as good" as the minimal mse model
tpred=predict(cv.fit,X) # Predictions on the test
data mte=apply((tpred-Y)^2,2,mean) # Compute
mse for the predictions
points(log(fit$lambda),mte,col="blue",pch="*") # overlay the mse predictions on the plot
#legend("topleft",legend=c("10 fold
CV", "Test"),pch="*",col=c("red", "blue")) coef.exact = coef(cv.fit, s =
0.5, exact = TRUE)
coef.apprx = coef(cv.fit, s = 0.5, exact =
FALSE) ans<-coef(cv.fit,
s=cv.fit$lambda.1se)
sink("//ifik.unibe.ch/users/Homes/cuenca/Desktop/Data_wolfberg/output.txt")
lapply(ans, print)
sink()
```

Supplementary figure 2.2. Script to build a linear discriminant analysis with the output of the logistic model

LDA

```
data1=read.table("Data_mc14_001.csv", header=TRUE, sep=";")
attach(data1)
names(data1)
library("MASS")
library("nnet")

#groups_logit <- multinom (Treatment ~ Abcb1a + Adh1 + Aldob + Atg16l1 + C3 +
Casp1
+ Ccl11 + Ccl12 + Ccl20 + Ccl25 + Ccl5 + Ccr1 + Ccr2 + Ccr5 + Ccr9 +
Cd55 + Chil1 + Cldn8
+ Col1a2 + Cr2 + Csta+ Cx3cl1 + Cx3cr1 + Cxcl1 + Cxcl10 + Cxcl11
+ Cxcl12 + Cxcl2 + Cxcl3 + Cxcl9 + Cxcr1 + Cxcr3 + Edn3 + Egr3 + Fpr1
+ Gcg
+ H2.Aa+ H2.Eb1 + Hsp90b1 + Hspa5+ Ifng + Il13 + Il17a + Il1b + Il1rn
+ Il23a
+ Il2ra + Il5 + Il6 + Irf5 + Isg15 + Itgb2 + Lcn2 + Ltb + Lyz1 +
Mmp10 + Mmp12+ Mmp1a + Mmp3 +
Mmp7 + Muc1 + Nod2 + Nos2 + Nr3c2 + Pck1 + Pecam1+ Reg1 +
S100a8 + S100a9 + Saa3 + Sele + Selenbp1 + Sell + Sod2 +
Stat1
+ Stat3 + Tdo2 + Tff1 + Timp1 + Tnf + Tyk2 + Ubd + Vwf, ,
data=data1, model=TRUE, Hess=TRUE)
summ<-
summary(groups_logit)
summ

#Equation
groups_lda <- lda (Treatment ~
Adh1+C3+Ccl12+Csta+Ccl25+Cxcl11+Egr3+Hspa5+Il5+Itgb2+Ltb+Muc1+Nos2+Nod2+Pecam
1+Reg2+S aa3
+Sod2+Tdo2)

summary(groups_lda)
ans=predict(groups_lda)
#http://stat.ethz.ch/R-manual/R-
patched/library/nnet/html/multinom.html ans$x[,2,2]
ans$x[,2]
a<-
(ans$x[,1])
b<-
(ans$x[,2])
d<-
c("Blue","Blue","Blue","Blue","Blue",8,8,8,8,8,1,1,1,1,1,"Orange","Orange","Orange","Orange","R
ed"," Re d","Red","Red","Red")
c<-cbind(a,b,d)
plot(c, col=c[,3],main="LDA with subset 19", xlab="LDA-1", ylab="LDA-
2",pch=16, cex=4,xlim=c(- 60,60),ylim=c(-7,7.5))
legend("top",legend=c("E.coli HS","PBS","Reversible Salmonella","Avirulent
Salmonella","Wild Type Salmonella"),pch=16 ,cex=1.5,col=c("Blue",8,1,"Orange","Red"))
groups_lda
#####Repeat with only four and try to
classify data3=read.table("Data_mc14_001b.csv", header=TRUE,
sep=";") attach(data3)

groups_lda3 <- lda (Treatment ~
```

```
Adh1+C3+Ccl12+Csta+Ccl25+Cxcl11+Egr3+Hspa5+Il5+Itgb2+Ltb+Muc1+Nos2+Nod2+Pecam
1+Reg2+S aa3
+Sod2+Tdo2)
```

```
summary(groups_lda3)
ans3=predict(groups_lda3)
#http://stat.ethz.ch/R-manual/R-
patched/library/nnet/html/multinom.html ans3$x[2,2]
ans3$x[,2]
a3<- (ans3$x[,1])
b3<-
(ans3$x[,2])
d3<-
c("Blue","Blue","Blue","Blue","Blue",8,8,8,8,8,"Orange","Orange","Orange","Orange","Red","Red"
,"Red ", "Red","Red")
c3<-cbind(a3,b3,d3)
plot(c3, col=c3[,3],main="LDA with subset 19-test", xlab="LDA-1", ylab="LDA-2",pch=16,
cex=4,xlim=c(- 10,10),ylim=c(-7,8))
legend("topleft",legend=c("E.coli HS","PBS","Reversible Salmonella","Avirulent
Salmonella","Wild Type Salmonella"),pch=16 ,cex=1.3,col=c("Blue",8,1,"Orange","Red"))
groups_lda
```

```
##### variables to test
data2=read.table("Data_mc14_001c.csv", header=TRUE,
sep=";") attach(data2)
ans2=predict(groups_l
da 3) a2<-
(ans2$x[,1])
b2<- (ans2$x[,2])
d2<-c(1,1,1,1,1)
c2<-cbind(a2,b2,d2)
points(c2, col=1,pch=16,
cex=4) c2
ans2
head(ans)
head(ans2
)
```

Chapter 3. Host-microbial IgA immune adaptation biases intestinal bacteria-bacteria competition to favor resident over immigrant strains

Author contributions

This manuscript describes the interaction between the adaptive immune system and the microbiota to outcompete an invasive pathogen. This work was possible thanks to the contribution of several authors:

- Animal Experimentation: Miguelangel Cuenca, Stefanie Buschor, Fernanda Coelho, Nicolas Studer and Miguel Terrazos.
- Native microbiota analysis: Miguelangel Cuenca, Nicolas Studer and Simone Herp
- Experiment design and conceptualization: Miguelangel Cuenca, Fernanda Coelho, Stefanie Buschor, Emma Slack and Siegfried Hapfelmeier
- LPS variation analysis: Miguelangel Cuenca and Emma Slack
- Construction of *Salmonella enterica* Typhimurium strains: Miguel Terrazos

Abstract

The mammalian intestinal microbiota is a host-specific stable consortium of host-adapted microorganisms that, amongst other beneficial functions, collectively provide protection against pathogen invasion while improving the host nutrition. To achieve this community the host must impose selective pressure by favoring host-compatible strains, in order to exclude bacterial invaders that can damage the delicate host-microbiota interaction. Here we describe the phenomenon where the combination of strain-specific IgA, a resident non-lethal *Salmonella enterica* Typhimurium (Stm) strain and a third as yet unknown bacterial adaptation, leads to the out-competition of an invading pathogenic Stm by the resident strains. The decrease in WT Stm colonization provides a partial protection against colitis and preserves the resident strain that in IgA absence would be lost. This approach explains how the adaptive immunity influences the bacteria-bacteria competition, leading to the formation of a stable and distinctive intestinal microbiota by improving the relative fitness of gut-resident commensals.

Introduction

The mammalian intestinal microbiota is a multi-species microbial consortium, acquired after birth and mostly composed of bacteria that engage in a beneficial (mutualistic) or neutral (commensal) relationship with the host organism. Mutualistic microbes have evolved to not cause damage to a healthy and immunocompetent host, and to promote health by co-metabolization of complex nutrients and biosynthesis of vitamins, by colonizing niches that are restricted to the gut lumen (body exterior), and by interfering with the invasion of microbial immigrants (that may be less adapted or pathogenic).

Any mutualistic relationship is based on bilateral actions for a common goal; therefore it requires a healthy intestinal ecology, which can provide an optimal environment to the resident species. The pre-colonization of the intestinal tract with certain bacterial strains has been shown previously to be protective against the invasion by related pathogenic immigrants due to metabolite depletion, exemplified by the inability of enterohemorrhagic *E. coli* 0157:H7 to infect a mouse that had been pre-colonized with commensal *E. coli* strains HS and Nissle 1917 (Leatham et al., 2009). Such metabolite depletion is normally induced by a consortium of bacteria, in a process called colonization resistance (Maltby et al., 2013). Colonization resistance of the intestinal pathogen *Salmonella enteric* serovar Typhimurium (*S. Typhimurium*, short: Stm) has been directly linked to the luminal out-competition of intestinal pathogens by a complex microbiota after the remission of inflammation (Endt et al., 2010).

A colonization resistance conferring microbiota is consistently formed in all mammalian hosts, despite of genetic, nutritional or environmental variability. This phenomenon suggests that the host actively facilitates the establishment of a defined and controlled microbiota, where most of the intestinal bacterial species are only transient (ecological succession and "tourist" species that do not stably colonize) and the main residents are represented mainly by host-adapted bacterial strains that are able to maintain a permanent colonization (Dishaw et al., 2014). It has further been observed that despite the high phylogenetic variability in the microbiota, most of the functional categories and metabolic pathways represented in the microbial metagenome are fairly conserved between hosts individuals (Ridaura et al., 2013).

The constitution of the intestinal microbiota has been hypothesized to require the continuous selective pressure imposed by the adaptive immune system (Dishaw et al., 2014). Human microbiology traditionally has focused mainly on the role of adaptive immune responses in pathogen eradication or control. However, new approaches have led to the more general concept that the adaptive immune system functions to "commensalize" any newcomer in the gut, potentially pathogenic or not, in order to maintain the disease-free co-existence (Forbes

et al., 2008; Gauger et al., 2007; McSorley et al., 2000; Palm et al., 2014). This concept is consistent with the fact that obligate pathogenic species, that have evolved the ability to escape this host control, are rare, whereas opportunistic pathogenic, commensal and mutualistic species are part of a difficult-to-categorize continuum that most hosts are associated with.

The main host mechanisms imposing selective pressure on the gut microbial community have been suggested to be immunoglobulin A (IgA)-, anti-microbial peptides-, and mucin 2- (muc2) mediated (Dishaw et al., 2014; Rogier et al., 2014). The modes of action of these different effector molecules are very broad. They can increase the distance from the microbial community to the epithelial cells, kill bacteria in a selectively or not-selective manner, reduce their motility (Forbes et al., 2008; Peterson et al., 2007a), inactivate virulence factors, agglutinate bacteria (Forbes et al., 2008), provide nutrients for competing bacterial species and also provide an anchoring site for bacterial adhesion (Rogier et al., 2014).

The neutralization of microbial virulence factors by host-controlled mechanisms phenotypically attenuates pathogens, which after losing their competitive edge, may be cleared from the gut through out-competition by resident species (Endt et al., 2010). Although all host-derived protective mechanisms are important for the control and containment of the intestinal microbiota, only the adaptive immune system can induce microbial species- and strain-specific immune responses, and one of the best characterized immune mechanisms modulating the gut microbiota is intestinal IgA.

The ability of IgA to selectively affect colonization of specific members of the microbiota has been recently shown in mice, where *B. theta* strains can gain intestinal fitness by capsule phase variation and loss of IgA binding (Peterson et al., 2007a). The adaptive immune system has also been shown to alter the rate of evolution of *E. coli* populations, as in RAG2^{-/-} mice (that lack T and B cells) an adaptive immune deficiency led to a more unpredictable fixation of adaptive *E. coli* mutations during intestinal colonization (Barroso-Batista et al., 2015). This finding is corroborated by evidence for an increased gut bacterial diversity in RAG1^{-/-} compared with the wild type mice, an observation that can be reversed by bone marrow transfer (Zhang et al., 2014).

Here, we show that bacteria-specific IgA can influence the bacterial-bacteria competition at the strain level between a resident bacterial strain and an invading pathogenic variant. This effect is generated by a tripartite interaction between bacterial serotype specific IgA, a host-driven bacterial adaptation, and a third as yet unidentified mechanism. The host-microbiota

interaction described here is clear evidence for a host-immunity-driven positive selection on host-adapted bacteria, supporting the hypothesis that the immune system protects the resident microbiota from potentially dangerous invaders.

Results

Establishment of permanent residency of STm strains with varying degrees of attenuation in non-colonization-resistant gnotobiotic mice

To study the dynamics of bacteria-host interactions following introduction of new species, we chose to use a novel gnotobiotic mouse model containing a microbial consortium of 12 defined mouse-derived intestinal bacterial species (oligo-MM). This model has been shown previously to be susceptible to non-typhoid invasive salmonellosis caused by *Salmonella enterica* Typhimurium associated with colitis symptoms developing within 3-4 days post infection, without the need to artificially induce infection susceptibility by antibiotic treatment (Fransen et al., 2015; Hapfelmeier et al., 2008) (Brugiroux, et al in press).

To study the possible protective effects of immune-controlled colonization of an intestinal pathogen a range of three isogenic mutant strains of STm with varying levels of attenuation were used: (i) a partially attenuated *sseD* mutant (attenuated STm) lacking T3SS-2 function and causing a containable, transient colitis, (ii) a cell wall auxotrophic STm mutant ($\Delta asd::tetRA$; $\Delta alrP$; $\Delta alrN$, $\Delta metC$) harboring the complete set virulence genes but unable to grow on nutrients provided by host or diet (CWA STm), and (iii) an avirulent *invG sseD* mutant strain of STm (avirulent STm) that, lacking T3SS-1 and T3SS-2, no longer causes measurable pathology.

Attenuated STm is a well characterized *sseD* mutant strain, a crucial component of the type three secretion system (T3SS) apparatus from the *Salmonella* pathogenesis island 2 (SPI-2), effectively reducing the ability of this strain to proliferate intracellularly and leading to a self-resolving colitis (Medina et al., 1999). CWA strains show a severe colonization phenotype *in vitro* and in germ-free animals since they are unable to synthesize the essential cell wall components D-alanine (D-Ala) and meso-Diaminopimelic acid (m-Dap), and hence cannot proliferate without external supply with D-Ala and m-Dap, two amino acids absent in diet or the host metabolism (Cuenca et al., 2016). As a consequence CWA STm cannot proliferate in host tissues, yet remain fully invasive as assessed with *in vitro* assays with limiting D-amino acids (**figure S3.1A**). Avirulent STm, in addition to *sseD*, harbours a mutation in *invG*, an indispensable component of T3SS-1, rendering it unable to actively invade cells as well as unable to intracellularly proliferate in macrophages, resulting in complete avirulence (Hapfelmeier et al., 2005).

Gnotobiotic wild-type oligo-MM mice were inoculated with 10^8 CFU of either attenuated, CWA or avirulent STm, and studied for least 22 days. Although CWA STm is entirely unable to proliferate *in vitro* or in germ-free animals, this strain was able to stably colonize the intestinal tract of oligo-MM colonized mice. We presume that our strain is able to uptake and metabolize cell wall precursors (MurAA) released by members of the oligo-MM microbiota, leading to colonization levels equivalent to the non-CWA strains ($7.1 \times 10^7 \pm$ confidence interval 1.9×10^7 CFU; **figure 3.1A**). Mice colonized with CWA STm were able to efficiently transmit this strain horizontally to other animals by co-habitation, ruling out this being a high dose selection artefact (**figure S3.1B**).

Permanent colonization with CWA or avirulent STm was not associated with intestinal inflammation, evidenced by baseline lipocalin 2 levels (**figure 3.1B**). Infection with attenuated STm induced a transient inflammation, resulting in an increase in fecal lipocalin 2 at day 11 and 14 (**figure 3.1B**), which was resolved by day 22 independent of the clearance of luminal colonization (**figure 3.1A**). In this model that requires no harsh antibiotic manipulation to study intestinal STm colonization we found no evidence for the selection of spontaneous avirulent "cheater" mutants that outcompete the more virulent strain over time (Diard et al., 2013), as we could confirm full invasiveness of *ex-vivo* reisolated bacterial clones *in vitro* (**figure S3.1A**).

The continuous colonization by both non-CWA strains was associated with live bacterial translocation to the mesenteric lymph nodes (MLN) recoverable at day 4, similar to what has been shown previously (Endt et al., 2010; Hapfelmeier et al., 2005). In contrast, this phenomenon was not observed with CWA STm despite its normal-level luminal colonization (**figure 3.1C**), most likely due to the short range of the bacteria-bacteria MurAA cross-feeding required for syntrophic growth of CRW STm.

Since we added three new strains of varying virulence to the oligo-MM microbiota, we decided to analyze the gut bacterial composition and look for compositional alterations. It has been described previously that inflammation can alter the gut community structure (Stecher et al., 2007), nevertheless we were unable to measure major alterations in the community structure, even during colitis-associated colonization with attenuated STm (**figure 3.1 E and F**). The newly formed 13 member structure in each case remained stable for at least 22 days, fully preserving all original community members as well as the newly integrated STm strain, regardless of STm genotype (**figure 3.1 E and F**).

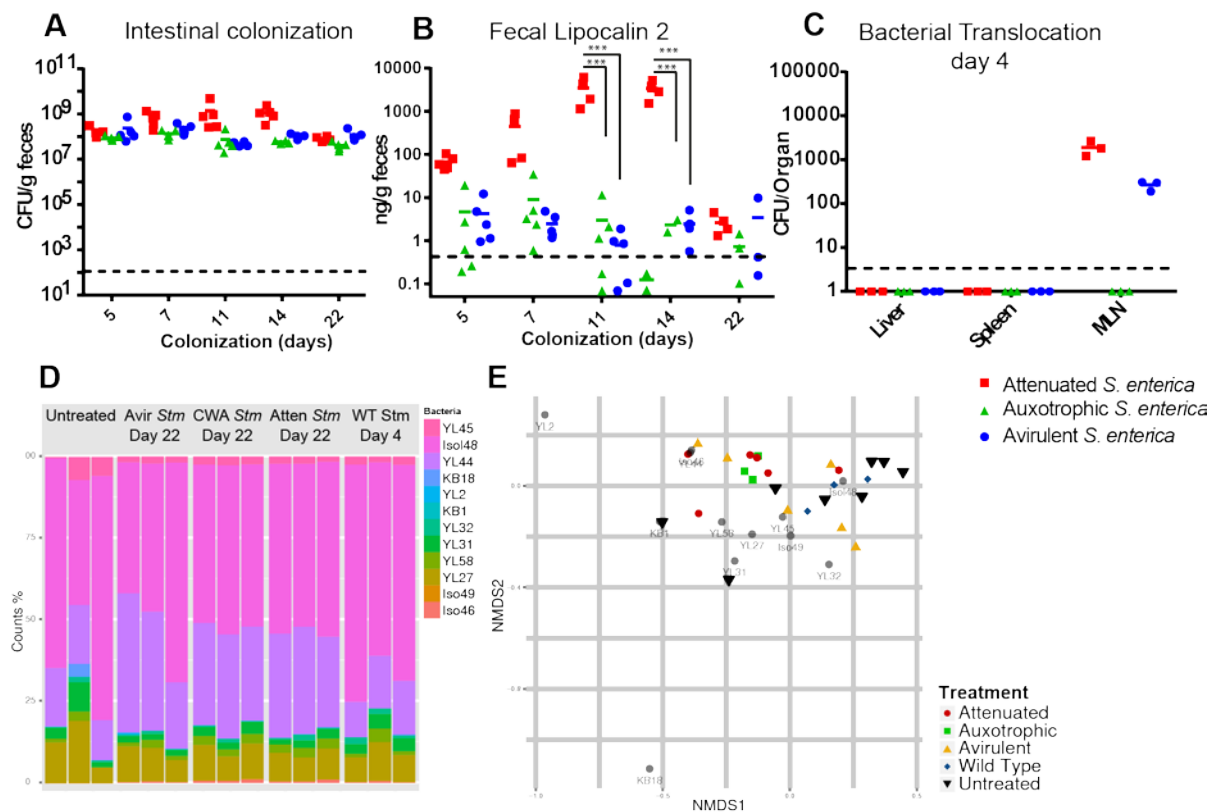


Figure 3.1. Different *Salmonella* strains stably colonize the gut of colonized mice. Mice were gavaged with 10^8 CFU of either attenuated, cell wall auxotrophic (CWA) or avirulent *Salmonella* and closely analyzed for 22 days. **(A)** Fecal CFU counts. **(B)** Lipocalin 2 concentration in feces (ANOVA with Tukey post-test). **(C)** Organ CFU counts. **(D)** Bar plots of microbiota composition. **(E)** Ordination plot of the microbiota composition, the gray circles mark the influence of individual strains. Symbols: *** p < 0.001, ** p < 0.01.

Long-term resident STm strains out-compete an isogenic wild-type invader strain, providing protection from infection

The finding that all three tested STm strains stably colonized the intestinal lumen suggested that the oligo-MM microbiota provides a viable niche for permanent *Salmonella* colonization, with little competition by other microbiota species. We therefore hypothesized that if STm pre-colonized mice were exposed to wild type STm, the fully virulent immigrant would compete for the same niche, leading to either co-existence of both strains or out-competition of the genetically deficient STm strains (the syntrophy-dependent CRW strain in particular) by the wild type strain.

To test this hypothesis, mice were gavaged with 10^8 CFU of attenuated, CWA, avirulent *S. typhimurium*, or PBS vehicle-only and allowed to equilibrate for 23 days before challenge with 10^8 CFU of the parental wild type STm strain by gavage. STm pre-conditioning for 23 days allows for the induction of microbiota-induced adaptive immunity and resolution of inflammation (see **figure 3.1B**, day 22). It has been established that murine wild type STm infection induces colitis starting from 8 to 12 hours post gavage in antibiotic-treated SPF

mice (Barthel et al., 2003) and from 3 to 4 days in the oligo-MM mice (Brugiroux, et al in press); thus, animals were sacrificed after 4 days of challenge infection (**figure 3.2A**).

Remarkably, the intestinal colonization levels of all of the attenuated pre-colonizer strains remained stable during the whole course of challenge infection (**figure 3.2B**), despite of the intuitive idea that the wild type should have an equal or increased fitness over the gene-deficient attenuated pre-colonizer strains. This maintenance of pre-colonization was associated with the constant decline in the luminal counts and accordingly a decreasing competitive index of wild-type STm (**figure 3.2C and D**). The unexpected out-competition of the wild type invader suggested that the pre-colonizer strain had acquired an ecological and/or a host-conferred advantageous (fitness-increasing) adaptation to the gut environment that does not benefit the newly immigrating strain.

The long-term STm colonization, by any of the 3 variant strains tested, conferred the mice with a strong protection against *Salmonella* induced colitis and mediated the shedding of the newcomer, as demonstrated by the greatly reduced intestinal CFU counts of the wild type strain, lower fecal lipocalin 2, reduced organ CFU counts and absence of intestinal pathology at day 4 post wild-type STm challenge compared to naïve mice (**figures 3.2C and 2E-G**). The protection observed in these mice is almost identical between the mice that were pre-conditioned with the attenuated strain (able to cause a self-limiting pathology), the CWA strain (able to invade epithelial cells, but not causing pathology or intestinal translocation), and the fully avirulent strain (well-colonizing, but unable to actively cause pathology), suggesting that long-term host-microbial adaptation, but neither pathogenesis, proliferation in host tissues nor any specific functionality of the main virulence factors T3SS-1 and -2 significantly affected the observed within host acquisition of a competitive edge over the isogenic virulent invader.

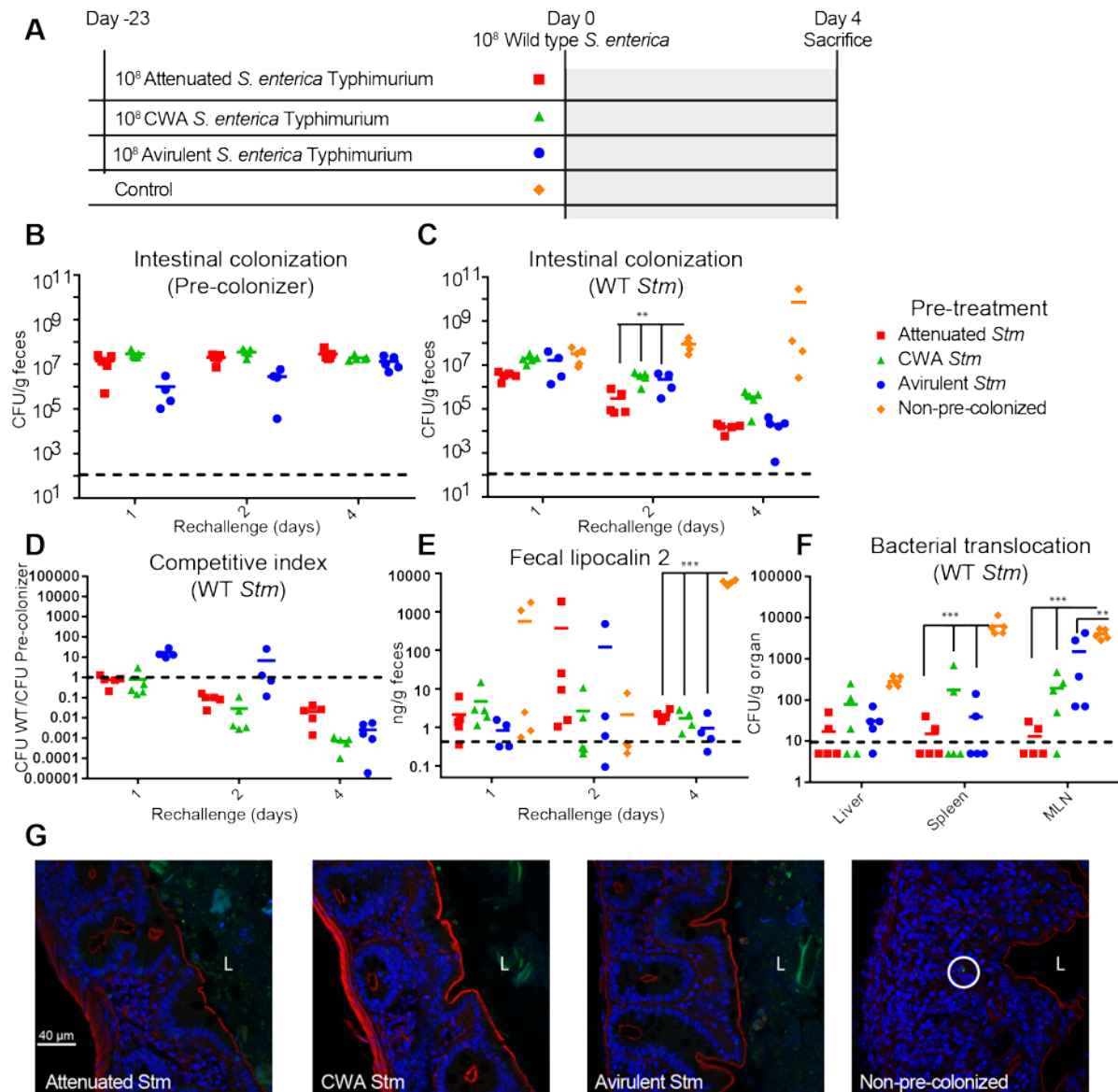


Figure 3.2. Pre-colonizing *Salmonella* strains out-compete the invading wild type *Salmonella*. (A) Mice Pre-colonized for 23 days with either attenuated, CWA, avirulent or a single dose of PBS were gavaged with 10⁸ CFU of wild type *Salmonella* and closely analyzed over 4 days. (B) Fecal CFU counts of the pre-colonizing strains of *Salmonella*. (C) Fecal CFU counts of wild type *Salmonella* (ANOVA with Tukey post-test). (D) Competitive index of wild type *Salmonella* against the pre-colonizing strain (ANOVA with Tukey post-test). (E) Lipocalin 2 concentration in feces (ANOVA with Tukey post-test). (F) Organ CFU counts (Liver, Spleen and Mesenteric Lymph Nodes) of wild type *Salmonella*. (G) Representative immunofluorescence stains at day 4; L marks the lumen, intracellular *Salmonella* in green, phalloidin in red and DAPI in blue. Symbols: *** p < 0.001, ** p < 0.01.

Long-lived plasma cell (LLPCs) depletion abolishes fitness advantage of resident CWA STm over invading wild type strain

To elucidate a mechanism for the observed out-competition of invading wild type STm by resident isogenic derivatives, we decided to dissect the two possible origins of host-bacterial co-adaptation that may evolve during intestinal long-term residency: first, the bacteria-specific adaptive immune response, and second, fitness increasing bacterial genetic adaptations.

In support of the first possible mechanism, it has been shown that specific IgA is able to modulate the intestinal fitness of bacteria based on differential binding to populations expressing variable outer membrane polysaccharide structures (Peterson et al., 2007a). To experimentally address this possibility we depleted IgA producing plasma cells and B cells in oligo-MM mice pre-conditioned by 23-day colonization with CWA STm one day before re-challenge with STm wild type, by combined treatment with anti-CD20 antibody and Bortezomib (Khodadadi et al., 2015).

Unlike in non-depleted control mice, out-competition of the wild-type invader strain by resident CWA STm was abolished in mice depleted of IgA-producing cells. These mice harbored a stable 1:1 ratio of both strains, despite of that fact that these mice had been co-caged with the control group until the day of plasma cell depletion (**figure 3.3A-C**). The depletion of LLPCs and B-cells did, however, not affect the organ colonization in these mice, suggesting a certain degree of persistence in the protection against systemic infection, possibly due to the long half-life of serum antibodies or a dominant role of T cells or other immune cell types (**figures 3.3D**).

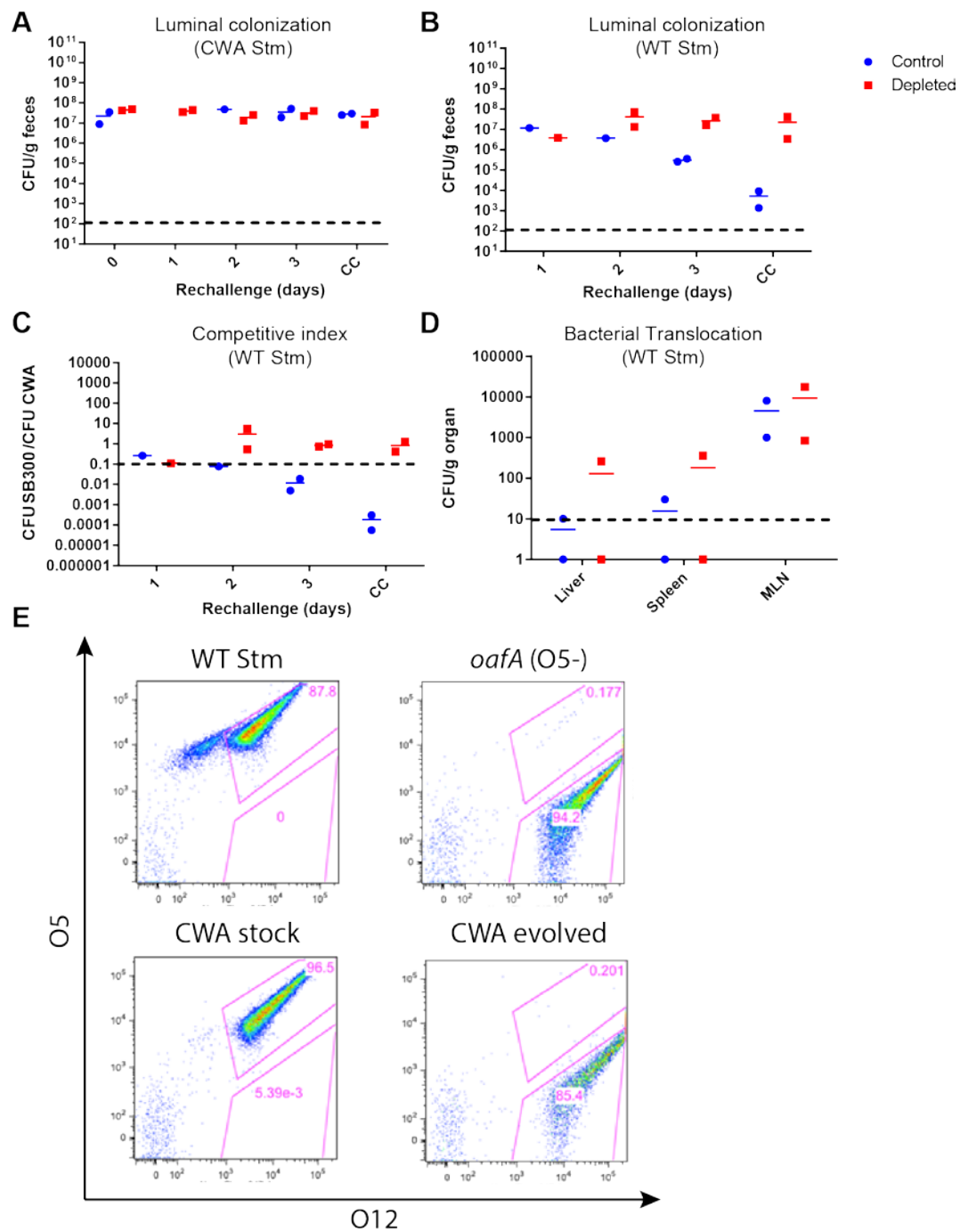


Figure 3.3. Depletion of long lived plasma cells cancels advantage of the resident CWA strain, and correlates with an LPS change in the pre-colonizer strain. Mice pre-colonized for 23 days with CWA were depleted of LLPCs, and one day later gavaged with 10^8 CFU of wild type STm. **(A)** Quantification of fecal colonization levels of the pre-colonizing strains of STm by selective plating. **(B)** Quantification of fecal colonization levels of wild type STm upon challenge infection by selective plating. **(C)** Competitive index (CI = WT Stm CFU / CWA Stm CFU). **(D)** Organ CFU counts (Liver, Spleen and Mesenteric Lymph Nodes) of wild type *Salmonella*. **(E)** O5/O12 LPS typing in original and evolved strains

The abolition of the competitive advantage of resident STm by the depletion of IgA suggested that long-term resident STm strain had evolved to escape IgA binding leading to a

fitness gain over the non-evolved immigrant. The LPS O-antigen is the main determinant of STm binding and protective intestinal IgA (Levinson et al., 2015; Michetti et al., 1992), and immunity driven LPS O-antigen phase variation leading to the spontaneous loss of the dominant O5 antigen, allows evasion of recognition by anti-O5 IgA without loss of invasiveness (Forbes et al., 2008; Michetti et al., 1992).

To assess if this bacterial adaptation mechanism could explain the observed luminal out-competition, we characterized the LPS composition of long term intestinal resident CWA Stm strain re-isolated after 34 days of colonization, in comparison to the original CWA STm stock. The standard Stm LPS is mainly composed of a mixture of O5 and O12 antigens, where the first possess an acetylation of a side chain abequose residue that is absent in the latter (Ilg et al., 2013).

We analyzed by flow cytometry the ability of specific anti-O5 and anti-O12 antibodies to bind to the bacterial LPS. We found that, as previously described, our lab stock of wild-type Stm grown *in vitro* is predominantly O5 and O12 antigen-double positive. Spontaneous shifts in the abequose acetylation rate (phase variation) generate minor subpopulations of O5- only serotype bacteria (**figure 3.3E**). The non-host-adapted CWA Stm lab strain was predominantly O5-/O12-double serotype positive, with a reduced serotype O5-only subpopulation (for unknown reasons), whereas the host-adapted long-term resident CWA strain had lost the expression of the abequose-acetylated O5 antigen (**figure 3.3E**). This observation is reminiscent of a previous report describing fitness-increasing evasion of IgA recognition by polysaccharide phase variants of *Bacteroides thetaiotaomicron* (Peterson et al., 2007a). Based on these data, we hypothesized that the ability of resident STm to outcompete the wild type STm immigration is related to the differential selective pressure imposed by O5-specific IgA, since most of it would bind the newcomer WT Stm and not the evolved CWA.

Sterile induction of STm-specific IgA combined with short-term pre-colonization with host-adapted CWA STm can partially rescue the observed protection phenotype

To address this hypothesis, we performed an orthogonally designed experiment selectively varying (i), the short-term resident strain (day-1) (original stock CWA strain versus 34-day host-adapted CWA strain) and (ii), the anti-STm IgA immunity of the mice (Moor et al., 2016)(orally immunized with 3 doses PAA-inactivated CWA STm O-12/5 or naïve; **figure 3.4A**). The main advantage of using the CWA strain over the avirulent or attenuated for this experiment is that the strict luminal containment guarantees that all bacteria-bacteria

competition is limited to the lumen, and not influenced re-seeding from persistently infected MLNs (Kaiser et al., 2013).

27 days after primary immunization with PAA-inactivated CWA STm (**figure 3.4**, green and red) or kept naïve (**figure 3.4** blue), all mice were short-term pre-colonized by gavage with either host adapted (**figure 3.4**, red and blue) or non-host-adapted CWA STm (**figure 3.4**, green), followed 1 day later by a challenge with 10^8 CFU of wild type STm for 4 days until sacrifice.

Pre-colonized-only mice (**figure 3.4B-D**, blue) showed intestinal out-competition of the CWA pre-colonizer by the wild type strain starting on day two, and lead to the total extinction of the evolved CWA by day 4 in almost all the mice of this group, suggesting that the difference in fitness between the pre-colonizer strain and the wild type invader cannot only be attributed to non-immunity-related fitness-increasing intestinal adaptations.

The mice that were immunized with PAA-inactivated and pre-colonized with non-host-adapted CWA STm showed a clear co-existence of the pre-colonizer strain with the wild type, that was absent in the naïve mice (**figure 3.4B-C**). This partial rescuing of the phenotype observed in figure 2, suggests that the adaptive immune response plays an important role in the preservation of the resident microbiota in combination with bacteria adaptation to IgA recognition. None the less we were unable to observe a statistically significant difference between the evolved and the stock CWA strains, despite the competitive index seeming different. A possible explanation to the absence of difference between the response between stock CWA and evolved CWA strains could be that the PAA-treated Stm induced an altered type of anti-LPS IgA. To address this possibility we repeated the experiment from figure 3.4 taking advantage of the transient colonization of CWA strains in germ-free mice to induce adaptive immune response independent of colonization (**figureS3.2A**). The results obtained from live bacteria IgA induction reinforce the observation of figure 4.3, discarding the idea that the non-functionality of PAA-treated induced IgA (**figureS3.2B-E**)

These results indicate that a killed-bacteria-induced adaptive immune response, in combination with a one day pre-colonization with a CWA strain (evolved or not) was able to partially restore the phenomena observed in a long term colonization. We conclude from this result that a second unknown mechanism of bacterial adaptation must contribute to the fitness increase of resident attenuated STm, in combination with the LPS O-antigen phase variation and the IgA immunity.

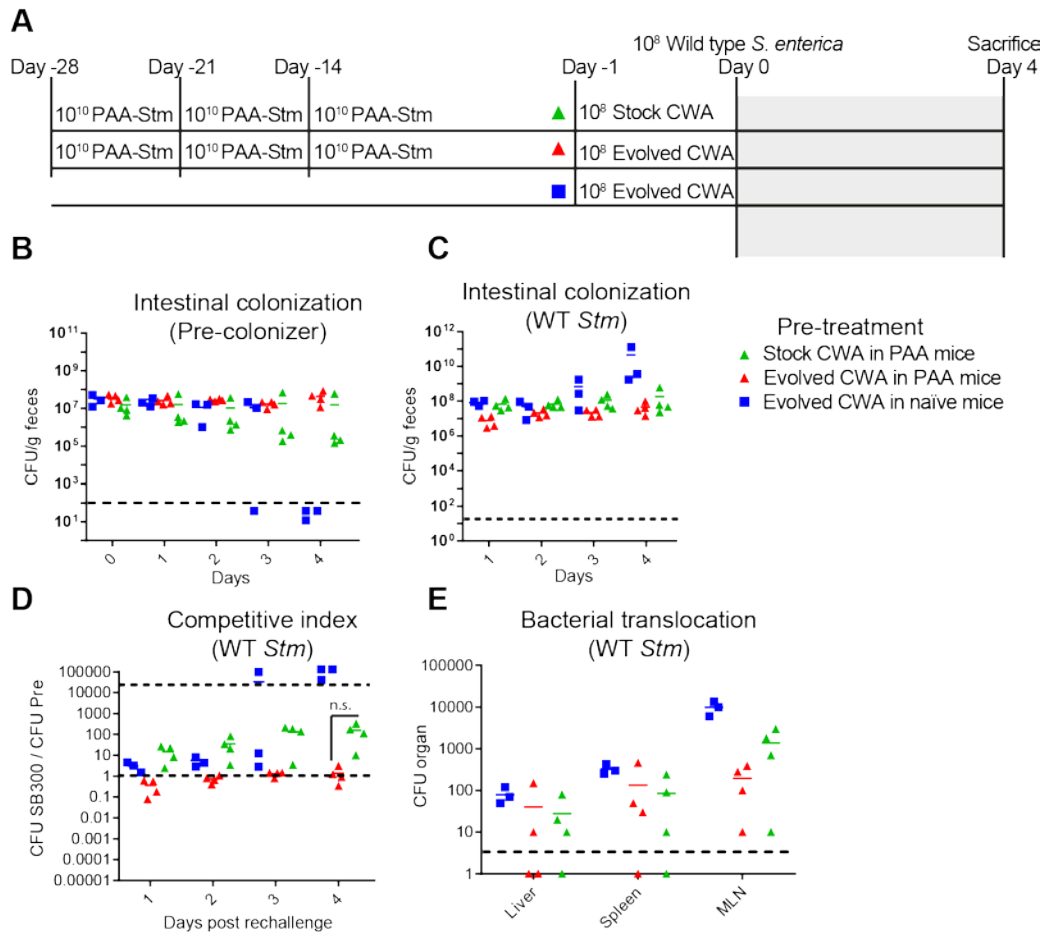


Figure 4. **The interplay between IgA and pre-colonization partially restore the out-competition.** Mice pre-treated with either PAA-Stm or PBS were the original CWA or an evolved CWA to assess the ability of out-compete WT *Stm*. **(B)** Fecal counts of precolonizer strain **(C)** Fecal counts of wild type *Salmonella*. **(D)** Competitive index of wild type *Salmonella* against the pre-colonizing strain. **(E)** Organ counts of wild type *Salmonella*. Symbols: *** $p < 0.001$, ** $p < 0.01$, n.s. not significant

Discussion

In this work we describe how the long term residency of three non-lethal *Salmonella* strains can lead to the out-competition of an isogenic WT *Stm* immigrant, protecting from STm-induced colitis. This *in vivo* advantage is independent of virulence factors or systemic colonization (Hapfelmeier et al., 2008), but dependent on the STm specific IgA host immune response. The out-competition of WT *Stm* cannot be explained merely by a niche occupation by the resident strain, since intestinal short-term residency, also of a long-term adapted strain in a naive mouse was not able to phenocopy the co-adapted resident-host interaction consisting of evolved bacteria and IgA-immunized host.

The independence of the out-competition from virulence factors is unexpected, since it has been described that virulent vaccines provide superior protection against infection, especially in bacterial infections. (Coward et al., 2014). Based on this notion, we hypothesized that the

transient inflammation induced by partially attenuated STm during establishment of long-term residency would lead to increased potency to out-compete wild-type Stm compared to the avirulent strains tested. This hypothesis proved to be wrong since all three strains tested (attenuated, avirulent, and CWA) were equally able to maintain their resident colonization levels, and outcompete the wild-type Stm strain.

The hypothesis that continuous inflammation would benefit WT Stm could not be fully verified or discarded. The high variability in lipocalin 2 at day 2 suggests that in some mice there was a transient increase in the neutrophil mediated activity, however all the long term colonized mice were able to out-compete wild-type Stm. The variability in inflammation correlated with the variability in the competitive index (**Figure 3.2 D and E**), further supporting the idea that the bacteria-bacteria competition is crucial for homeostasis.

It has been shown previously that IgA can modify the *in vivo* fitness of bacterial strains, based on their ability to be recognized by IgA (Peterson et al., 2007b). Based on this we explored the hypothesis that the host-imposed selective pressure was dependent on secretory IgA, and we tested it by depletion of IgA-producing LLPCs. The depletion of plasma cells abolished the competitive advantage of the pre-colonizer strain, leading to a continuous co-existence of both strains. This phenomenon suggests that the continuous selective pressure effected by specific IgA is a crucial factor in the differentiation between resident and immigrant strains.

The idea that the main function of IgA is to increase the competitiveness of resident microbiota against pathogens is strongly supported by current evidence. It has been shown that colitogenic bacteria are more likely to induce IgA responses than the non-colitogenic counterpart (Palm et al., 2014), and the excessive IgA-mediated responses against commensals are an important factor in the development of colitis (Wenzel et al., 2014).

The precise mechanism of how IgA may alter luminal bacterial survival is not fully understood. It has been reported that the ratio between capsule mutants and WT *B. thetaiotaomicron* can be increased up to 100 fold in presence of IgA directed against the capsule (Peterson et al., 2007a). It has also been shown that the clustering of dividing cell populations can lead to differential exclusion of certain clones from the lumen (K. Moor, E. Slack and coworkers, unpublished data). Besides a fitness-decreasing effect of IgA, it has been shown that IgA can impair the function of the *Salmonella* T3SS, effectively neutralizing the virulence factors (Forbes et al., 2008; Levinson et al., 2015; Michetti et al., 1992).

The continuous selective pressure imposed on the microbiota by the reactivity of IgA is possibly the driving force to select O5 LPS negative strains of Stm. Since it is known that IgA

can reduce the fitness of the recognized bacteria (Peterson et al., 2007a) it is conceivable that the ability to generate variations of LPS antigens may increase *in vivo* fitness. This continuous bacteria-host interplay eventually leads to a vast array of different IgA to accumulate over time, reducing the possibility of a newcomer non-adapted tourist to establish.

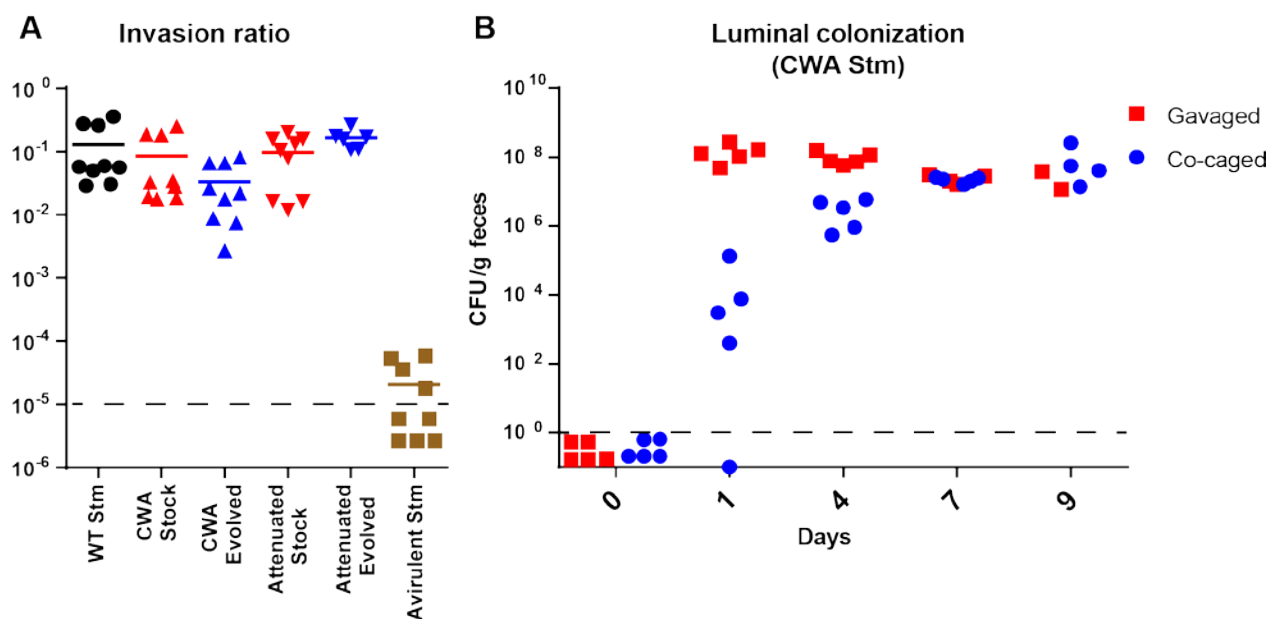
Since IgA on its own is not able to clear *Salmonella* from the gut (Endt et al., 2010), we tried to recapitulate the observed mutualistic Stm-IgA synergic interaction by sterile immunization of the animals with PAA-inactivated Stm, followed by a one day pre-colonization (Moor et al., 2016). This procedure was able to avoid the extinction of the CWA strain by immigration of wild-type Stm, evidenced in a stable 1:1 colonization ratio, which was lost in the non-immunized group that generated no Stm-binding IgA. Nonetheless, the combination of these two factors was still unable to fully confer out-competition of immigrating wild-type Stm. One possible explanation for this incomplete effect was that the IgA was artificially generated by immunization with PAA-killed instead of live organisms, potentially structurally altered by the harsh oxidation of important antigenic determinants. This hypothesis could be rejected based on the fact that the immunization with live bacteria (**Figure S3.2**) generated an identical out-competition phenotype.

Our current inability to completely re-capitulate the WT Stm out-competition by separating immunization from pre-colonization suggests that we could not detect all contributing mechanisms. We therefore hypothesize that the pre-colonizer strain needs to colonize for a longer time than one day to fully adjust to the luminal environment, since the strains were adapted to the *in vitro* conditions. The mechanism of this adaptation is probably by increased expression of scavenging proteins or a metabolic adaptation, leading to an environmental advantage over the WT Stm strain.

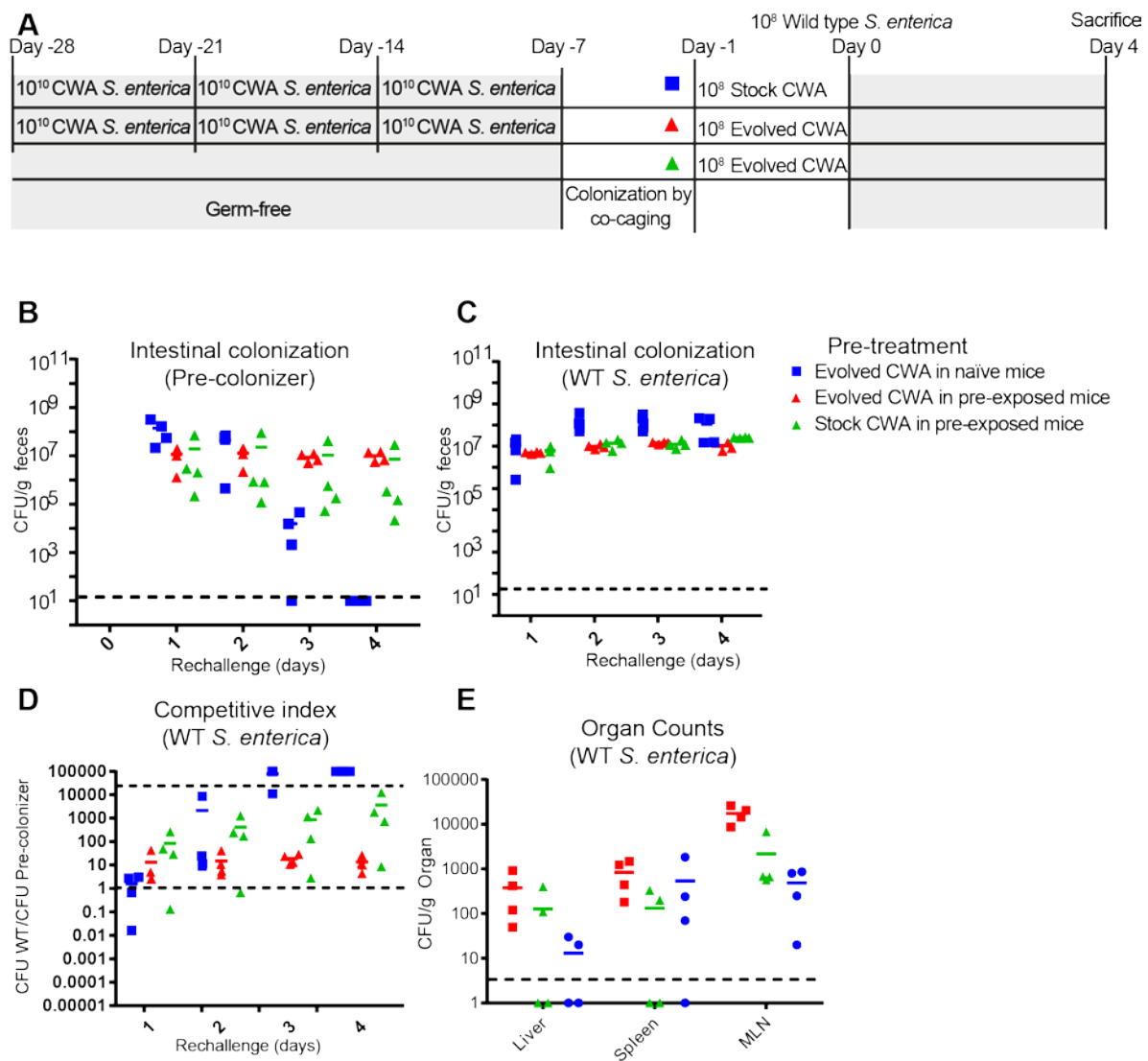
In conclusion, we maintain our hypothesis that the metabolic competition by a host-adapted resident microbial strain in combination with the ability of strain-specific IgA to decrease the fitness of newly immigrating microbial strains, act synergistically to exclude pathogenic or other tourist species. Our data further support the concept that the intestinal adaptive immune system favors the species enrichment of the resident microbiota and improves consortial stability (Dishaw et al., 2014). This mechanism sheds new light on the host-mediated microbiota regulation, since most previous studies have only been able to describe nutrient-related species variation.

The identification of the precise mechanism of metabolic adaptation/competition or IgA-mediated species depletion will be subject of future work and may crucial to better understand the ecological succession in the gut.

Supplementary Figures:



Supplementary figure 1. **In vitro** and **In vivo** testing of the *Salmonella* strains. **(A)** *In vitro* invasion ratio of the different strains used. HeLa cells were exposed to 10^6 CFU (MOI=5) of either wild type, CWA stock, CWA evolved (long term re-isolates from *Salmonella* (day 34), attenuated stock, attenuated evolved or avirulent and the intracellular CFU were measured by plating after 80 min. **(B)** Intestinal colonization of mice co-caged with mice gavaged with CWA *Salmonella*.



Supplementary figure 2. PAA-treatment simulates the immune activation induced by live bacteria. (A) Germ-free mice pre-treated three times with either CWA or PBS were permanently colonized by co-caging with a oligo-MM colonized mouse. After a week of oligo-MM colonization these mice were pre-colonized with either CWA stock or evolved, and one day after re-challenged with WT *Stm*. **(B)** Fecal counts of the pre-colonizer strain. **(C)** Fecal counts of wild type *Salmonella*. **(D)** Competitive index of wild type *Salmonella* against the pre-colonizing strain. **(E)** Organ counts of wild type *Salmonella*.

Table S1. Bacterial strains and plasmids

Strain/ Plasmid	Strain name	Relevant genotype/phenotypes/description	Source, Reference
WT <i>Salmonella enterica</i> Typhimurium	SL1344/ SB300	Wild type	W.D. Hardt (Hoiseth and Stocker, 1981)
Attenuated <i>Salmonella enterica</i> Typhimurium	M556	<i>sseD::aphT</i>	W.-D. Hardt (Hapfelmeier et al., 2004)
Avirulent <i>Salmonella enterica</i> Typhimurium	M557	<i>DinvG</i> ; <i>sseD::aphT</i>	W.-D. Hardt (Hapfelmeier et al., 2004)
CWA <i>Salmonella enterica</i> Typhimurium	HA630	$\Delta asd::tetRA$; $\Delta alrP$; $\Delta alrN$, $\Delta metC$	This study
	HA623	Δasd ; $\Delta alrP$; $\Delta alrN$, $\Delta metC$	This study
	HA615	Δasd ; $\Delta alrP$; $\Delta alrN$, $\Delta metC::tetA-sacB$	This study
	HA614	Δasd ; $\Delta alrP$; $\Delta alrN$	This study
	HA613	Δasd ; $\Delta alrP$; $\Delta alrN::tetA-sacB$	This study
	HA612	Δasd ; $\Delta alrP$;	This study
	HA611	Δasd ; $\Delta alrP$; $::tetA-sacB$	This study
	HA610	Δasd ;	This study
	HA609	Δasd ; $::tetA-sacB$	This study
	HA608	$\Delta metC::tetA-sacB$	This study
	HA607	$\Delta alrN::tetA-sacB$	This study
	HA606	$\Delta alrP$; $::tetA-sacB$	This study
	HA605	Δasd ; $::tetA-sacB$	This study
pM965		Constitutive GFP-expression plasmid, Amp ^R	W.-D. Hardt, (Stecher et al., 2004)
pSIM6		Lambda red recombination plasmid	D. Court, (Thomason et al., 2014)
T-Sack		<i>E. coli</i> W3110, designed as multiple template <i>tetA-sacB</i> , <i>amp</i> , <i>cat</i> and <i>kan</i>	D. Court, (Li et al., 2013)

Table S2. Primers used in this study

Name	Description	Sequence
SB300-alrNmutF	<i>alrN::tetA-sacB</i> cassette construction forward	CCAAGTGGACCGGTGACGCCTTAGCCTGAATTAGGTTA ATCAAAGGGAAAACTGTCCATATGC
SB300-alrNmutB	<i>alrN::tetA-sacB</i> cassette construction backwards	CAACGTTTGCATAGCGCGCATAACTGATAAAGGAAGTGAA TCCTAATTTTTGTTGACACTCTATC
SB300-asd-mutF	<i>asd::tetA-sacB</i> cassette construction forward	GAACCACACGCAGGCCCGATAAGCGCTGCAATAGCCACT A ATCAAAGGGAAAACTGTCCATATGC
SB300-asd-mutB	<i>asd::tetA-sacB</i> cassette construction backwards	CGCGCATACACAGCACATCTCTTTGCAGGAAAAAACGCT TCCTAATTTTTGTTGACACTCTATC
SB300-alrP-mutF	<i>alrP::tetA-sacB</i> cassette construction forward	GATGAGTAACTCTCCGTCATTCTTTTAAACAAGGAATTCAA TCCTAATTTTTGTTGACACTCTATC
SB300-alrP-mutB	<i>alrP::tetA-sacB</i> cassette construction backwards	CCGATAAGCGCAAGCGCCACCCGGCCCGCGCTATT TA ATCAAAGGGAAAACTGTCCATATGC
SB300-metC-mutF	<i>metC::tetA-sacB</i> cassette construction forward	TAGTTTAGACATCCAGACGGTTAAAATCAGGAAACGCAAC TCCTAATTTTTGTTGACACTCTATC
SB300-metC-mutB	<i>metC::tetA-sacB</i> cassette construction backwards	CGGAAATTGTCTGCATATATGTCCATCCCCGGCAACTTTA ATCAAAGGGAAAACTGTCCATATGC
SB300-alrN-rmvF	<i>alrN::tetA-sacB</i> cassette removal forward	CCCAAGTGGACCGGTGACGCCTTAGCCTGAATTAGGTT A TTCACCTTCCTTTATCAGTTATGCGCGCTATGCAAACGTTG
SB300-alrN-rmvB	<i>alrN::tetA-sacB</i> cassette removal backwards	CAACGTTTGCATAGCGCGCATAACTGATAAAGGAAGTGAA TAACCTAATTCAGGCTAAGGCGTCGACCGGTCCACTTGG G
SB300-asd-rmvF	<i>asd::tetA-sacB</i> cassette removal forward	GAACCACACGCAGGCCCGATAAGCGCTGCAATAGCCACT A AGCGTTTTTTTCTGCAAAGAGATGTGCTGTGTATGCGCG
SB300-asd-rmvB	<i>asd::tetA-sacB</i> cassette removal backwards	CGCGCATACACAGCACATCTCTTTGCAGGAAAAAACGCT TAGTGGCTATTGCAGCGCTTATCGGGCCTGCGTGTGGTT C
SB300-alrP-rmvF	<i>alrP::tetA-sacB</i> cassette removal forward	GATGAGTAACTCTCCGTCATTCTTTTAAACAAGGAATTCAA TAAATACGCGGCGGGCCGGGTGGCGCTTGCGCTTATCC GG
SB300-alrP-rmvB	<i>alrP::tetA-sacB</i> cassette removal backwards	CCGATAAGCGCAAGCGCCACCCGGCCCGCGCGTATT TA TTGAATTCTTGTGTTAAAAGAATGACGGAGAGTTACTCATC
SB300-metC-rmvF	<i>metC::tetA-sacB</i> cassette removal forward	TAGTTTAGACATCCAGACGGTTAAAATCAGGAAACGCAAC TAAAGTTGCCGGGGATGGACATATATGCAGACAATTTCCG
SB300-metC-rmvB	<i>metC::tetA-sacB</i> cassette removal backwards	CGGAAATTGTCTGCATATATGTCCATCCCCGGCAACTTTA GTTGCGTTTCTGATTTTAACCGTCTGGATGTCTAAACTA
SB300-alrN-ctl-F	<i>alrN</i> check forward	GTTTGGCGGCATGATTTGGA
SB300-alrN-ctl-B	<i>alrN</i> check backwards	CACCTTAGGCTGGACGATGG
SB300-asd-ctl-F	<i>asd</i> check forward	TAAGCGCTGCAATAGCCACT
SB300-asd-ctl-B	<i>asd</i> check backwards	TTGCGACTTTGGCTGCTTTT
SB300-alrP-ctl-F	<i>alrP</i> check forward	GGTACGGTTCTGTCTGACGTT
SB300-alrP-ctl-B	<i>alrP</i> check backwards	TATTACCGGATGACGGCGTG
SB300-metC-ctl-F	<i>metC</i> check forward	GCCAGGGTGCAGATGGTTAT
SB300-metC-ctl-B	<i>metC</i> check backwards	GACGCAACAAACGCAGACTT
SB300-asd-tetRA-F	<i>asd::tetRA</i> cassette forward	GCGCGCATACACAGCACATCTCTTTGCAGGAAAAAACG CTTTAAGACCCACTTTTCACATT
SB300-asd-tetRA-B	<i>asd::tetRA</i> cassette backwards	AACCACACGCAGGCCCGATAAGCGCTGCAATAGCCACTA CTAAGCACTTGTCTCCTG

Materials and Methods

Animal colonization experiments

Germ-free animals were re-derived from C57BL/6 mice and maintained germ-free in flexible film isolators in the Genaxen Foundation Clean Mouse Facility (CMF) of the University of Bern as described (Macpherson and McCoy, 2014). Mice colonized with oligo-MM from birth were also bred and maintained in the CMF. For experiments, the mice were transferred to experimental flexible film isolators for the duration of the pre colonization or PAA-Stm treatment. After the end of the pre-treatment the experimental mice were aseptically transferred to autoclaved sealseal-plus IVCs under positive pressure (Tecniplast, Italy) in a barrier unit of the Genaxen Clean Mouse Facility. Cage changes were carried out under strictly aseptic conditions. In all experiments animals were provided with sterile mouse chow (Kliba 3437; autoclaved) and autoclaved water ad libitum. All experiments were performed according to protocols approved by the Bernese Cantonal Ethical committee for animal experiments and carried out in accordance with Swiss Federal law for animal experimentation (license number BE91/14 and BE 36/15).

To generate contamination-free bacterial inoculums, NaCL (0.3M), D-Ala (200 µg/mL) and Dap (50 µg/ mL) supplemented autoclaved LB medium in sterile-filter-sealed flasks, was aseptically inoculated from single colonies of the test bacterium and incubated shaking at 150 rpm at 37°C for 16 hours. Bacteria were harvested by centrifugation (10 min, 4816 x g, 4°C) in a sterile aerosol-proof assembly, washed in autoclaved sterile PBS and concentrated to a density of 5×10^8 CFU/mL in sterile PBS, performed aseptically under a sterile laminar airflow. The bacterial suspensions were aseptically aliquoted in autoclaved plastic tubes and sealed in a sterilized secondary containment. The sterile tubes containing the inocula and the mice were aseptically imported into a sterilized laminar flow hood, and each animal inoculated with 200 µL of bacterial suspension (containing 1×10^8 CFU in sterile PBS, at a density of 5×10^8 CFU/mL) by gavage, carried out wearing sterile surgical gowns and sterile surgical gloves. Fresh fecal pellets were collected aseptically, suspended in sterile PBS, and plated in serial dilutions on D-Ala/ Dap-supplemented or non-supplemented MacConkey II agar and incubated aerobically at 37°C for 24 hours.

Long-lived plasma cell depletion

To deplete long lived plasma cells and B-cells, mice were injected I.V under sterile conditions with anti-CD20 (10mg/kg; 18B12 IgG2a, Biogen USA) and Bortezomib (0.75 mg/kg; Millennium Pharmaceuticals USA) diluted in 100µL (Khodadadi et al., 2015).

Bacterial culture

LB medium (Sigma-Aldrich) was used as the standard growth media. MacConkey was used as the standard media for fecal pellet counts. Where required, the following supplements were added to the media: ampicillin (Sigma, 100 µg/mL), tetracycline (Sigma, 12.5 µg/mL), kanamycin (Sigma, 50 µg/mL), meso-diaminopimelic acid (Sigma, 50 µg/mL), D-alanine (Sigma, 200 µg/mL).

PAA-inactivation of STm

Wild type *Salmonella enterica* Typhimurium was cultured in 500 mL LB (NaCl 0.3M) shaking at 150 rpm at 37°C for 16 h. Bacteria was harvested as described above and resuspended in 10 mL of 0.1% per-acetic acid in water for one hour. The bacterial particles were washed three times with PBS by centrifugation and suspended at a density of 10^{11} particles/ mL. The bacterial suspensions were aseptically aliquoted in autoclaved plastic tubes and sealed in a sterilized secondary containment. The sterile tubes containing the inocula and the mice were aseptically imported into plastic film isolators, and each animal inoculated with 200 µL of bacterial particle suspension (containing 2×10^{10} CFU in sterile PBS, at a density of 2×10^{11} CFU/mL) by gavage

Bacterial genetic engineering

All bacterial strains used or generated in this study are specified in S1 Table. The *Salmonella enterica* Typhimurium SB300, M556 and M557 were kindly provided by Wolf-Dietrich Hardt (Hapfelmeier et al., 2004). The strain HA630 was generated by sequential P22 transduction of the individual mutations, and using lambda Red recombineering to remove the *tetA-sacB* cassettes with the appropriate “rmv” primers. All single deletions were carried out individually in four strains (HA605-HA608) with the Court Lab Lambda Red recombineering method (Li et al., 2013), using the pSIM6 plasmid and the *tetA-sacB* cassette. To generate the *tetA-sacB* or *tetRA* cassettes PCR was performed using the gene appropriate “mut” primer and the T-SACK strain (*tetA-sacB*) or a Tn10 based cassette (*tetRA*) (Li et al., 2013). All deletions were confirmed by PCR using the appropriate “ctl” primer. All primers are described in table S2

Fluorescent imaging

The distal 3 cm of the cecum were fixed in 4% PFA in PBS for 24 h, and then transferred to a 20% Sucrose solution for 24-48 h. The fixed cecum was then embedded in OTC media, and flash frozen with liquid nitrogen. Sections of 7 µm thickness were cut and rinsed twice in PBS and one time in PBS/2% BSA. Sections were stained with a PBS/2% BSA solution containing

DAPI (Sigma-Aldrich, USA, 0.01 mg/mL final concentration) and Phalloidin-Atto 647N (Sigma-Aldrich, USA, 0.04 nmol/mL final concentration) for 30min. Sections were rinsed again twice in PBS and one time in PBS/2%BSA and mounted under Vectashield (Vector laboratories, USA). Images were acquired using a Zeiss LSM710 Laser scanning microscope with a 40X oil objective (three z-stacks with 3 μ m spacing, 150 μ m square sections, independent mode channels).

Gentamicin protection assay

HeLa (Kyoto) cells were seeded into 24-well dishes and grown for 1 day to obtain 80% confluency. The cells were cultured in Dulbecco modified Eagle medium (DMEM) containing 10% fetal bovine serum (FBS). During the whole procedure cells were incubated at 37°C under an atmosphere containing 5% CO₂. The adherent cells were washed three times with Hanks' buffered salt (HBSS) and covered with 500 μ L HBSS, 10 min before cells were infected with bacteria. Cultures of the appropriate strain were grown in 10 mL 0.3 M NaCl LB for 16 h, shaking at 150 rpm, at 37°C, diluted 1:20 into 40 mL fresh 0.3M NaCl LB media, and subcultured for 5 h under the same conditions. Bacteria were then washed once in PBS and diluted to an OD₆₀₀ of 0.6. HeLa cells were infected with 5 μ L of the resulting bacterial suspension per well and were incubated in HBSS for 50 min. To kill extracellular bacteria, HeLa cells were washed three times with HBSS and incubated in 500 μ L DMEM containing 10% FBS and 400 μ g/mL gentamicin, for 30 min. This provides a total infection time of 80 min. HeLa cells were afterwards washed three times with PBS and lysed in 0.1% sodium-deoxycholate/PBS. The CFUs of intracellular bacteria and the infectious dose were determined by plating of appropriate dilutions on D-Ala and m-Dap supplemented LB agar. The intracellular (= gentamicin protected) CFUs were calculated as a ratio of the whole inoculum.

Lipocalin-2 ELISA

Fecal Lipocalin-2 was measured using the solid phase Sandwich ELISA Mouse Lipocalin-2/NGAL DuoSet (R&D Systems, USA). The assay was performed according to the manufacturer's instructions, except for the horseradish peroxidase, HRP-SA which was used from Biolegend (USA). Fecal pellets from mice were dissolved in 0.5 mL sterile PBS, and debris were spun down (7000 rpm, 5min). The supernatant was used as a sample, and a dilution series was made (1:3 dilution, 6 dilutions). Of the standard a dilution series was made in duplicates (1:3 dilution, 12 dilutions). The OD₄₀₅ was measured using a thermomax microplate reader (Molecular Devices, USA) Data was analyzed using graph pad Prism program. A four parameter dose-response curve was fitted, using equal hill slopes for all

samples on the same plate. Samples with low OD₄₀₅ values resulting in a curve fit with R² values below 0.95 were defined below detection limit. By comparison with the standard, the EC₅₀ was used to calculate the absolute amount of Lipocalin-2 per sample.

Live bacterial flow cytometry for LPS-O-antigen typing

The appropriate *Salmonella* strain was grown in 0.2 µm membrane-filtered LB broth overnight at 37°C and 150 rpm. 500 µL of culture was gently pelleted for 3 min at 4816 x g in a Heraus Fresco 21 centrifuge and suspended with 500 µL of sterile-filtered 2% BSA/ 0.005% NaN₃/ PBS. One microliter of this solution was transferred to a new clean 1.5 mL tube and incubated for 5 minutes at room temperature with anti-O5 (Difco Salmonella O antisera Factor 5 #226601) and anti-O12 antibodies (STA5 EBV-transformed B cell supernatant). The bacteria was washed once with 500 µL of sterile-filtered 2% BSA/ 0.005% NaN₃/ PBS and pelleted for 3 min at 4816 x g in a Heraus Fresco 21. The supernatant was discarded and the pellet was re-suspended in 200 µL of 2% BSA/ 0.005% NaN₃/ PBS containing BV421-anti-Rabbit (secondary to anti O5, Biolegend) and Ax647-anti-hIgG (secondary to anti O12, Jackson)

Data analysis and statistical analysis

All data analysis was done using the Prism statistical programs. The appropriate statistics are explained in the legend of each figure

Acknowledgements

We thank the Clean Mouse Facility for all the animal work, Jens Stein for kindly providing the anti-CD20 antibody, Wolf Dietrich-Hardt for providing the original WT Stm strain, Fabian Blank, Carlos Wotzkow and the MIC for their support with the microscopes. This work was funded by the grants ERC 281904 and SNF 310030_138452.

References

- Barroso-Batista, J., Demengeot, J., and Gordo, I. (2015). Adaptive immunity increases the pace and predictability of evolutionary change in commensal gut bacteria. 6, 8945.
- Barthel, M., Hapfelmeier, S., Quintanilla-Martínez, L., Kremer, M., Rohde, M., Hogardt, M., Pfeffer, K., Rüssmann, H., and Hardt, W. (2003). Pretreatment of mice with streptomycin provides a *Salmonella enterica* serovar Typhimurium colitis model that allows analysis of both pathogen and host. 71, 2839-2858.

Coward, C., Restif, O., Dybowski, R., Grant, A.J., Maskell, D.J., and Mastroeni, P. (2014). The effects of vaccination and immunity on bacterial infection dynamics in vivo. *10*, e1004359.

Cuenca, M., Pfister, S.P., Buschor, S., Bayramova, F., Hernández, S.B., Cava, F., Kuru, E., Van Nieuwenhze, M.S., Brun, Y.V., Coelho, F.M., et al. (2016). D-Alanine-Controlled Transient Intestinal Mono-Colonization with Non-Laboratory-Adapted Commensal *E. coli* Strain HS. *11*, e0151872.

Diard, M., Garcia, V., Maier, L., Remus-Emsermann, M.N., Rol, Regoes, R., Ackermann, M., Hardt, W., and Regoes, R.R. (2013). Stabilization of cooperative virulence by the expression of an avirulent phenotype. *Nature* *494*, 353-356.

Dishaw, L.J., Cannon, J.P., Litman, G.W., and Parker, W. (2014). Immune-directed support of rich microbial communities in the gut has ancient roots. *47*, 36-51.

Endt, K., Stecher, B., Chaffron, S., Slack, E., Tchitchek, N., Benecke, A., Van Maele, L., Sirard, J., Mueller, A.J., Heikenwalder, M., et al. (2010). The microbiota mediates pathogen clearance from the gut lumen after non-typhoidal *Salmonella* diarrhea. *PLOS Pathogens* *6*, e1001097.

Forbes, S.J., Eschmann, M., and Mantis, N.J. (2008). Inhibition of *Salmonella enterica* serovar typhimurium motility and entry into epithelial cells by a protective antilipopolysaccharide monoclonal immunoglobulin A antibody. *76*, 4137-4144.

Fransen, F., Zagato, E., Mazzini, E., Fosso, B., Manzari, C., Aidy, El, S., Chiavelli, A., D'Erchia, A.M., Sethi, M.K., Pabst, O., et al. (2015). BALB/c and C57BL/6 Mice Differ in Polyreactive IgA Abundance, which Impacts the Generation of Antigen-Specific IgA and Microbiota Diversity. *Immunity* *43*, 527.

Gauger, E.J., Leatham, M.P., Mercado-Lubo, R., Laux, D.C., Conway, T., and Cohen, P.S. (2007). Role of motility and the flhDC Operon in *Escherichia coli* MG1655 colonization of the mouse intestine. *75*, 3315-3324.

Hapfelmeier, S., Müller, A.J., Stecher, B., Kaiser, P., Barthel, M., Endt, K., Eberhard, M., Robbiani, R., Jacobi, C.A., Heikenwalder, M., et al. (2008). Microbe sampling by mucosal dendritic cells is a discrete, MyD88-independent step in DeltainvG *S. Typhimurium* colitis. *The Journal Of Experimental Medicine* *205*, 437-50.

Hapfelmeier, S., Ehrbar, K., Stecher, B., Barthel, M., Kremer, M., and Hardt, W. (2004). Role of the *Salmonella* pathogenicity island 1 effector proteins SipA, SopB, SopE, and SopE2 in

Salmonella enterica subspecies 1 serovar Typhimurium colitis in streptomycin-pretreated mice. *Infection And Immunity* 72, 795-809.

Hapfelmeier, S., Stecher, B., Barthel, M., Kremer, M., Müller, A.J., Heikenwalder, M., Stallmach, T., Hensel, M., Pfeffer, K., Akira, S., et al. (2005). The *Salmonella* pathogenicity island (SPI)-2 and SPI-1 type III secretion systems allow *Salmonella* serovar typhimurium to trigger colitis via MyD88-dependent and MyD88-independent mechanisms. *J. Immunol.* 174, 1675-85.

Hoiseth, S.K., and Stocker, B.A. (1981). Aromatic-dependent *Salmonella typhimurium* are non-virulent and effective as live vaccines. *Nature* 291, 238-9.

Ilg, K., Zandomenighi, G., Rugarabamu, G., Meier, B.H., and Aebi, M. (2013). HR-MAS NMR reveals a pH-dependent LPS alteration by de-O-acetylation at abequose in the O-antigen of *Salmonella enterica* serovar Typhimurium. *Carbohydrate Research* 382, 58.

Kaiser, P., Slack, E., Grant, A.J., Hardt, W., and Regoes, R.R. (2013). Lymph Node Colonization Dynamics after Oral *Salmonella Typhimurium* Infection in Mice. *PLOS Pathogens* 9, e1003532.

Khodadadi, L., Cheng, Q., Alexander, T., Sercan-Alp, Ö., Klotsche, J., Radbruch, A., Hiepe, F., Hoyer, B.F., and Taddeo, A. (2015). Bortezomib Plus Continuous B Cell Depletion Results in Sustained Plasma Cell Depletion and Amelioration of Lupus Nephritis in NZB/W F1 Mice. 10, e0135081.

Leatham, M.P., Banerjee, S., Autieri, S.M., Mercado-Lubo, R., Conway, T., and Cohen, P.S. (2009). Precolonized human commensal *Escherichia coli* strains serve as a barrier to *E. coli* O157:H7 growth in the streptomycin-treated mouse intestine. 77, 2876-2886.

Levinson, K.J., De Jesus, M., and Mantis, N.J. (2015). Rapid Effects of a Protective O-Polysaccharide-Specific Monoclonal IgA on *Vibrio cholerae* Agglutination, Motility, and Surface Morphology. *Infection And Immunity* 83, 1674.

Li, X., Thomason, L.C., Sawitzke, J.A., Costantino, N., and Court, D.L. (2013). Positive and negative selection using the tetA-sacB cassette: recombineering and P1 transduction in *Escherichia coli*. *Nucleic Acids Research* 41, e204.

Macpherson, A.J., and McCoy, K.D. (2014). Standardised animal models of host microbial mutualism. 8, 476-486.

- Maltby, R., Leatham-Jensen, M.P., Gibson, T., Cohen, P.S., and Conway, T. (2013). Nutritional basis for colonization resistance by human commensal *Escherichia coli* strains HS and Nissle 1917 against *E. coli* O157:H7 in the mouse intestine. *Plos ONE* 8, e53957.
- McSorley, S.J., Cookson, B.T., and Jenkins, M.K. (2000). Characterization of CD4+ T cell responses during natural infection with *Salmonella typhimurium*. *164*, 986-993.
- Medina, E., Paglia, P., Nikolaus, T., Müller, A., Hensel, M., and Guzmán, C.A. (1999). Pathogenicity island 2 mutants of *Salmonella typhimurium* are efficient carriers for heterologous antigens and enable modulation of immune responses. *Infection And Immunity* 67, 1093-9.
- Michetti, P., Mahan, M.J., Slauch, J.M., Mekalanos, J.J., and Neutra, M.R. (1992). Monoclonal secretory immunoglobulin A protects mice against oral challenge with the invasive pathogen *Salmonella typhimurium*. *Infection And Immunity* 60, 1786-1792.
- Moor, K., Wotzka, S.Y., Toska, A., Diard, M., Hapfelmeier, S., and Slack, E. (2016). Peracetic Acid Treatment Generates Potent Inactivated Oral Vaccines from a Broad Range of Culturable Bacterial Species. *Frontiers In Immunology* 7, 34.
- Palm, N.W., de Zoete, M.R., Cullen, T.W., Barry, N.A., Stefanowski, J., Hao, L., Degnan, P.H., Hu, J., Peter, I., Zhang, W., et al. (2014). Immunoglobulin A coating identifies colitogenic bacteria in inflammatory bowel disease. *158*, 1000-1010.
- Peterson, D.A., McNulty, N.P., Guruge, J.L., and Gordon, J.I. (2007a). IgA response to symbiotic bacteria as a mediator of gut homeostasis. *2*, 328-339.
- Peterson, D.A., McNulty, N.P., Guruge, J.L., and Gordon, J.I. (2007b). IgA Response to Symbiotic Bacteria as a Mediator of Gut Homeostasis. *Cell Host & Microbe* 2, 328.
- Ridaura, V.K., Faith, J.J., Rey, F.E., Cheng, J., Duncan, A.E., Kau, A.L., Griffin, N.W., Lombard, V., Henrissat, B., Bain, J.R., et al. (2013). Gut microbiota from twins discordant for obesity modulate metabolism in mice. *341*, 1241-1244.
- Rogier, E.W., Frantz, A.L., Bruno, M.E.C., and Kaetzel, C.S. (2014). Secretory IgA is Concentrated in the Outer Layer of Colonic Mucus along with Gut Bacteria. *3*, 390-403.
- Stecher, B., Hapfelmeier, S., Müller, C., Kremer, M., Stallmach, T., and Hardt, W. (2004). Flagella and chemotaxis are required for efficient induction of *Salmonella enterica* serovar Typhimurium colitis in streptomycin-pretreated mice. *Infection And Immunity* 72, 4138-50.

Stecher, B., Robbiani, R., Walker, A.W., Westendorf, A.M., Barthel, M., Kremer, M., Chaffron, S., Macpherson, A.J., Buer, J., Parkhill, J., et al. (2007). *Salmonella enterica* serovar typhimurium exploits inflammation to compete with the intestinal microbiota. *5*, 2177-2189.

Thomason, L.C., Sawitzke, J.A., Li, X., Costantino, N., and Court, D.L. (2014). Recombineering: genetic engineering in bacteria using homologous recombination. *106*, 1.16.1-1.16.39.

Wenzel, U.A., Magnusson, M.K., Rydström, A., Jonstrand, C., Hengst, J., Johansson, M.E., Velcich, A., Öhman, L., Strid, H., Sjövall, H., et al. (2014). Spontaneous Colitis in Muc2-Deficient Mice Reflects Clinical and Cellular Features of Active Ulcerative Colitis. *Plos ONE* *9*, e100217.

Zhang, H., Sparks, J.B., Karyala, S.V., Settlage, R., and Luo, X.M. (2014). Host adaptive immunity alters gut microbiota. *The ISME Journal* *9*, 770.

General Discussion

In this work we developed and tested a new bacterial tool for the study of the host-microbiota interaction. This tool, referred to as cell wall auxotrophic (CWA) bacteria, was first fully characterized for the human commensal *E. coli* HS. We were able to determine the extent of CWA bacterial survival under non-permissive conditions, measure their mean half-life in germ-free animals, and establish the similarity to the wild type bacteria-host interaction (Cuenca et al., 2016). This characterization allowed us to simulate a short-lived colonization with a commensal, safely return the mice to germ-free status and elicit a long-lived immune response towards that strain. Despite this being done in the past by Hapfelmeier *et al*, we offer now a more reliable system and a full characterization of all the properties, expanding our understanding of the effects of cell wall starvation (Hapfelmeier et al., 2010).

Transient bacterial colonization using CWA bacteria provides a method to expose bacteria-naïve germ-free mice to live antigens, but without compromising their axenic hygiene status. The microbiota conditioning of germ-free animals may therefore be used for the immune normalization of germ-free mice, potentially correcting several of the known alteration of their immune system, like neutropenia, enlarged cecum size, irregular mucus or disrupted immune responses (Balmer et al., 2014; Jakobsson et al., 2015; Macpherson and McCoy, 2014).

In line, the finding that CWA bacterial strains were able to emulate the early aspects of a bacterial colonization led us to speculate if it would also be possible to recapitulate the early signaling events of a pathogen infection. For this purpose we exposed germ-free mice to a CWA strain of *Salmonella enterica* Typhimurium (Stm) and measured the early mucosal transcriptional response pattern. We found that transient CWA Stm infection effectively emulated (and was limited to) the host responses occurring during the first few hours of wild type infection, independent of intestinal damage, invasion into deep tissues, or permanent pathogen colonization. Our findings showed that the induction of the early intestinal innate response by Stm is damage-independent but virulence factor-dependent. This induction is comparable to the NLRC4 dependent epithelial cell expulsion observed by Sellin *et al*, where they show that the primary line of defense starts occurring as early as 6 hours post infection in the antibiotic treated model (Sellin et al., 2014).

The ability to emulate short-duration pathogenic or commensal bacteria-host interactions opens up new possibilities for studying the importance of the sequential bacterial colonization or the effects of bacterial pre-exposition in the colonization process, independently of the permanent colonization of the gut. It also allows determining the longevity of the immune responses after the antigen has been removed, the source of very heated discussions in the

mucosal immunology field (Bredholt et al., 2014; Hapfelmeier et al., 2010; Mattioli and Tomasi, 1973).

Besides the opportunity to address basic immunology questions, the CWA system can be used to study a complex microbiota interaction. Indeed, the process of colonization of the gut and the consequent host-microbiota interplay can be exquisitely well studied using this system, as we were able to establish a CWA Stm long term colonization system, which does not lead to disease.

Utilizing the - rather unexpected - long term luminal colonization of the CWA Stm in gnotobiotic mice harboring a reduced-complexity microbiota, as well as other modified Stm strains, we were able to characterize the ability of the host to directly affect the bacterial fitness in a species- and strain-specific manner. The continuous bacteria-specific selective pressure imposed by IgA, in combination with bacterial adaptation protected the resident strain and suppressed the establishment of a wild type Stm immigrant. This finding is reminiscent of the advantage that certain strains can have due to surface carbohydrate variation (Peterson et al., 2007)

Although the mechanism of how IgA alters luminal bacteria survival still remains incompletely understood, our findings provide evidence for an active IgA-driven process to preserve resident bacteria. This observation goes in line with the hypothesis that the adaptive immune system promotes of a stable and beneficial resident microbiota (Dishaw et al., 2014), and the continuous bacterial fitness-increasing adaptation (Degnan et al., 2014). An important unexplored area of this work is the non-genetic adaptations in bacteria that might be induced by a short stay in the gut. It has been shown in the past that once a strain manages to fully colonize the gut, it is able to deplete nutrients and prevent the colonization of newcomers (Maltby et al., 2013). This aspect should be further explored to assess if this is an important factor in the out-competition of similar strains.

Future work may explore the possibilities for utilizing these interactions to change the community structure of the microbiota therapeutically, for more effective prevention of intestinal infection than currently achievable with traditional vaccination approaches.

References

Balmer, M.L., Schürch, C.M., Saito, Y., Geuking, M.B., Li, H., Cuenca, M., Kovtonyuk, L.V., McCoy, K.D., Hapfelmeier, S., Ochsenbein, A.F., et al. (2014). Microbiota-derived compounds drive steady-state granulopoiesis via MyD88/TICAM signaling. *J. Immunol.* 193, 5273-83.

- Bredholt, G., Brokstad, K.A., Pathirana, R.D., Aarstad, H.J., Tondel, C., and Cox, R.J. (2014). Longevity of B-Cell and T-Cell Responses After Live Attenuated Influenza Vaccination in Children. *Journal Of Infectious Diseases* 211, 1541.
- Cuenca, M., Pfister, S.P., Buschor, S., Bayramova, F., Hernandez, S.B., Cava, F., Kuru, E., Van Nieuwenhze, M.S., Brun, Y.V., Coelho, F.M., et al. (2016). D-Alanine-Controlled Transient Intestinal Mono-Colonization with Non-Laboratory-Adapted Commensal *E. coli* Strain HS. *Plos ONE* 11, e0151872.
- Degnan, P.H., Barry, N.A., Mok, K.C., Taga, M.E., and Goodman, A.L. (2014). Human Gut Microbes Use Multiple Transporters to Distinguish Vitamin B12 Analogs and Compete in the Gut. *Cell Host & Microbe* 15, 47.
- Dishaw, L.J., Cannon, J.P., Litman, G.W., and Parker, W. (2014). Immune-directed support of rich microbial communities in the gut has ancient roots. 47, 36-51.
- Hapfelmeier, S., Lawson, M.A.E., Slack, E., Kirundi, J.K., Stoel, M., Heikenwalder, M., Cahenzli, J., Velykoredko, Y., Balmer, M.L., Endt, K., et al. (2010). Reversible microbial colonization of germ-free mice reveals the dynamics of IgA immune responses. 328, 1705-1709.
- Jakobsson, H.E., Holmén-Larsson, J., Schütte, A., Ermund, A., Rodríguez-Piñeiro, A.M., Arike, L., Wising, C., Svensson, F., Bäckhed, F., and Hansson, G.C. (2015). Normalization of Host Intestinal Mucus Layers Requires Long-Term Microbial Colonization. *Cell Host & Microbe* 18, 582-92.
- Macpherson, A.J., and McCoy, K.D. (2014). Standardised animal models of host microbial mutualism. *Mucosal Immunology* 8, 476.
- Maltby, R., Leatham-Jensen, M.P., Gibson, T., Cohen, P.S., and Conway, T. (2013). Nutritional basis for colonization resistance by human commensal *Escherichia coli* strains HS and Nissle 1917 against *E. coli* O157:H7 in the mouse intestine. *Plos ONE* 8, e53957.
- Mattioli, C.A., and Tomasi, T.B. (1973). The life span of IgA plasma cells from the mouse intestine. *The Journal Of Experimental Medicine* 138, 452-60.
- Peterson, D.A., McNulty, N.P., Guruge, J.L., and Gordon, J.I. (2007). IgA Response to Symbiotic Bacteria as a Mediator of Gut Homeostasis. *Cell Host & Microbe* 2, 328.
- Sellin, M.E., Müller, A.A., Felmy, B., Dolowschiak, T., Diard, M., Tardivel, A., Maslowski, K.M., and Hardt, W. (2014). Epithelium-Intrinsic NAIP/NLRC4 Inflammasome Drives Infected Enterocyte Expulsion to Restrict *Salmonella* Replication in the Intestinal Mucosa. *Cell Host & Microbe* 16, 237.

Miguelangel Cuenca

Address: Frohberweg 11 Bern 3012, Switzerland
Phone: (+41) 79 646 0892
Nationality: Spanish / Venezuelan
Date of birth: February 6th, 1987
Email: miguelangel.cuenca.vera@gmail.com
<https://ch.linkedin.com/in/miguelangel-cuenca-a67b8517>

Education

- 2012-2016 **PhD in Immunology**
University of Bern, Switzerland
Committee: Siegfried Hapfelmeier, Emma Slack-Wetter and, Philippe Krebs
External referee: Nassos Typas
- 2013 **Computational biology, practical course**
European Molecular Biology Organization
- 2011-2012 **Master in biochemistry, molecular biology and biomedicine**
Universidad Complutense de Madrid, Spain
Supervisor: Daniela Xavier Dias
- 2011 **Mathematical modelling for infectious diseases dynamics, practical course**
Wellcome Trust Genome Centre, United Kingdom
- 2003-2009 **Bachelor degree in biology**
Universidad Simón Bolívar, Venezuela
-

Experience

- 2012-2016 **PhD candidate, University of Bern**
Project: Exploring the pathogen-commensal continuum: Cell wall auxotrophic bacteria in gnotobiotic mice
Design and lead two independent research projects
Providing scientific support to several projects
Complex data analysis and script writing using R or perl
Establishment and maintenance of international collaborations
Communicating results in international conferences for a technical audience
Communicating results for general audience
Co-supervision master and lab rotation students
- 2011-2012 **Master Student, Universidad Complutense de Madrid**
Project: Genetic Scale Metabolic Reconstruction of *Rhodococcus ruber*
Design a simple pipeline for bacterial metabolic reconstruction
Perform downstream NGS analysis
Translate the obtained results in to a continuation wet-lab project
- 2009-2011 **Research assistant, Instituto De Biomedicina - Universidad Central de Venezuela**
Main tasks:
Patient interview and selection for the research project
Data analysis using multivariate statistics
Laboratory analysis of patients samples
- 2008 **Intern, Quimbiotec**
Main tasks:
Standardization of quality control procedures for human recombinant insulin
Performing laboratory techniques for product quality assessment
Writing reports conforming to the European Pharmacopeia standards

Skills

Computational Skills	Multivariate statistical analysis Intermediate R scripting Basic Perl programming Intermediate mathematical modelling Downstream NGS processing Complex statistical analysis
Laboratory Skills	Bacterial site-directed genetic manipulation Phage genetics Cell culture and <i>in vitro</i> infections Gnotobiotic mice experimentation and defined microbiota colonization General immunology techniques (ELISA, FACS, Western blot) Cell isolation from tissues for flow cytometry analysis
Soft skills	Able to explain complex scientific problems effectively Good project management Excellent problem solving skills Excellent teaching skills Ability to effectively work under stress
Languages	Spanish: Native English: Advanced German: Beginner

Publications (accepted)

M, Cuenca, S P. Pfister, S Buschor, F Bayramova, S B. Hernandez, F Cava, E Kuru, M S. Van Nieuwenhze, Y V. Brun, F M. Coelho and S Hapfelmeier. **D-Alanine-Controlled Transient Intestinal Mono-Colonization with Non-Laboratory-Adapted Commensal E. coli Strain HS**. (2016) PloS ONE 11, e0151872.
ML. Balmer, C M. Schurch, Y Saito, M B. Geukin, H Li, **M Cuenca**, L V. Kovtonyuk, K D. McCoy, S Hapfelmeier, AF. Ochsenbein, M G. Manz, E Slack, and AJ. Macpherson
Microbiota-Derived Compounds Drive Steady-State Granulopoiesis via MyD88/TICAM Signaling. (2014)The Journal of Immunology, 193: 5273-5283

Publications (in preparation)

M Cuenca, S Buschor, M Terrazos, N Studer, F Matos-Coleho, S Hapfelmeier **Specific IgA disfavors an intestinal pathogen by mediating out-competition by resident bacteria** *In preparation*
S Buschor, M Cuenca, S Hapfelmeier. **An early time window of epithelial susceptibility determines severity of Citrobacter rodentium A/E infection** *In preparation*

Prizes

Best short talk. **Rigi workshop 2016 “Systems and Synthetic Biology of Microbes”**
Third prize. **GCB -Science Slam**. <https://tube.switch.ch/videos/a0502082>

References

Siegfried Hapfelmeier Siegfried.hapfelmeier@ifik.unibe.ch
Emma Slack-Wetter emma.slack@micro.biol.ethz.ch
Philippe Krebs philippe.krebs@pathology.unibe.ch

Declaration of Originality

Last name, first name:

Matriculation number:

I hereby declare that this thesis represents my original work and that I have used no other sources except as noted by citations.

All data, tables, figures and text citations which have been reproduced from any other source, including the internet, have been explicitly acknowledged as such.

I am aware that in case of non-compliance, the Senate is entitled to withdraw the doctorate degree awarded to me on the basis of the present thesis, in accordance with the “Statut der Universität Bern (Universitätsstatut; UniSt)”, Art. 69, of 7 June 2011.

Place, date

Signature